The Sensitivity of Tropical Radiative Budgets to Cloud Distribution and the Radiative Properties of Clouds

By
David O'C. Starr

Department of Atmospheric Science
Colorado State University
Fort Collins, Colorado

Colorado
State
University

Department of
Atmospheric Science

Paper No. 270

THE SENSITIVITY OF TROPICAL RADIATIVE BUDGETS

TO CLOUD DISTRIBUTION AND THE

RADIATIVE PROPERTIES OF CLOUDS

By

David O'C. Starr

Department of Atmospheric Science

Colorado State University

Fort Collins, Colorado

80523

June, 1976

ABSTRACT

THE SENSITIVITY OF TROPICAL RADIATIVE BUDGETS TO CLOUD DISRIBUTION AND THE RADIATIVE PROPERTIES OF CLOUDS.

The research reported in this paper defines the constraints, which data analysis techniques must meet if the GATE Radiation Subprogram accuracy objectives are to be met, in terms of the conventional independent variables used in radiative transfer computations. The need for an objective cloud field determination scheme and the proposed methods of deducing the radiative divergence fields from cloud field data and other pertinent meteorological data are reviewed in light of the GATE RSP proposed resolution and accuracy requirements.

The sensitivity of the radiative divergence fields to inaccuracies in the cloud field description is investigated by means of broadband radiative transfer models for the short wave ($0.3\ \mu m$ - $3\ \mu m$) and long wave ($3.0\ \mu m$ - $55\ \mu m$) spectral regions. Specifically, the maximum allowable uncertainties in the description of each of the bulk cloud radiative properties, cloud height, and areal cloud cover are determined for various cloud types, such that the RSP proposed accuracy in the radiative heating rates of $\pm 0.2°C \cdot day^{-1}$ for 200 mb thick atmospheric layers may be achieved. The situation of multi-layered cloud configurations is treated. The case of simultaneous uncertainties in the description of various cloud parameters is also investigated. The data presented are most applicable to the determination of the radiative divergence on the GATE A/B and B-scales. Objective cloud field determinations are constrained to meet these criteria if the RSP objectives are to be met.

The sensitivity of the fields of radiative divergence to uncertainties in the vertical moisture and temperature structure is evaluated. The effects of aerosols are also discussed. In addition, the sensitivity of the radiative fluxes at the surface to the specification of the temperature, moisture and cloud fields is determined.

Based on the results, recommendations are made concerning the development of an objective cloud field determination scheme and the development of adequate methods of deducing the fields of radiative divergence for the GATE areas.

David O'C. Starr
Atmospheric Science Department
Colorado State University
Fort Collins, Colorado 80523
Spring, 1976

ACKNOWLEDGEMENTS

TABLE OF CONTENTS

LIST OF TABLES

LIST OF FIGURES

LIST OF SYMBOLS

a, b, c, d - weighting factors

a_c — short wave broadband cloud absorptivity

c_p — specific heat of air at constant pressure

g — acceleration of gravity

H — irradiance

K — short wave irradiance

p — pressure

q_v — mixing ratio of water vapor

Q — radiative heating rate

t — time

t_a — short wave transmissivity of the free atmosphere

t_c — short wave cloud transmissivity

T — temperature

TQ — radiative heating rate of the total atmospheric column

α — percent area cloud cover

δx — maximum allowable uncertainty in x

Δp — pressure thickness of a layer

Δp_c — pressure thickness of a cloud layer

Δx, Δy — dimension of horizontal resolution

ε^* — effective infrared broadband cloud emissivity

ε_s — effective infrared broadband surface emissivity

θ — solar zenith angle

λ — wavelength

ρ_c — short wave broadband cloud reflectivity

ρ_s — short wave broadband surface reflectivity

σ — Stefan-Boltzman constant

Φ - geopotential height

($\uparrow$)   - upward

($\downarrow$)   - downward

SUBSCRIPTS

B   - base

CB   - cloud base

CT   - cloud top

IR   - infrared

o   - top of atmosphere

R   - total radiation

s   - surface

SW   - short wave

T   - top

I. INTRODUCTION

The field phase of the GARP* Atlantic Tropical Experiment (GATE) (ISMG, 1975) was carried out during the period 15 June to 23 September 1974. The observing network encompassed the tropical zone of Africa, the Atlantic Ocean, and Central and South America (Figs. 1 and 2) and was adequate for the study of tropical scale interactions ranging from one to 10,000 kilometers. Seventy nations participated in the experiment providing resources including 39 research ships, 13 highly instrumented aircraft, several satellites, numerous ground stations, and some 4,000 scientists and technicians. The deployment of observing platforms was configured to correspond to scales of meteorological phenomena in the tropics (Table 1). The experiment was designed to explore the role of the tropics in the general circulation of the atmosphere as part of the overall GARP objectives. This involves describing the basic state of the atmosphere on scales corresponding to meteorological phenomena such that investigations of the interaction of the different scales may be carried out. Parameterization schemes for moist convection, boundary layer processes and the large scale effects of radiation may then be developed. Subsequently, improved numerical models of the global circulation should be forthcoming.

The goal of the research reported in this paper is to specify the output information and accuracy required of objective cloud field determinations, such that the GATE Radiation Subprogram objectives may be fulfilled. A primary objective of the RSP is to determine the vertical profiles of radiation fluxes and of radiative temperature change at the time and space resolution of the A/B, B and C-scales. The importance

---

* Global Atmospheric Research Program

1
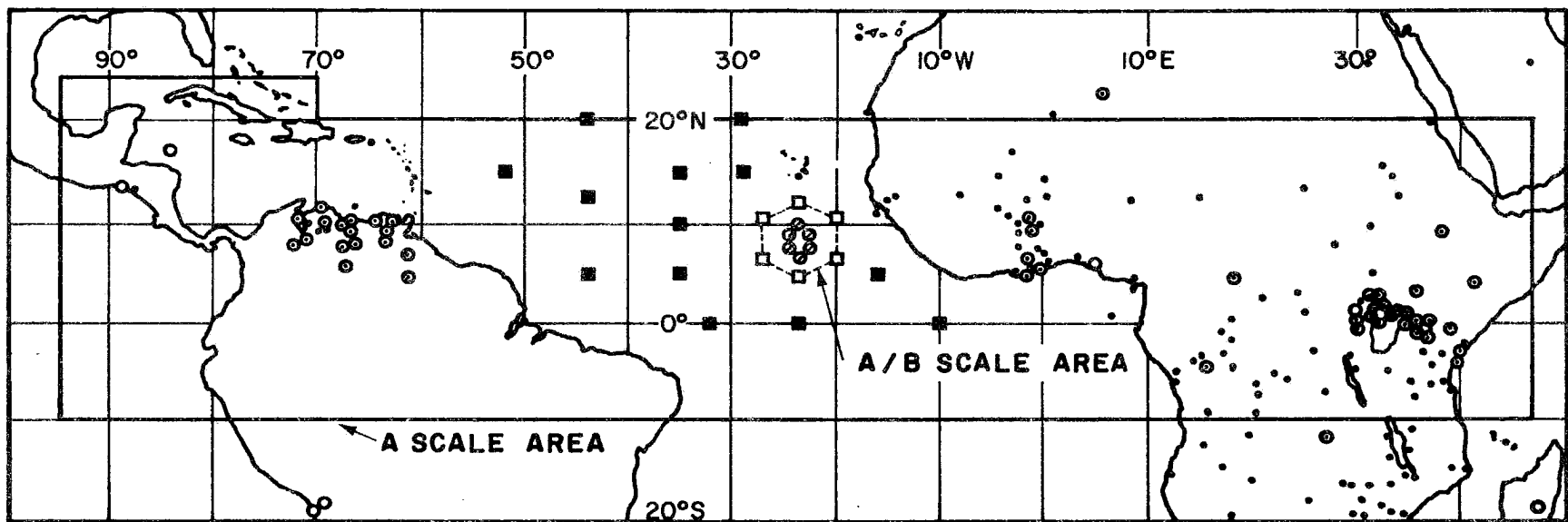
Figure 1. GATE A, A/B, and B-scale areas and the surface radiation observing network.

● Weather observation stations reporting total radiation measurements, solar radiation measurements, sky radiation measurements or radiation measurements in general; points plotted according to WMO Publication No. 9.

⊘ B-scale ship positions

□ A/B-scale ship positions

○ Stations which global solar radiation measurements are published by the Main Geophysical Observatory in Leningrad.

■ A-scale ship positions

Ship positions are valid for Phase I. Further information is available in ISMG, 1975.
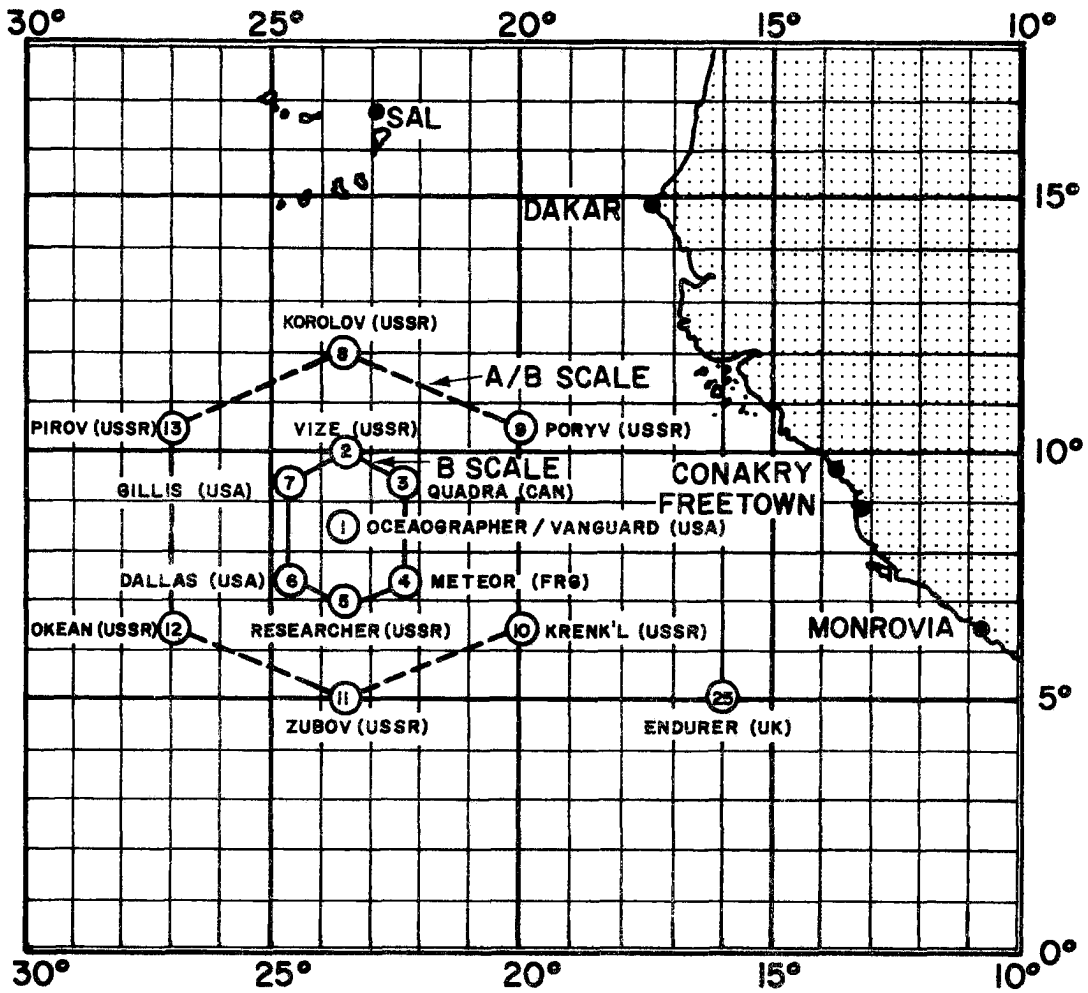
Figure 2. GATE A/B, and B-scale ship positions for Phase I.
Numbers refer to ship locations as given in the
Ship Operation Plan, GATE Report No. 10.

Table 1. Scales of Tropical Disturbances.

Scale	From (km)	To (km)	Name
A	10^3	10^4	Wave scale
B	10^2	10^3	Cloud-cluster scale
C	10	10^2	Mesoscale
D	1	10	Cumulus scale

of radiative processes in the development of tropical disturbances such as tropical waves and cloud clusters is well documented in the literature. Reed and Recker (1971) have reported that the net radiative temperature change in a tropical wave disturbance is of the same order of magnitude as the total diabatic heating. Albrecht and Cox (1975) have demonstrated the sensitivity of the vertical motion fields associated with tropical waves to the phase difference of the convective and radiative heating. The importance of net radiative temperature change for the energetics of cloud clusters has been clearly pointed out by the investigations of Yanai, et al (1973), Nitta and Esbensen (1973), and Nitta (1975). Yanai, et al (1973) have shown that the contribution of the radiative heating to the vertical flux of total heat (a measure of activity of cumulus convection) is of the same order of magnitude as all other terms. Further evidence for the importance of radiative processes in the development of tropical disturbances has been pointed out in papers by Gray (1972), Gille and Krishnamurti (1972), and Pelissier (1972). The highly heterogeneous cloud fields of the tropics force a highly variable contribution of radiation to the energetics. Thus, the determination of the spatial and temporal distribution of radiative fluxes and heating is necessary for an adequate description of the basic state of the atmosphere on the various scales.

The RSP has stated the desired accuracy of radiative heating rate determinations as $\pm 0.2°C \cdot day^{-1}$ for a 6 to 12 hour period over 200 mb thick atmospheric layers. This implies that the net fluxes be known to a relative accuracy of ± 2.4 W$\cdot$m^{-2} per 200 mb. It has been estimated (Kraus, et al., 1973) that the number of direct observations of radiative fluxes was only 3% of those needed to fulfill the resolution

requirements of the RSP. Thus, analysis techniques are needed to generate the required fields of radiative fluxes and temperature change from the direct observations and other pertinent meteorological data. Various methods have been proposed for this task (Vonder Haar, et al., 1974). These are: (1) a computation from state parameters incorporating the direct application of the radiative transfer equation, utilizing laboratory and theoretically derived coefficients, to the observed distributions of water vapor, carbon dioxide, ozone, aerosols, and clouds within a volume at a given time; (2) a semi-empirical method based upon an application of the radiative transfer equation, utilizing in-situ measurements of atmospheric transmissivity in four spectral intervals representative of the contributions of water vapor, carbon dioxide, clouds and the earth's surface, to the observed distributions of those parameters; (3) a compositing technique where mean vertical profiles of radiative divergence, constructed from the statistics of direct in-situ observations for various conditions, are area-weighted according to the observed structure at a given time. A fundamental input quantity necessary for the successful application of any of these techniques is a description of the three dimensional cloud fields present. That is, the spacial and temporal distribution of clouds in the GATE area is absolutely required for the description of the radiative energy component.

In this study, the various methods proposed to solve for the fields of radiative temperature change are reviewed with respect to the resolution and accuracy requirements of the RSP, the input data required, the overall feasibility and the implications for an objective cloud field determination. The sensitivity of the radiative heating rates to uncertainties in the specification of the cloud fields is determined.

Specifically, the impact of uncertainties in the vertical location, areal coverage, and radiative properties of clouds on the radiative heating rates is evaluated. In light of the Radiation Subprogram resolution and accuracy requirements, a tolerable range of uncertainty of the cloud field description is specified. Objective cloud field determinations must be constrained to meet these criteria if the RSP objectives are to be met.

The sensitivity of the fields of radiative divergence to uncertainties in the vertical moisture and temperature structure is evaluated. The effects of aerosols are also discussed. In addition, the sensitivity of the radiative fluxes at the surface to the specification of the temperature, moisture and cloud fields is determined.

II. THE REQUIREMENTS OF A RADIATIVE DIVERGENCE DETERMINATION

The resolution and specific output formulation of an objective cloud field determination scheme are dependent upon the intended application. This work is directed toward utilizing cloud field information as an input for a determination of radiative fluxes and radiative temperature change. The complexity and ultimate feasibility of such a scheme are largely determined by the requirements of the method of incorporating the cloud fields into a radiative divergence determination. In turn, the radiative divergence determination is required to meet an accuracy requirement of $\pm0.2°C\cdot day^{-1}$ for a 200 mb thick layer. The radiative temperature change of a volume of the atmosphere is caused by the divergence of net radiation in that volume. Assuming horizontal homogeneous stratification and employing the hydrostatic assumption, the relationship between net flux divergence and radiative temperature change for an atmospheric layer is given by:

$$Q_R \equiv \left(\frac{\partial T}{\partial t} \right)_{Rad.} = \frac{-g}{c_p} \frac{\Delta H_{NET}}{\Delta p} \qquad (2.1)$$

where ΔH_{NET} is the divergence of net radiative flux in the pressure layer Δp, g is the acceleration due to gravity, c_p is the specific heat of dry air at constant pressure, T is temperature, and t is time. The radiative heating rate, Q_R, may be partitioned further into a short wave or solar component ($\lambda=0.3~\mu m \rightarrow 3.0~\mu m$) and a long wave or infrared component ($\lambda=3.0~\mu m \rightarrow 55~\mu m$). Thus,

$$Q_R = Q_{IR} + Q_{SW} . \qquad (2.2)$$

These definitions apply for all subsequent discussions unless otherwise noted.

Effectively, the required precision of relative flux determinations in the vertical is fixed by the accuracy requirements of the heating rate. This relationship has been noted by Kraus, et al, (1973). The accuracy of radiative heating rates deduced from observed radiative fluxes as a function of the precision of the flux measurements for various layer pressure thicknesses is shown in Fig. 3. To specify radiative heating rates to a vertical resolution exceeding Δp = 200 mb requires the relative net flux be specified to a precision greater than ± 2.4 $W \cdot m^{-2}$ at each level. To observationally verify determinations to this precision is state of the art. Therefore, the accuracy requirements can be meaningfully maintained for a vertical resolution not exceeding $\Delta p \simeq$ 200 mb. That is, a vertical resolution of $\Delta p \sim$ 200 mb is the desired output formulation of a radiative divergence determination. This is not to imply that additional partitioning based upon theoretical reasoning, empirical evidence, or computations is not possible. Such partitioning, while not directly verifiable, would have great utility for investigations of boundary layer or outflow layer interactions. However, additional partitioning must be done subsequent to and constrained to agree with the values specified at the coarser vertical resolution. This would insure the highest level of confidence in the radiative fields determined. It must also be noted here that to generate a useful product, the radiative heating rates need to be specified in a standard format. This study will consider a vertical partitioning of layers as:

$$
\begin{aligned}
\text{Layer 1} &\rightarrow p = \;\; .1 \rightarrow 200 \text{ mb} \\
\text{Layer 2} &\rightarrow p = 200 \rightarrow 400 \text{ mb} \\
\text{Layer 3} &\rightarrow p = 400 \rightarrow 600 \text{ mb} \\
\text{Layer 4} &\rightarrow p = 600 \rightarrow 800 \text{ mb} \\
\text{Layer 5} &\rightarrow p = 800 \rightarrow \text{surface .}
\end{aligned}
\tag{2.3}
$$
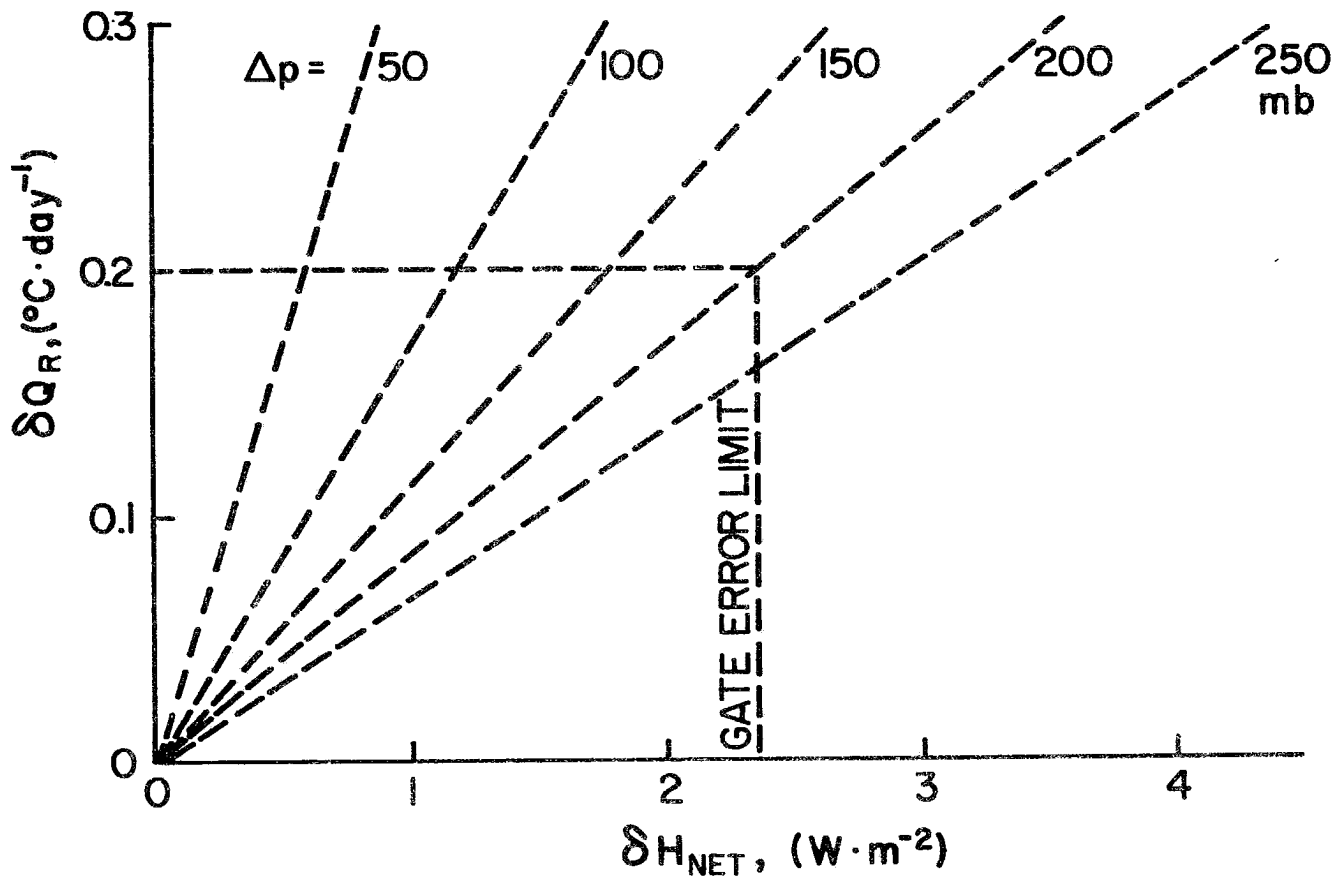
Figure 3. Relationship between the error in the individual measurements of the net radiative fluxes, δH_{NET}, and the induced error in radiative divergence, δQ_R, for different layer thicknesses, Δp. The RSP proposed accuracy requirement of $\delta Q_R = \pm 0.2°C \cdot day^{-1}$ for a 200 mb thick layer and the corresponding limiting allowable error in the individual net flux measurements of $\delta H_{NET} = 2.4 \ W \cdot m^{-2}$ is noted. (after Kraus, et al, 1973)

The area enclosed by the B-scale array is $\sim 7.2 \times 10^4$ km^2.
When considering the horizontal resolution required for the radiative
divergence determination, it must be noted that the desired output
products for studies of the type reported by Yanai, et al (1973) are
values averaged over areas. That is, a profile of radiative temperature
change at a particular grid point is not useful unless it is representative
of the entire grid area corresponding to that point. Betts (1975) has
stated that for A/B and B-scale studies, area averaged values of the
radiative divergence would be necessary on a scale of 0.5° latitude by
0.5° longitude, $\sim 3 \times 10^3$ km^2. The grid adopted for this study is that
shown in Fig. 4. The dashed lines partition the area into grid boxes
for which the radiative divergence must be specified. C-scale studies
will require a horizontal resolution, in the sense noted above, of
$\sim 10^2$ km^2.

The temporal resolution desired, as stated by the Radiation Subprogram,
is six to twelve hours. However, the lifetimes of convective systems
with scales ranging from squall lines to cloud clusters in the tropical
East Atlantic during the GATE have been found to be relatively short.
Analysis of radiometric data obtained from the SMS geosynchronous
satellite during the GATE, Martin (1975), suggests that over 50% of the
convective systems in the tropical east Atlantic, excluding those which
merged with or separated from other systems, exhibited lifetimes of less
than 24 hours. Only 15% persisted for more than 48 hours. Within
these systems, diurnal and semi-diurnal modes of convective activity
have also been found in the radar data taken by ship Quadra during
Phases I and II of the GATE (Marks, 1975). The lifetimes of individual
cells are much less than the system as a whole. Thus, to resolve changes
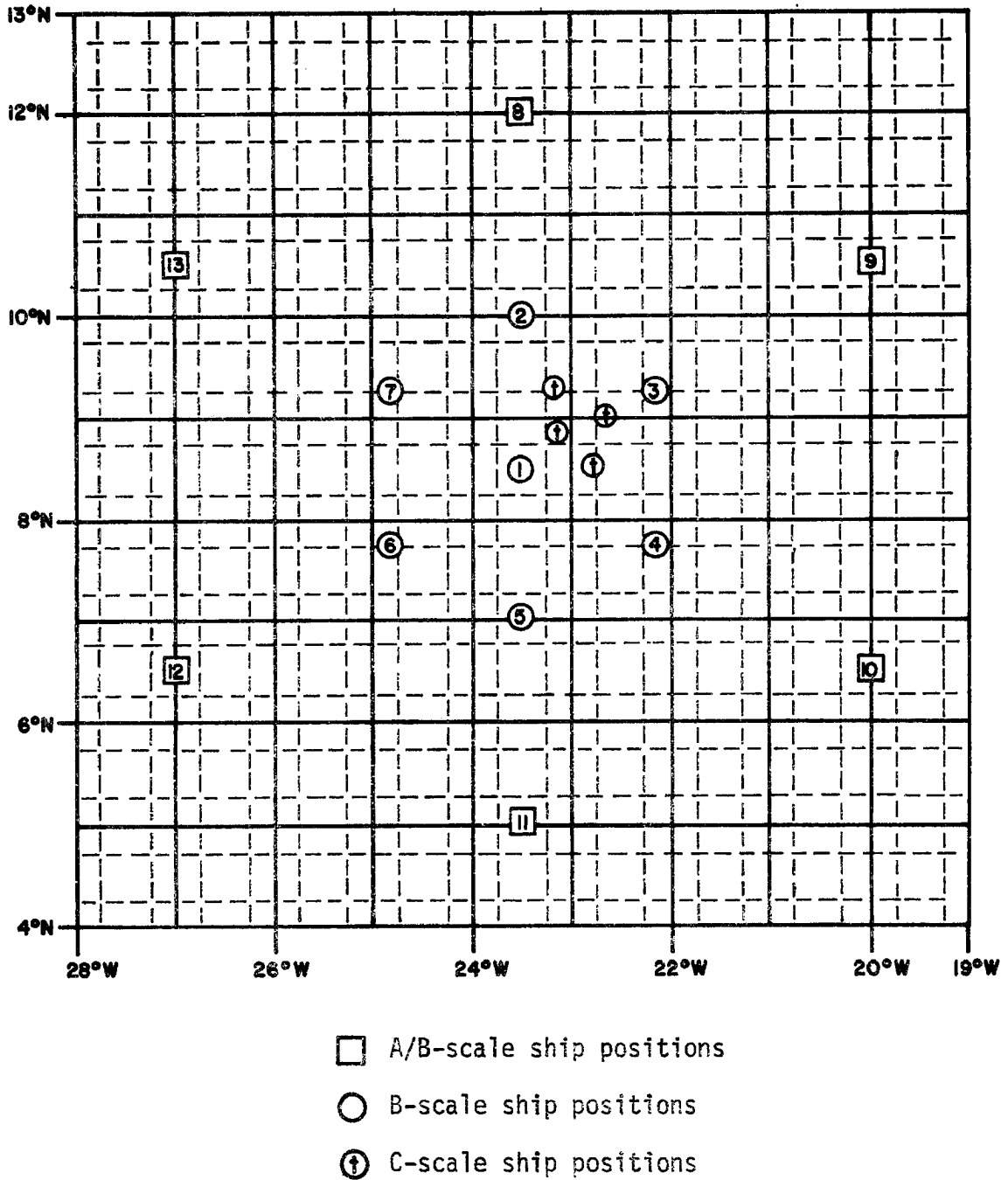
Figure 4. Proposed grid for GATE A/B and B-scale radiation analysis. Values of Q_R must be specified for each of the dashed grid boxes for a vertical resolution of 200 mb every 1-3 hours. The GATE A/B, B, and C-scale ship arrays are drawn for Phase III.

in the radiative fields associated with the growth and dissipation stages of B and C-scale convective systems, a resolution of one to three hours is desirable. To account for the contribution of solar fluxes to the radiative temperature change requires an integration in time to account for the changing solar geometry. A resolution of one to three hours would be appropriate to adequately resolve this variance.

III. METHODS FOR DETERMINING THE RADIATIVE DIVERGENCE

The determination of radiative fluxes and the radiative divergence in the atmosphere may be accomplished in several ways. Rodgers (1972) has reviewed the general aspects of the various types of schemes with special emphasis on their application to numerical modeling of atmospheric processes. Three general types of methods are most applicable to meeting the Radiation Subprogram objectives for the GATE. These are: computations from state parameters, semi-empirical methods and compositing techniques.

A. Computation from State Parameters

The computation of radiative divergence in the troposphere from state parameters requires the integration of the radiative transfer equation. Methods of varying complexity exist for this integration. Kondratyev (1972) has summarized many of the simplified fast methods employed in dynamical and climatological models. The accuracy and resolution of these fast methods are too coarse for the purposes of the Radiation Subprogram. The improvement of this type of model should result from the more detailed analysis envisioned by the RSP. A more complex and accurate procedure is to use the classical radiative transfer equation for horizontally homogeneous layers. This method utilizes frequency integrated transmission/emission functions over small spectral intervals (i.e., a band model). A typical band model is detailed in section IV.A. For the computation, the vertical distributions of the following atmospheric quantities are needed:

clouds	aerosols
temperature	ozone
water vapor	carbon dioxide

together with the surface pressure. The transmission/emission functions for atmospheric parameters are based on laboratory and theoretical determinations. The effect of molecular scattering is also taken into account.

The various formulations of band models which are currently in use, often yield somewhat different results. This disagreement arises through the use of different numerical methods of integration and different emissivity data. For example, Stone and Manabe (1968) have compared the technique given by Manabe and Strickler (1964) and Manabe and Wetherald (1967) to that reported by Rodgers and Walshaw (1966) for the infrared portion of the spectrum. They showed disagreement in the radiative cooling exceeding the GATE RSP desired accuracy for the clear sky case. No account was made for aerosol contributions.

Roach (1961), Kondratyev and Nikolsky (1968), Cox (1969), Kuhn and Stearns (1971), Kondratyev (1971), Cox, et al (1972), and Paltridge (1973) have shown that numerical computations often do not agree with observations, even for observed cloudless conditions. This disagreement is often ascribed to the presence of aerosols. Bignell (1970), Cox (1973) and Grassl (1974) have attempted to account for this effect in the continuum portion of the spectrum. They have postulated a water vapor pressure broadening effect to account for the discrepancy in the lower troposphere. Cox (1969) has stated that the presence of very thin cirrus clouds, which are not visible to a ground observer, may be the cause of the disagreement at upper levels.

At present, the typical band models take no account of the radiative effects due to aerosols such as dust and oceanic haze. More lengthy and complex methods, which still employ simplifying assumptions,

may be used (e.g. Yamamoto, et al., 1974; and Herman and Browning, 1975). However, their applicability to the GATE region has yet to be verified. In section III.E., the potential magnitude of the aerosol influence on the radiative heating is discussed.

From the above discussions, it is evident that, even for cloud free conditions, extensive verification of the accuracy of band models will be necessary.

For cloudy conditions, the radiative transfer about the clouds is handled by using bulk coefficients to describe the radiative characteristics of clouds. That is, the shortwave absorptivity and reflectivity and the long wave effective emissivity of the cloud are assumed to be independent of wavelength. The sensitivity of a typical calculation to the bulk properties prescribed can be quite large. This is particularly true for high clouds as is demonstrated in Chapter IV.

The natural variability of the bulk radiative properties of clouds has been observed to be large. Cox (1976) has reported large variations in the observed infrared properties of tropical clouds. The bulk solar properties, which are dependent upon the microphysical structure of the clouds, much as the infrared properties are, may also vary substantially. The variation of bulk solar properties with changing solar zenith angle has also been shown to be large (Kondratyev, 1969). Thus, the emissivity, absorptivity, reflectivity, and corresponding solar geometry for a particular cloud feature must also be regarded as necessary input data to a calculation from state parameters. The cloud is assumed to be of semi-infinite horizontal extent for the band computation. McKee and Cox (1974) have shown by more exact methods that for clouds of finite

horizontal extent, errors as great as 25% may be anticipated in the vertical fluxes of solar radiation when using this assumption.

An additional matter of concern with the band models is the computational feasibility. An integration of a typical model (described in section IV.A.) uses approximately 30 seconds of computer time on a CDC-6400 at 70k core for a single geographic point. To generate area average values of radiative divergence to the desired accuracy under the highly heterogeneous cloud conditions of GATE will require integrations at a large number of points for statistical significance. To resolve areas of cumulus activity, a horizontal resolution of $\Delta x = \Delta y \leq 10$ km may be necessary. The input parameters, especially the water vapor mixing ratio, aerosol concentration, clouds and the bulk radiative cloud properties will need to be specified at this resolution. This implies $\sim 7 \times 10^2$ integrations at a specific time to resolve the B-scale area. This procedure would be repeated every 1-3 hours for each day of the GATE. The amount of computer time required is prohibitive. Thus, some area averaging of input parameters is necessary to reduce the amount of computations. The accuracy of this type of scheme under this constraint has not been verified.

Detailed modelling of the radiative transfer is possible utilizing more complex methods. Kattawar, et al (1973) and McKee, et al (1974) have developed methods where photon paths are followed individually by random procedures. These models are too time consuming for operational use. Their value is to aid in the development of adequate parameterizations for the radiative effect of cloud fields in terms of bulk coefficients.

B. The Semi-Empirical Method

The semi-empirical method is applicable to the calculation of the infrared radiative divergence profiles. Smith and Shen (1975) have reported that, based upon theoretical calculations using the model of Rodgers and Walshaw (1966), the total spectrally integrated infrared radiative divergence may be accurately approximated from a linear combination of the radiative divergence profiles for four optimum spectral intervals. That is

$$\frac{\partial T}{\partial t}(p)_{TOTAL} = \sum_{i=1}^{4} a_i \frac{\partial T}{\partial t}(p, \Delta\lambda_i) \qquad (3.1)$$

where a_i is an empirically determined weighting coefficient and

$$
\begin{aligned}
\Delta\lambda_1 &= 6.1 - 6.5 \ \mu m \\
\Delta\lambda_2 &= 10.9 - 11.4 \ \mu m \\
\Delta\lambda_3 &= 12.5 - 13.9 \ \mu m \\
\Delta\lambda_4 &= 16.7 - 26.3 \ \mu m.
\end{aligned}
\qquad (3.2)
$$

The longwave divergences in the four spectral intervals are representative samples of the total tropospheric radiative divergence due to water vapor, carbon dioxide, clouds and the earth's surface. During the GATE, measurements of the upward and downward longwave fluxes of radiation integrated over the entire longwave spectrum and in these optimum spectral intervals were taken from the Convair 990 aircraft. The integrated radiative transfer equation was used to determine the radiative divergence for the entire spectrum and each of the spectral intervals. This enabled the specification of the empirical weighting factors, a_i, through a regression analysis. The computation of the total infrared radiative divergence profile may then be accomplished through the calculation of the radiative divergence for the four spectral

intervals, provided the atmospheric transmission functions for these intervals are known as a function of the vertical distributions of temperature, moisture, and cloud amount. The CV-990 aircraft experiment observed the radiance in the required spectral intervals, from the atmosphere and clouds, at viewing angles from zenith to nadir. Vertical profile soundings were conducted through clear air and through clouds. This enables the flux transmissivity of the atmosphere and clouds to be derived using established techniques (Smith, et al., 1972).

This method is more efficient than the band models. It has the advantage of being based on observed relationships and flux transmissivities obtained in-situ. Account is made for the atmospheric parameters most responsible for observed variations in the distribution of radiative temperature change. The absolute accuracy of the method should be tested with independent data. The method must account for the varying contribution of aerosols. The severity of this constraint may be seen in section III.E. Also, the transmissivity data related to clouds must be sufficient to account for all types of clouds that contributed significantly to the distribution of radiative fields. An additional scheme would be needed to account for the radiative processes in the short wave portion of the spectrum. To achieve computation feasibility, area averaging of the input parameters will be necessary.

C. The Compositing Technique

The compositing technique relies on observations of radiative flux divergence and concurrent atmospheric parameters. This method has been discussed by Cox (1971b, 1972). During the GATE, a large amount of observations of the radiative fluxes were taken from ship, satellite,

aircraft and radiometersonde platforms (Cox and Kraus, 1975). The radiometersonde instrument RMS error has been given by Johnson and Kuhn (1966) as less than $\pm 0.25°C$ per day. The broadband, hemispheric pyranometer and pyrgeometer instruments flown on aircraft have a precision of ± 3.4 $W \cdot m^{-2}$ (Albrecht, et al., 1974; and Cox, 1975). This implies radiative divergence may be determined to $\pm 0.29°C$ per day for a 200 mb thick layer of the atmosphere. Therefore, this basic data approaches the desired accuracy. The aircraft flight configurations included a stacked mode and a profiling mode. Thus, flux divergence profiles for heterogeneous cloud fields and various vertical cloud structures have been obtained. Mean profiles of radiative divergence corresponding to particular types of cloud configurations can be constructed. The basis of the compositing method is that the flux divergence profile for a particular vertical distribution of atmospheric parameters is representative for areas where such a structure is observed. Cox (1968) has concluded that the horizontal variations of temperature and moisture in the tropics are not statistically related to the flux divergence profiles. This conclusion was based on exami-nation of several hundred radiationsonde ascents. The implication is that clouds are the primary modulators of radiative divergence in the tropics. That this conclusion is justified may be clearly seen from Fig. 5. Figure 5 is a comparison of the root mean square deviation of computations of the infrared cooling made from BOMEX rawinsonde temper-ature and moisture profiles collected during the period 31 May to 9 June, 1969 and radiationsonde observations of infrared cooling during the same period. The RMS deviation for the calculated case, which contains no clouds, is as much as a factor of five less than the RMS deviation for
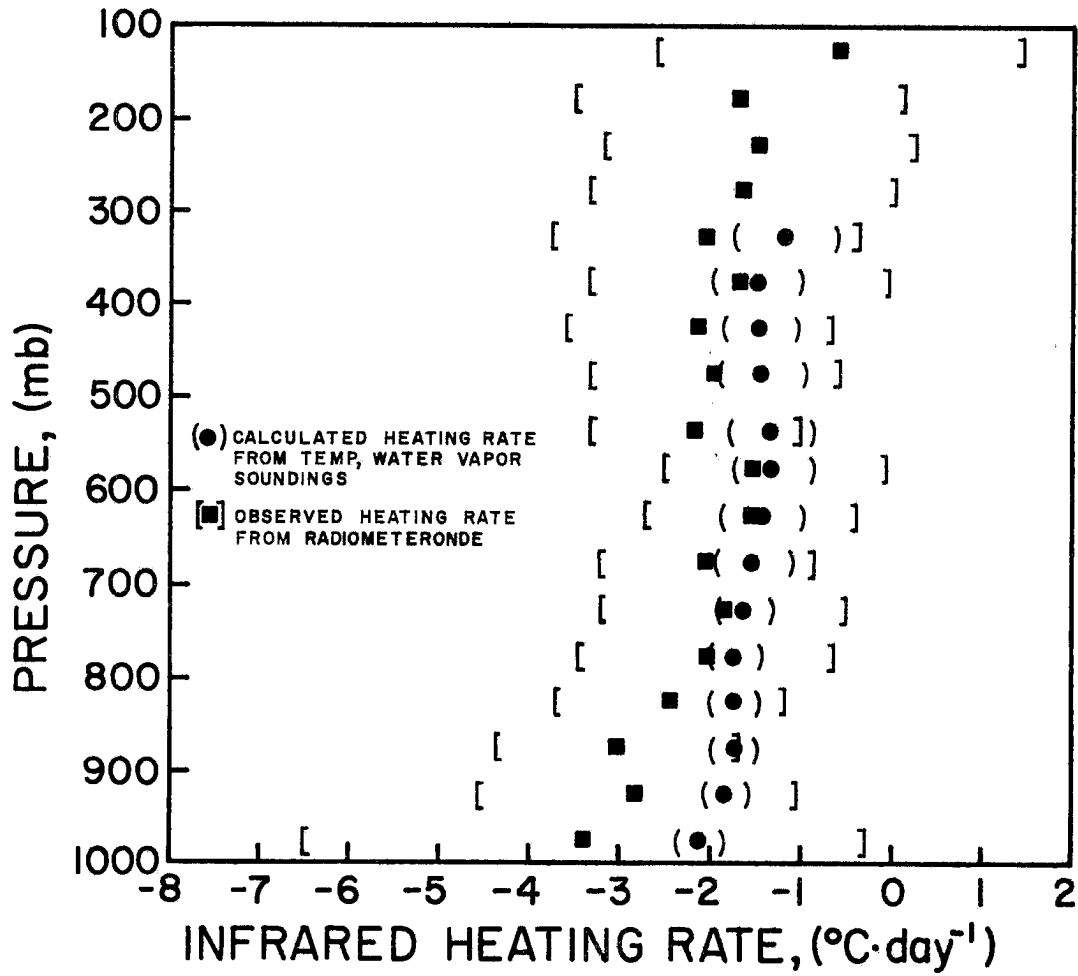
Figure 5. Comparison of the mean and RMS deviations of
observed and calculated infrared heating rates
for the BOMEX period 30 May - 9 June, 1969,
(from Cox, 1968).

the observed cases. Thus, clouds are the most important factor
influencing horizontal gradients of radiative heating in the tropical
atmosphere.

Therefore, with a description of the cloud fields present at a
particular time in an atmospheric volume, the mean radiative divergence
profiles corresponding to the types of cloud fields present may be area
weighted to yield a representative profile for that volume. Since mean
profiles for each typical cloud configuration are to be used, the larger
the volume, the more representative the results. Thus, the resolution
is limited by the degree of confidence desired. It must be verified that
individual profiles have been obtained for all significant cloud config-
urations in the GATE area. The magnitude of potential deviations from
the mean for a volume at a particular time as a function of volume must
be ascertained. It may also be necessary to stratify the typical
profiles according to the variations of other atmospheric parameters,
especially water vapor and aerosols, to increase the accuracy to
acceptable levels. Profiles must also be constructed to account for
effects due to varying solar zenith angle. The advantages of this
method are: it is based on the observed fields of flux divergence;
primarily only one independent variable, the cloud structure, is needed;
and the feasibility in terms of computer and data resources is good.

D. Implications of the Methods for an Objective Cloud Field Determination

All methods proposed thus far for the determination of the radiative
divergence fields for GATE require the specification of the cloud fields
present as a primary input. To achieve computational feasibility for
the computation from state parameters or the semi-empirical method,

statistics as to the areal extent of individual vertical cloud structures within an otherwise homogeneous volume will be required. The compositing technique has the same requirement. Thus, it is the statistics of the three dimensional cloud fields within a volume that is required and not the vertical structure at a few geographic points. Additional information as to the bulk radiative properties of particular cloud features is required for the computation from state parameters and is desirable for both the semi-empirical and compositing technique.

E. The Influence of Atmospheric Aerosols

Yamamoto, et al (1974) have shown that the extinction of solar radiation in the visible wavelengths due to aerosol absorption is significant. Reynolds, et al (1975) have observed extinction of solar radiation, which they attributed to aerosols, to be of the same magnitude as gaseous extinction during BOMEX.* Prospero and Carlson (1972) document the presence of aerosols of African origin in the BOMEX region. Kondratyev, et al (1976) have shown from observations that the radiative effects of dust aerosols of Saharan origin are large in the GATE region. The dust "cloud" may reflect greater than 5% of the downward solar flux. It may also absorb up to 15%. In addition, the angular distribution of the downward solar flux becomes much more diffuse downstream from the dust "cloud". This tends to enhance the reflectivity of the ocean surface. The effect in the infrared is to partially compensate the solar warming anomaly due to the dust. Kondratyev, et al (op. cit.) have stated that the radiative effect of the low level oceanic haze layer is relatively neutral. Thus, the dust aerosols of Saharan origin

---

* Barbados Oceanographic and Meteorological Experiment.

are the primary radiatively active aerosols in the GATE area. They have also found that the horizontal boundaries of the dust "clouds" are distinct and may be deduced from satellite radiometric data. The dust "cloud" is normally limited in vertical extent to the 600 mb to 900 mb layer. Thus, a dust "cloud" may typically induce an anomaly of $+4°C \cdot day^{-1}$ to $+5°C \cdot day^{-1}$ in the instantaneous heating rate of this layer. It is noted that exact computations of the radiative effect of aerosols are lengthy and complex. It is also questionable whether or not sufficient data on the composition, size distribution, and concentration of aerosols have been obtained to enable such calculations to be performed at the desired space and time resolution. Therefore, an empirical method of accounting for the effect of a dust layer is desireable in a radiative divergence determination. The potential magnitude of the heating anomaly implies that at least ten distinct stratifications of aerosol influence must be resolved in order to achieve the RSP accuracy goals. However, the data of Kondratyev, et al (op. cit.) suggests that, when there is a Saharan dust outbreak into the GATE area, the radiative effect is somewhat uniform. Thus, only a few stratifications of aerosol influence may need to be resolved once the presence of the dust "cloud" is established.

IV. SENSITIVITY OF THE RADIATIVE DIVERGENCE TO THE CLOUD FIELDS

An automated, efficient objective cloud field determination scheme is desired. Since it is doubtful that any scheme will be able to describe the cloud fields present during the GATE in their fullest detail, the sensitivity of the radiative temperature change to errors in the cloud field description must be evaluated. In this section, the sensitivity of the radiative fields to inaccuracies in the bulk radiative properties of clouds, cloud height, vertical extent and areal cloud cover is investigated. The situation of disturbed conditions with a multi-layered cloud configuration is also treated. The analyses presented in this chapter were performed in an independent fashion. In this regard, it must be noted that the sensitivities derived for the bulk radiative properties and cloud height, which are presented, represent the maximum limiting constraint. This arises because these analyses implicitly assume the areal cloud cover is 100% and, thus, the perturbation of the radiative field is maximized when compared to the case of broken or scattered cloudiness. The situation of simultaneous uncertainty in all cloud parameters is treated in Chapter V.

A. The Radiative Transfer Models

Broadband radiative transfer models were used to simulate the radiative transfer in the short wave (0.3 μm - 3.0 μm) and the long wave (3.0 μm - 55 μm) spectral intervals. The assumption of horizontal homogeneity of atmospheric parameters was made for both transfer models. Clouds were assumed to have infinite horizontal extent and uniform bulk radiative properties.

A simplified isothermal, broadband flux emissivity transfer program with a vapor pressure broadened continuum absorption reported by Cox (1973) was used to simulate the terrestrial fluxes. Account was made for the molecular emission of the continuum, rotational and 6.3 μm spectral bands of water vapor; the 15 μm band of carbon dioxide; and the 9.6 μm band of ozone. Compensation was made for the overlap of the rotational band of water vapor and the 15 μm band of carbon dioxide. Flux emissivities used in the calculation are those reported variously by Walshaw (1957), Smith (1969), and Cox (1973).

The transfer of infrared radiation through a cloud layer was modelled in terms of a broadband layer emissivity, Fig. 6. The effective emissivity (Kuhn, 1963; and Cox, 1976) is defined:

$$\epsilon^*(\uparrow) = \frac{H_B(\uparrow) - H_T(\uparrow)}{H_B(\uparrow) - \sigma T_T^4} \qquad \text{for the upward irradiance,} \qquad (4.1)$$

$$\text{and} \quad \epsilon^*(\downarrow) = \frac{H_B(\downarrow) - H_T(\downarrow)}{\sigma T_B^4 - H_T(\downarrow)} \qquad \text{for the downward irradiance.} \qquad (4.2)$$

The quantities $H(\uparrow)$ and $H(\downarrow)$ refer to the upward and downward infrared irradiances, respectively. The subscripts T and B refer to the top and bottom of the cloud layer, respectively. σ is the Stefan-Boltzman constant and T is the temperature. The effective emissivity defined in this manner implicitly includes the effects of emission by gases within the cloud layer and scattering by cloud hydrometers. The differing sources for the upwelling and downwelling irradiance streams imply differing spectral distributions of energy. The interaction of these irradiance streams with clouds is spectrally dependent and thus different upward, $\epsilon^*(\uparrow)$, and downward, $\epsilon^*(\downarrow)$, effective emissivities are

$$\blacktriangledown H_T(\downarrow) \qquad \blacktriangle H_T(\uparrow)=\epsilon^*(\uparrow)\cdot\sigma\, T_T^4+(1-\epsilon^*(\uparrow))\cdot H_B(\uparrow)$$

$$\triangle P_C \qquad\qquad \text{CLOUD}$$

$$\blacktriangledown H_B(\downarrow)=\epsilon^*(\downarrow)\cdot\sigma\, T_B^4+(1-\epsilon^*(\downarrow))\cdot H_T(\downarrow) \qquad \blacktriangle H_B(\uparrow)$$
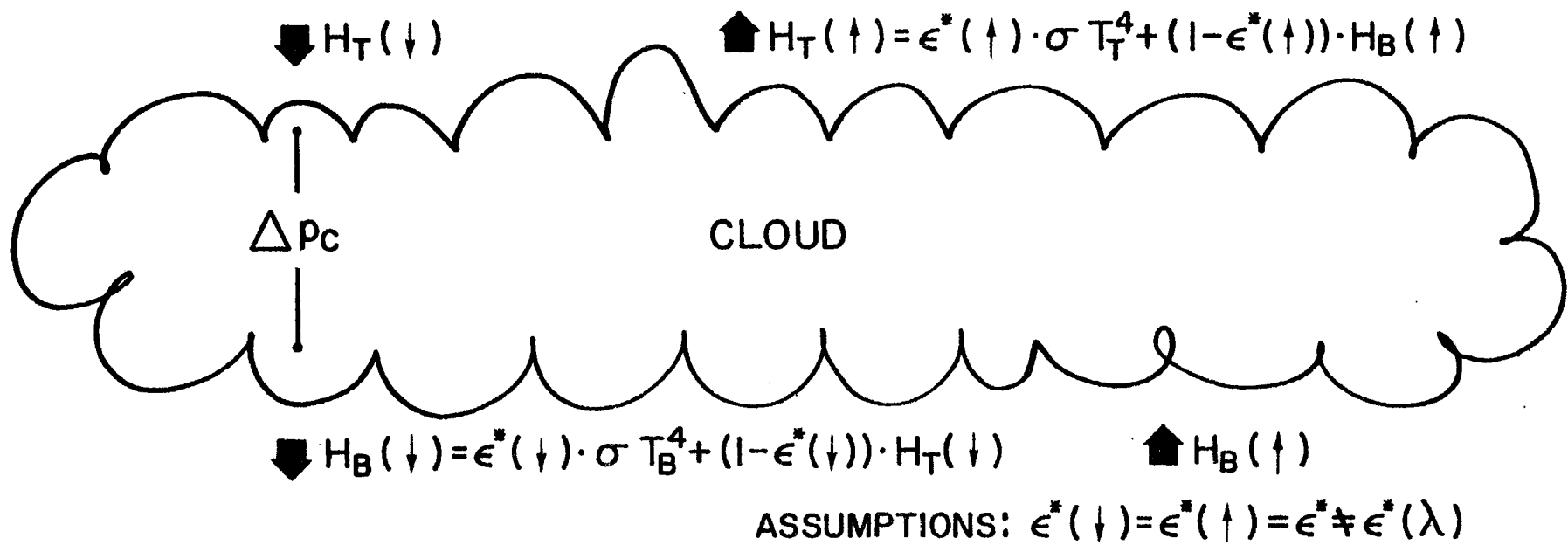
$$\text{ASSUMPTIONS: } \epsilon^*(\downarrow)=\epsilon^*(\uparrow)=\epsilon^* \neq \epsilon^*(\lambda)$$

INFRARED HEATING RATE IN CLOUD LAYER

$$Q_{IR}=\left\{H_T(\downarrow)+H_B(\uparrow)-H_T(\uparrow)-H_B(\downarrow)\right\}\cdot\frac{g}{C_p}\cdot\frac{1}{\Delta P_C}$$

Figure 6. Model of infrared radiative transfer at cloud boundaries.

needed. This has been discussed by Cox (1976). However, it is found that for a sensitivity analysis, the assumption that:

$$\epsilon^*(\uparrow) = \epsilon^*(\downarrow) = \epsilon^* \qquad (4.3)$$

does not adversely affect the results. Errors due to the grey body assumption are not evaluated here.

A simplified broadband flux transmissivity transfer model was used to simulate the short wave radiative transfer. The model treats absorption of solar radiation by water vapor, carbon dioxide, and ozone; scattering by molecules in the free atmosphere; and the absorption, reflection and transmission of solar radiation by cloud layers. The absorption data for the gaseous constituents as a function of absorber amount, are those given by Manabe and Möller (1961). Overlap between absorption bands of the different gases was ignored as was any contribution due to aerosols. The solar geometry is specified uniquely by the day of the year, latitude and time of day. For this study, all computations were carried out for 7°N latitude and Julian Day 225 (i.e. August 13). The solar constant was taken as 1360 $W \cdot m^{-2}$ (≈ 1.95 $ly \cdot min^{-1}$). The instantaneous heating rates, computed at 23 time steps from sunrise to local noon, were multiplied by twice the time increment and summed to yield the total integrated short wave heating through the day. Thus, the results are normalized such that atmospheric parameters, including clouds, are assumed to be constant for the entire day. In this work, the short wave heating rate, Q_{SW}, is the total integrated short wave heating per day unless specifically defined as an instantaneous heating rate. Therefore, whereas the results pertaining to the infrared component may be interpreted as either daily or instantaneous values, the analysis for the short wave component is only directly applicable

to the daily situation. To convert the short wave heating rate, Q_{SW}, as it is used here, to the average instantaneous short wave heating rate for the daylight hours, one must multiply the value of Q_{SW} by 1.96. The factor of 1.96 represents the ratio of the total number of hours in a day to the number of hours of daylight at 7°N on Julian Day 225. In a similar manner, the sensitivities for the short wave component may be converted to the average instantaneous situation during the daylight hours by dividing by 1.96. The sensitivities, modified to represent the daily average instantaneous situation, are the limiting quantities for analysis on a time scale of less than one day. It must be noted that even if the results presented here for the short wave component and also for the combined short wave and long wave analysis are transformed to correspond to the average instantaneous situation, they may only qualitatively represent the true sensitivity of the instantaneous rates at a specific time and solar geometry.

Tests were made to evaluate the effect of surface reflectivity upon the short wave heating rates. Comparing the solar heating in the case of no surface reflectivity and in the case of a surface reflectivity of 0.10, increased heating of less than 0.1 C°day^{-1} resulted in any 200 mb thick atmospheric layer. Therefore, except for the cloud free case, the reflected irradiance from the surface was ignored.

Thin clouds were assumed to be non-diffuse transmitters as in Fleming and Cox (1974). All reflected irradiance was assumed to be diffuse as was that which is transmitted by a thick cloud. The optical thickness of layers of the atmosphere downstream from a cloud was scaled by the diffusivity factor 1.66, formed by a hemispheric integration of optical thickness over a solid angle, as in Goody (1964), for computing

the absorption of reflected and transmitted diffuse irradiance. A schematic diagram of the treatment of solar irradiance, H, at the cloud boundaries is shown in Fig. 7. The transfer of short wave radiation through a cloud layer was modelled in terms of two broadband radiative properties, the cloud reflectivity, ρ_c, and the cloud absorptivity, a_c. The short wave reflectivity and absorptivity are defined as:

$$\rho_c = \frac{H_T(\uparrow)}{H_T(\downarrow)} \qquad (4.4)$$

and

$$a_c = 1 - \rho_c - \{ \frac{H_B(\downarrow)}{H_T(\downarrow)} \} \qquad (4.5)$$

where $H(\uparrow)$ and $H(\downarrow)$ refer to the upward and downward short wave irradiances, respectively. The subscripts T and B refer to the top and base of the cloud layer, respectively. It is noted that the cloud transmissivity, t_c, is defined as:

$$t_c = \frac{H_B(\downarrow)}{H_T(\downarrow)} \qquad (4.6)$$

The cloud reflectivity and absorptivity are assumed to be independent of wavelength. Errors due to this assumption are not evaluated here.

The mixing ratio of carbon dioxide was assumed to be constant with height and equal to $0.4666 \ g \cdot kg^{-1}$. The mixing ratio of ozone was a composite of vertical soundings which have been compiled by the Meteorological Branch, Canadian Department of Transportation, for West Africa for the month of July, Fig. 8. The total NTP depth was 0.273 cm.

The profiles of temperature and water vapor mixing ratio as a function of pressure were those given by Williams and Gray (1973), Fig. 9. This sounding is a composite of 537 rawinsonde soundings

(SUN) $H(\downarrow)_{p=0} = (SOLAR\ CONSTANT) \cdot COS\,\Theta$

$\Theta = SOLAR\ ZENITH\ ANGLE$

$H_T(\downarrow)$

$H_T(\uparrow) = g_c \cdot H_T(\downarrow)$

Δp_c

CLOUD

$H_B(\downarrow) = (1 - g_c - a_c) \cdot H_T(\downarrow)$

$H_B(\uparrow) = H_{RAY}(\uparrow)$

ASSUMPTIONS: $g_c^* \neq g_c(\lambda)$

$a_c^* \neq a_c(\lambda)$
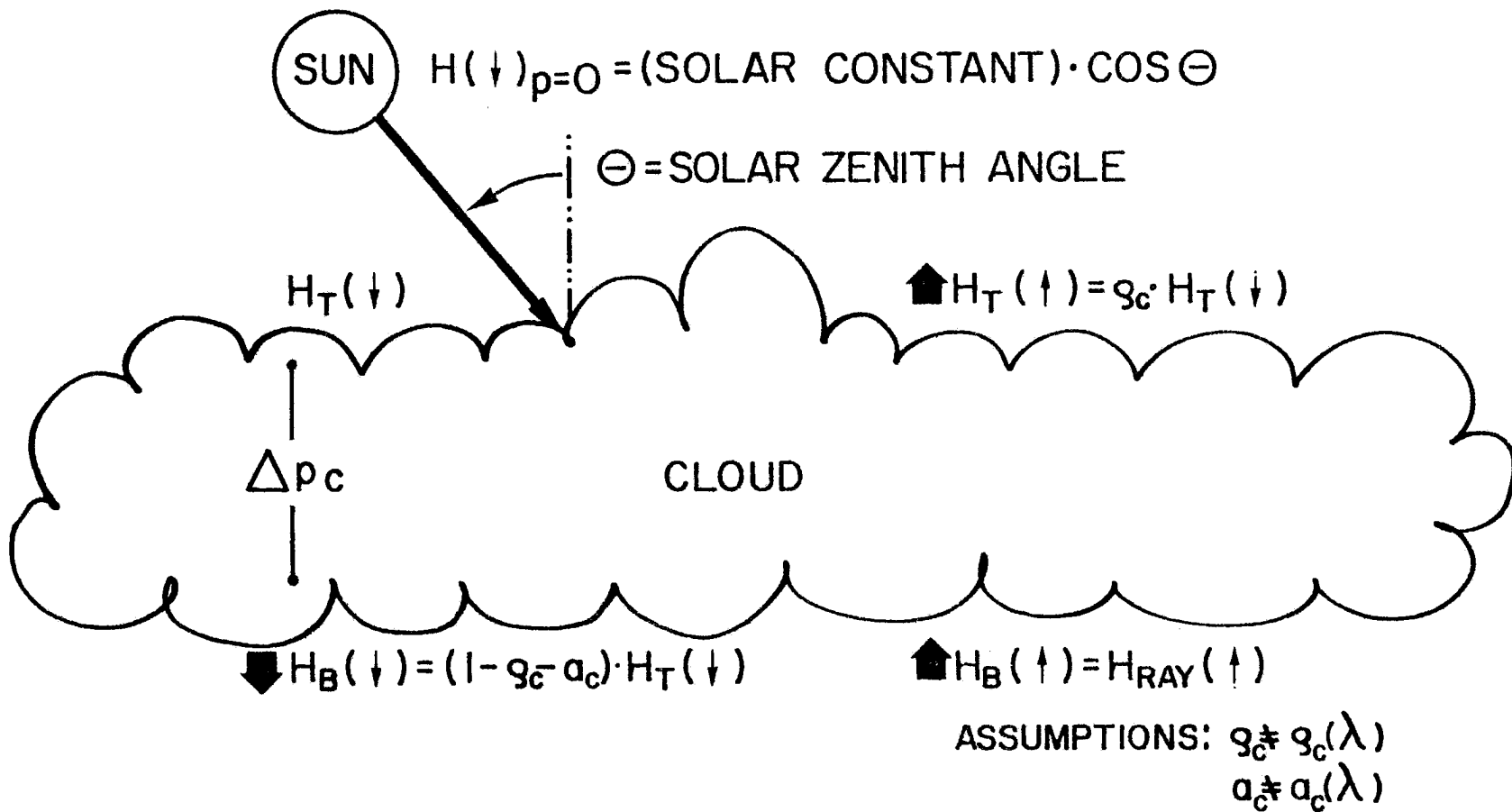
SHORT WAVE HEATING RATE IN CLOUD LAYER

$$Q_{SW} = \left\{ H_T(\downarrow) + H_B(\uparrow) - H_T(\uparrow) - H_B(\downarrow) \right\} \cdot \frac{g}{C_p} \cdot \frac{1}{\Delta p_c}$$

Figure 7. Model of short wave radiative transfer at cloud boundaries.
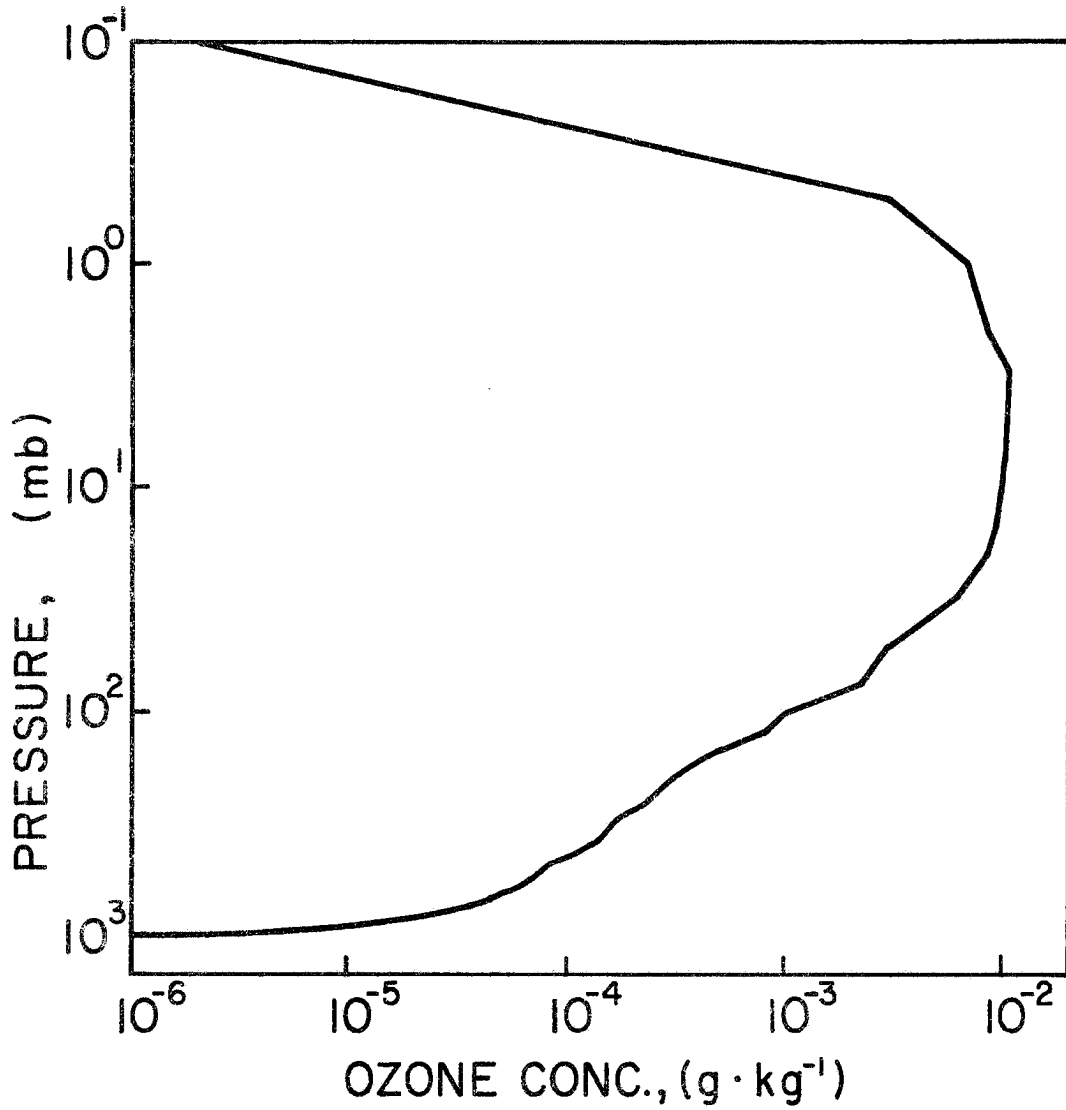
Figure 8. Vertical profile of the ozone mixing ratio used in model study. Data represents an average of individual soundings compiled by the Canadian Department of Transportation for the West Africa region for the month of July.
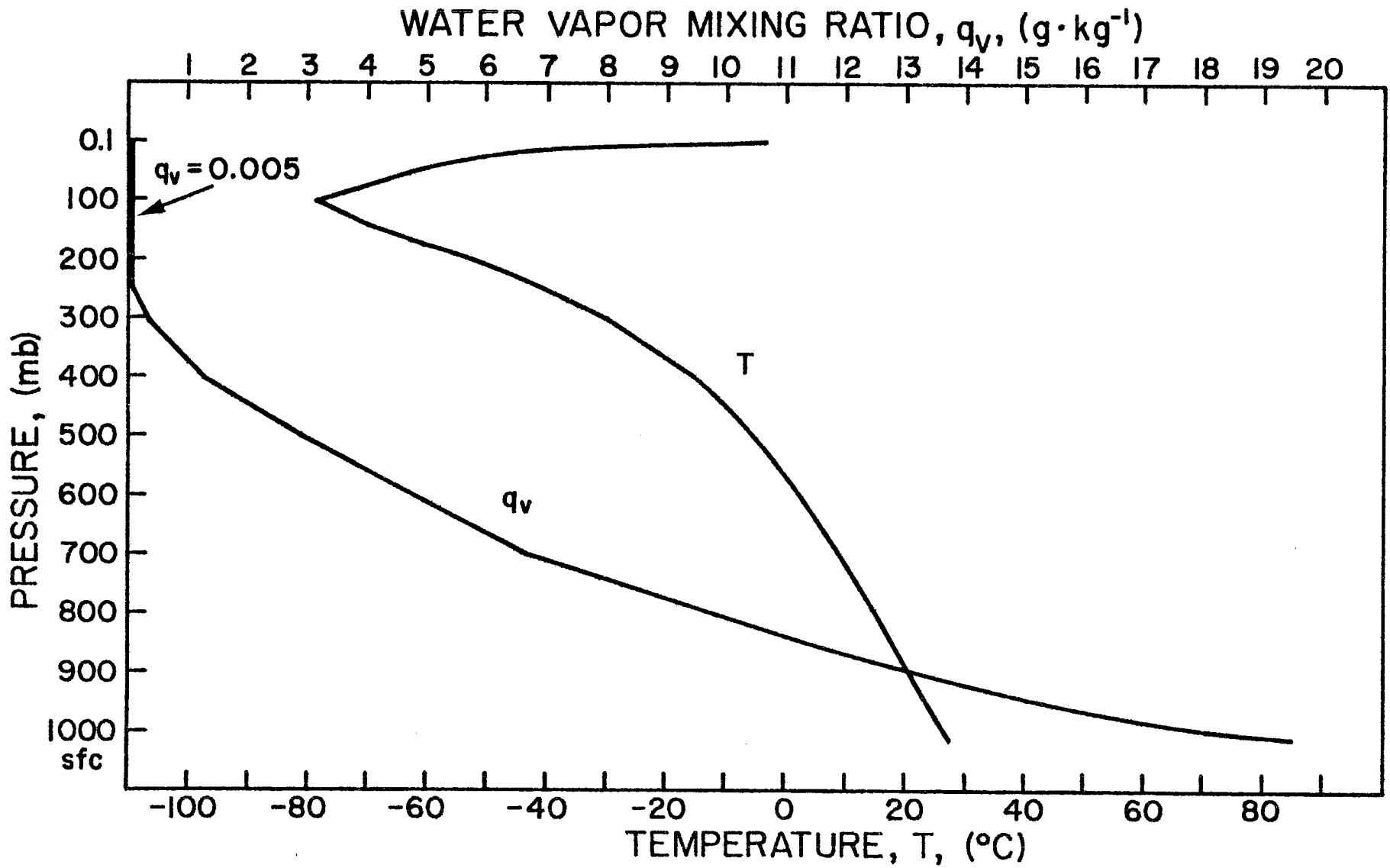
Figure 9. Vertical profile of temperature and water vapor mixing ratio used in model study. (after Williams and Gray, 1973)

representative of conditions in conservative cloud clusters in the western tropical North Pacific. Ruprecht and Gray (1974) have noted that this sounding differs only slightly from a composited mean cluster environment sounding. It is similar to the sounding given by Jordan (1958) for the West Indies "hurricane season". Ruprecht and Gray (1974) have shown that significant deviations from the mean moisture profile occur within a given cluster and for a cluster as a whole. They have reported the mean deviation of water vapor mixing ratio for any level does not exceed ±20%. Tests made with this radiative transfer model yielded the result that to achieve an accuracy of $Q_R = \pm 0.2°C$ per day^{-1}, random errors must not exceed ±0.2 $g \cdot kg^{-1}$ in the mean water vapor mixing ratio for a layer in layers 2, 3, and 4. The allowable random error in the mixing ratio for layers 1 and 5 is approximately ±0.03 and 2.0 $g \cdot kg^{-1}$, respectively. A systematic error in the water vapor mixing ratio of ±0.5 $g \cdot kg^{-1}$ in layers 3, 4, and 5 does not change the Q_R of any layer by more than ±0.2°C·day^{-1}. A systematic error of ±0.2 $g \cdot kg^{-1}$ in layers 2, 3, 4, and 5 does not alter the Q_R of any layer by more than ±0.2°C· day^{-1}. Random or systematic errors in the mean temperature of a layer or layers must be less than ±2.5°C to fulfill the Radiation Subprogram accuracy requirement.

Since the author desires to evaluate the sensitivity of the radiative temperature change to inaccuracies in the cloud field description, the mean sounding was employed. It is felt to be representative of conditions in which tropical clouds are likely to be present. Effects due to variations from the mean sounding upon the sensitivities derived in this work are noted where it is appropriate.

In Fig. 10, the computed long wave, short wave, and total radiative heating rates (Q_{IR}, Q_{SW}, and Q_R, respectively) are given for the mean sounding in clear sky conditions. The surface albedo was 0.04. A plotted point represents the mean heating rate in the corresponding 200 mb thick layer.

B. Sensitivity of the Infrared Component

1. Cloud Emissivity

The most significant radiative cloud property in the infrared spectral interval is the effective broadband infrared emissivity, ε^*. The ε^* of a particular cloud is dependent upon the microphysical structure of that cloud, (i.e., the liquid water content, drop size distribution, the water phase and the geometry and orientation of ice crystals - if they are present) integrated through the geometric thickness of the cloud. The natural variability of these parameters in clouds is significant. Consequently, the range of ε^* values associated with naturally occurring clouds may be assumed to be significant. Differences in the spectral distribution of incident radiant fluxes upon clouds and the subsequent interaction with the microphysical structure result in differences of ε^*. Cox (1976) has observed the large natural variability of ε^* for tropical clouds.

The total atmospheric infrared heating rate, TQ_{IR}, where

$$TQ_{IR} = \int_{p_T\ =\ 0.1\ mb}^{p_0\ =\ 1013\ mb} Q_{IR}(p')\ dp' \cdot \left(\frac{1}{p_0 - p_T}\right) \qquad (4.7)$$

as a function of cloud top pressure, p_{CT}, for clouds of differing ε^* is depicted in Fig. 11. For this figure, the clouds were assumed to be 100 mb thick. The range of TQ_{IR} for a given range of cloud ε^* is seen
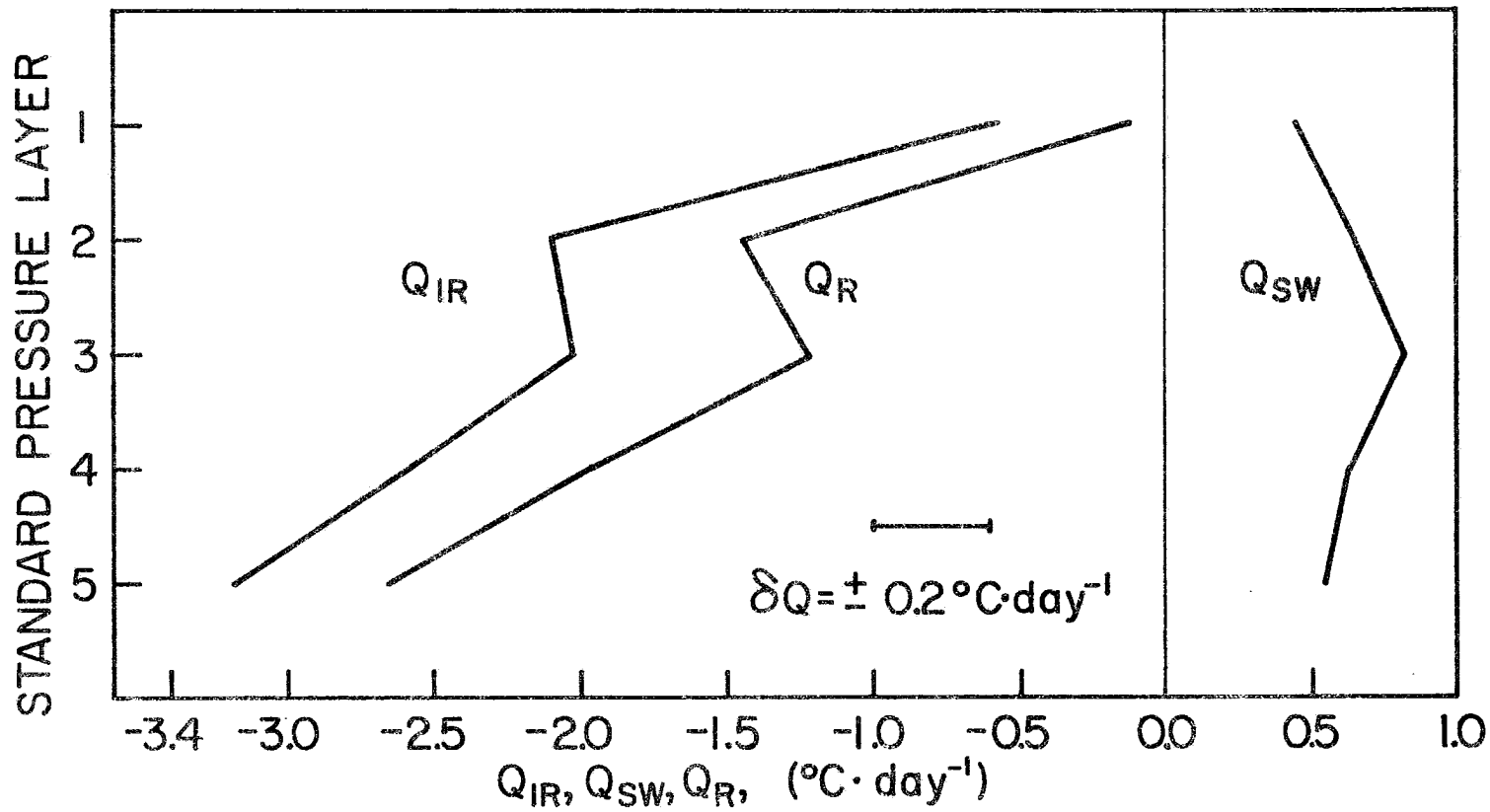
Figure 10. Daily radiative heating rate for clear sky conditions and the short wave and infrared components for each standard layer of the model atmosphere. The RSP proposed maximum allowable uncertainty in the radiative heating rate for a standard layer is noted.
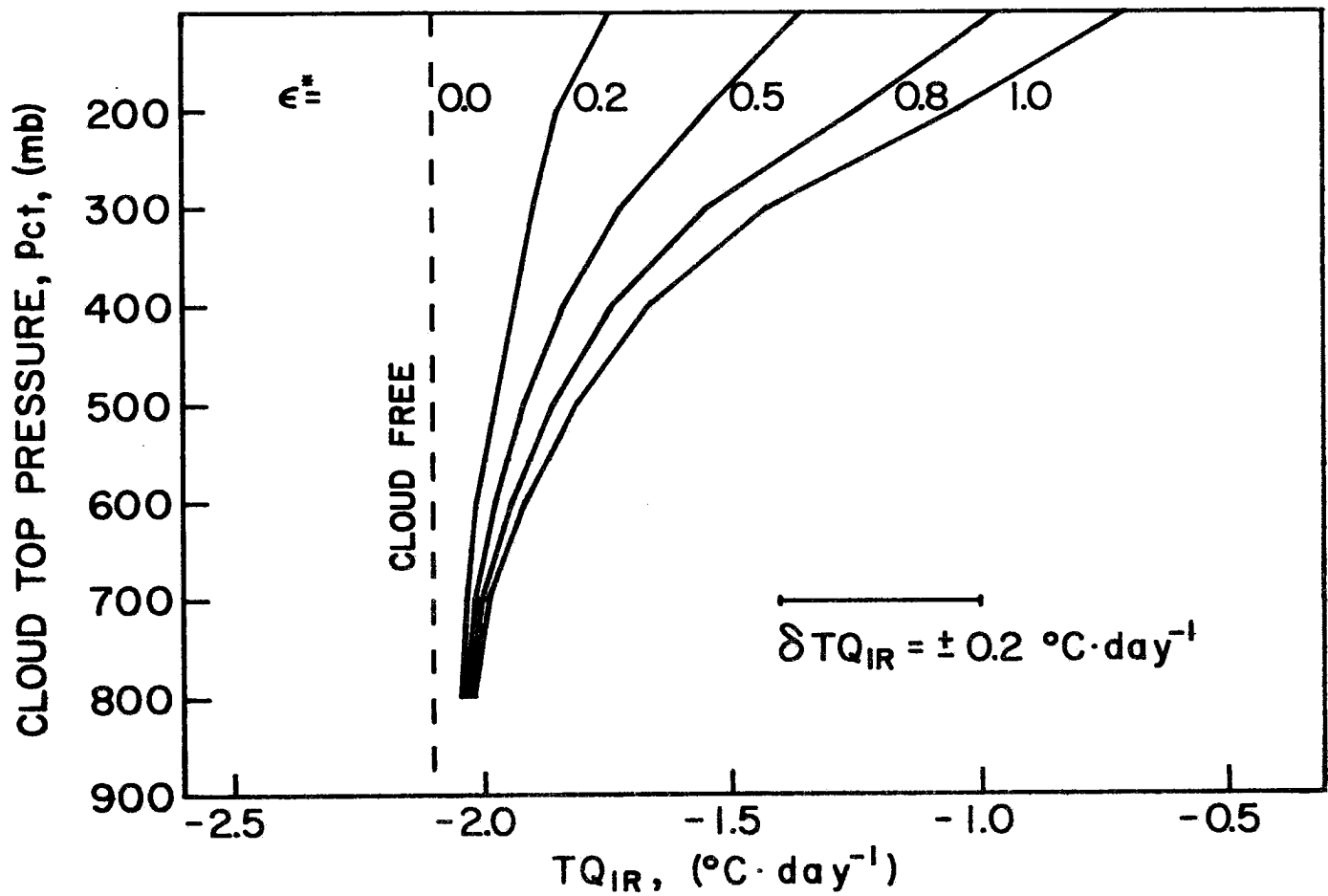
Figure 11. Infrared heating rates for the total atmospheric column for 100 mb thick clouds of various heights and effective infrared broadband emissivities. The dashed curve denotes the clear sky infrared heating.

to increase dramatically with decreasing p_{CT}. For clouds with p_{CT} greater than approximately 400 mb, the range of TQ_{IR} possible for emissivities from $\varepsilon^* = 0.0$ (i.e., cloud free) to $\varepsilon^* = 1.0$ (i.e., black cloud) is less than 0.4°C per day. Thus, the TQ_{IR} may be approximated to within ± 0.2°C per day by assuming $\varepsilon^* \simeq 0.5$. This implies that for a cloud below 400 mb, which approximates tropical water clouds, the ε^* need not be known to fulfill an accuracy requirement of ± 0.2°C per day for the entire atmospheric column. For upper level ice clouds, i.e. cirroform, at the 150 mb level, the ε^* must be known to within ± 0.10 to achieve this degree of accuracy. This large sensitivity of Q_{IR} to the ε^* prescribed for cirroform clouds has been previously noted by Manabe and Strickler (1964) and Cox (1971a). The effect of decreasing the cloud thickness, ΔP_c, upon the sensitivity of TQ_{IR} to variations in ε^* is slight.

The sensitivity of the infrared heating rate in each standard layer to the effective emissivity specified for 100 mb thick clouds at various levels of the atmosphere may be seen in Table 2. The data entries are the maximum allowable uncertainty in the effective infrared broadband emissivity, $\delta\varepsilon^*$, of the cloud, such that an accuracy of $\delta Q_{IR} = \pm .2$°C per day may be achieved for the corresponding layer. An asterisk, *, implies that $\delta\varepsilon^* > \pm 0.5$. Thus, these layers are relatively insensitive to the emissivity of the corresponding cloud. It is noted that the most sensitive layers are generally the layer the cloud occurs within and the layer below. Table 3 is the same as Table 2 except that the cloud is assumed to be 50 mb thick. The sensitivity for a layer decreases with decreasing cloud thickness. Uniform variations of atmospheric water vapor of $\pm 20\%$ at all levels alter $\delta\varepsilon^*$ by less than ± 0.01.

Pct LAYER	100	200	300	400	500	600	700	800
1	+0.13	+0.15	+0.28	*	*	*	*	*
2	+0.08	+0.08	+0.04	+0.12	*	*	*	*
3	+0.21	+0.13	+0.04	+0.31	+0.04	+0.13	*	*
4	+0.22	+0.15	+0.13	+0.12	+0.04	+0.27	+0.04	+0.15
5	+0.28	+0.19	+0.17	+0.17	+0.16	+0.14	+0.04	+0.16
$\delta\epsilon^*_{MAX}$	+0.08	+0.08	+0.04	+0.12	+0.04	+0.13	+0.04	+0.15

Table 2. Maximum allowable uncertainty in the effective infrared broad-band emissivity, $\delta\epsilon^*$, of a 100 mb thick cloud such that an accuracy in the infrared radiative divergence of $\delta Q_{IR} = \pm 0.2°C \cdot$ day^{-1} for each standard pressure layer may be achieved (see Eq. 2.1) for various cloud top heights, p_{CT}, in mb. The bottom row lists the limiting uncertainty allowed such that all standard layers meet the Radiation Subprogram accuracy requirements. An asterisk denotes a value of $\delta\epsilon^* > \pm 0.5$ in magnitude.

Pct LAYER	100	200	300	400	500	600	700	800	900
1	±0.09	∓0.42	*	*	*	*	*	*	*
2	±0.13	±0.16	∓0.11	*	*	*	*	*	*
3	±0.25	±0.16	±0.11	∓0.30	∓0.10	*	*	*	*
4	±0.26	±0.17	±0.16	±0.15	±0.11	*	∓0.14	*	*
5	±0.33	±0.22	±0.21	±0.20	±0.20	±0.17	±0.12	*	*
$\delta\epsilon^{*}_{MAX}$	±0.09	±0.16	±0.11	±0.15	∓0.10	±0.17	±0.12	*	*

Table 3. Maximum allowable uncertainty in the effective infrared broad-band emissivity, $\delta\epsilon^{*}$, of a 50 mb thick cloud such that an accuracy in the infrared radiative divergence of Q_{IR} = ±0.2°C· day^{-1} for each standard pressure layer may be achieved (see Eq. 2.1) for various cloud top heights, p_{CT}, in mb. The bottom row lists the limiting uncertainty allowed such that all standard layers meet the Radiation Subprogram accuracy requirements. An asterisk denotes a value of $\delta\epsilon^{*}$ > ±0.5 in magnitude.

In the bottom row of Table 2, the maximum uncertainty such that an accuracy of $\delta Q_{IR} = \pm 0.2\,°C$ per day may be achieved for all 200 mb thick layers for a cloud at a given level is noted. These data are graphically displayed in Fig. 12. The solid curves correspond to the data in Tables 2 and 3. The data were computed for the standard pressure layers noted in Eq. 2.3. It is evident that the jagged shape of these curves is largely due to proximity of cloud boundaries to standard pressure levels. The dashed curves were computed from the same data for a cloud centered pressure layer scheme. That is, the values of $\delta\varepsilon^*$ were computed for a 200 mb thick layer centered on the cloud and for the adjacent 200 mb thick layers. Thus, these curves portray, in a more general way, the maximum uncertainty in the effective, broadband, infrared cloud emissivity allowed such that the desired accuracy for all the standard pressure layers may be attained. An interesting result is that for a given cloud pressure thickness, the magnitude of $\delta\varepsilon^*$ is approximately a constant for a cloud at most levels of the tropical atmosphere. The exceptions are that when there are very high clouds, the sensitivity increases and that when there are clouds in the lower troposphere, Q_{IR} is insensitive.

To evaluate these results, we first consider water clouds. Yamamoto, et al (1970) have deduced broadband infrared emissivities for model water clouds of various thicknesses based upon theoretical calculations. They have concluded that for water clouds thicker than 100 meters, the broadband emissivity is nearly unity. Zdunkowski and Crandall (1971), Hunt (1973) and Paltridge (1974) have reported similar results for limited spectral intervals in the infrared. However, their results imply a thickness of up to 500 meters is required before a water cloud may be considered black. The author notes that the effective broadband infrared
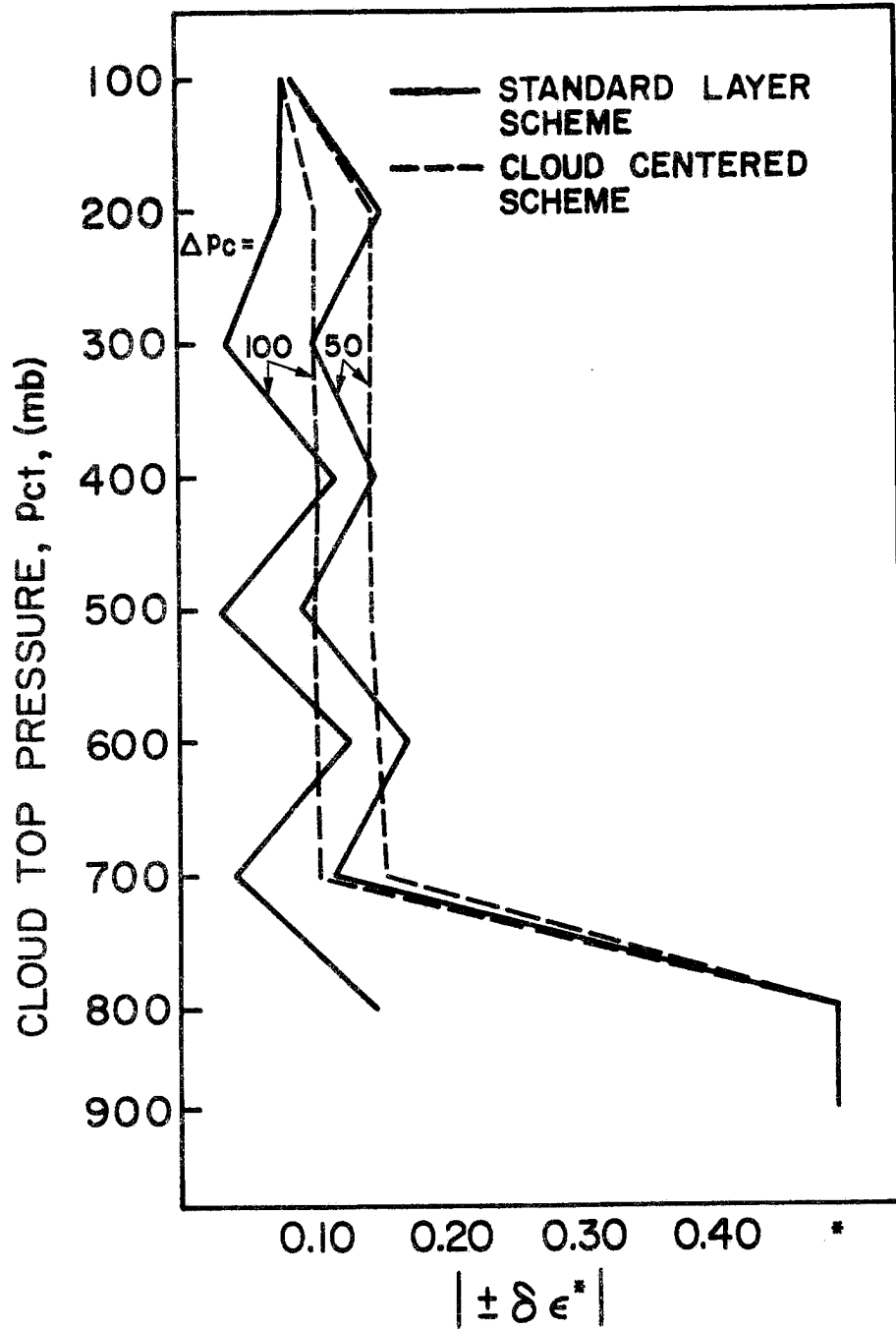
Figure 12. Magnitude of the maximum allowable uncertainty in the effective infrared broadband emissivity, $\delta\epsilon^*$, of a cloud, such that an accuracy on the infrared radiative divergence, δQ_{IR}, of $\pm 0.2°C\cdot$day may be achieved for all standard or cloud centered pressure layers as a function of cloud top height. (i.e. if $\delta\epsilon^* = \pm x$, then $|\pm \delta\epsilon^*| = x$)

emissivity, ε^*, employed in this study is always greater than the broadband emissivity used in the studies noted above as it includes the effect of reflected infrared radiation. Therefore, theoretical calculations imply that for a moderately thick water cloud the ε^* is nearly unity and the possibility of a real variation in ε^* exceeding the tolerable limits of uncertainty noted in Fig. 12 is slight. This fact may be reconciled with the observations of Cox (1976) by noting that his sample includes thin clouds. Furthermore, the presence of non-uniform cloud tops, i.e. turrets, and the possibility that all broken cloud observations were not eliminated from the data set may also contribute to the large variation of ε^* observed. We have shown that Q_{IR} does not vary substantially with the ε^* specified for a lower tropospheric cloud. Thus, only for the thin water cloud occurring in the mid-troposphere is there a need to specify an ε^* less than unity with some degree of accuracy. However, it has also been shown that as the cloud becomes thinner and thinner, the radiative effect becomes smaller and the tolerable range of uncertainty of the corresponding ε^* increases. For the thin cloud, the $\delta\varepsilon^*$ is greater than ± 0.15. Additional information from the Radiation Subprogram data analysis of specific aircraft observations of this type of cloud as to the proper values of ε^* will be needed.

Clouds exhibiting the most significant influence on the vertical distribution of Q_{IR} are the upper tropospheric ice clouds. The effective emissivity for a cloud of this type must be known to within ± 0.08 in order to deduce the Q_{IR} for each layer to the proposed accuracy. Measurements by Kuhn and Weickman (1969), Davis (1971), and Cox (1976) have shown that a wide range of ε^* values occurs in natural cirroform clouds. Jacobowitz (1970) and Fleming and Cox (1974) have performed

calculations confirming that a large range of ε^* may be expected in cirrus clouds. Hansen (1971), Shenk and Curran (1973), and Platt (1975) have proposed methods to deduce cirroform emissivities from satellite data. However, the accuracy of these types of schemes for operational use needs to be verified. It is apparent that with the high degree of sensitivity of Q_{IR} to the value of ε^* specified and the wide range of ε^* encountered in naturally occurring cirroform clouds, specific values of ε^* for particular cirroform clouds will be needed to meet the proposed accuracy requirement. Observational data obtained during the GATE Field Phase may be the only way to resolve this problem.

When the cloud boundary is in close proximity to a standard pressure level, the sensitivity of Q_{IR} to the ε^* prescribed increases by at least a factor of two over the case when the cloud is deep within the layer. In light of the above discussions, this effect will not severely limit the accuracy of calculations when water clouds are present. However, in the case of ice clouds, this effect serves to emphasize the necessity for specific accurate information on the ε^* of an ice cloud. One encouraging fact is that the middle and lower tropospheric Q_{IR} is relatively insensitive to the ε^* prescribed for an upper level ice cloud, Tables 2 and 3. Thus, even if it is not possible to attain the proposed accuracy for all layers, the values deduced for the lowest layers will be representative.

2. Cloud Height

In order to evaluate the sensitivity of Q_{IR} for the standard layers to uncertainties in the cloud height, a series of computations were made for water clouds, thin and thick ice clouds, and clouds of large vertical

extent. For convenience, a plot of pressure as a function of geopotential height for the mean tropical atmosphere is given in Fig. 13.

All data presented in this section were derived under two basic assumptions. First, the standard layer(s) in which the cloud boundaries occur were assumed to be known. If the layer(s) in which the cloud boundaries occur are not known, the vertical distribution of Q_{IR} exhibits errors substantially exceeding the desired accuracy. Second, it was assumed that the cloud boundaries were not coincident with or in very close proximity to the standard pressure levels. This was done to simplify the analyses. If a cloud boundary is in close proximity to a standard pressure level, the tolerable uncertainty in the boundary location decreases greatly. This is due to the large cooling and warming in the region of cloud top and cloud base, respectively. Very accurate information on the boundary locations is needed in this case. Further discussion of this problem is given in following sections.

The maximum allowable uncertainty of cloud top location, δp_{CT} for 50 mb thick black water clouds such that the proposed RSP accuracy requirement may be fulfilled is revealed in Table 4. These clouds were assumed to exist at levels of 925 mb to 500 mb. The entries are the allowable δp_{CT} such that an accuracy of $\delta Q_{IR} = \pm 0.2°C$ per day may be achieved for a given layer for clouds occurring above, within, or below that layer. An asterisk denotes a sensitivity of $\delta p_{CT} > \pm 500$ mb.

The radiative divergence in layers above the standard layer in which a water cloud occurs is relatively insensitive to the location of cloud top. This is due to the small quantity of water vapor in the upper layers. The middle tropospheric water cloud requires the most accurate location. This results because of the radiative interaction
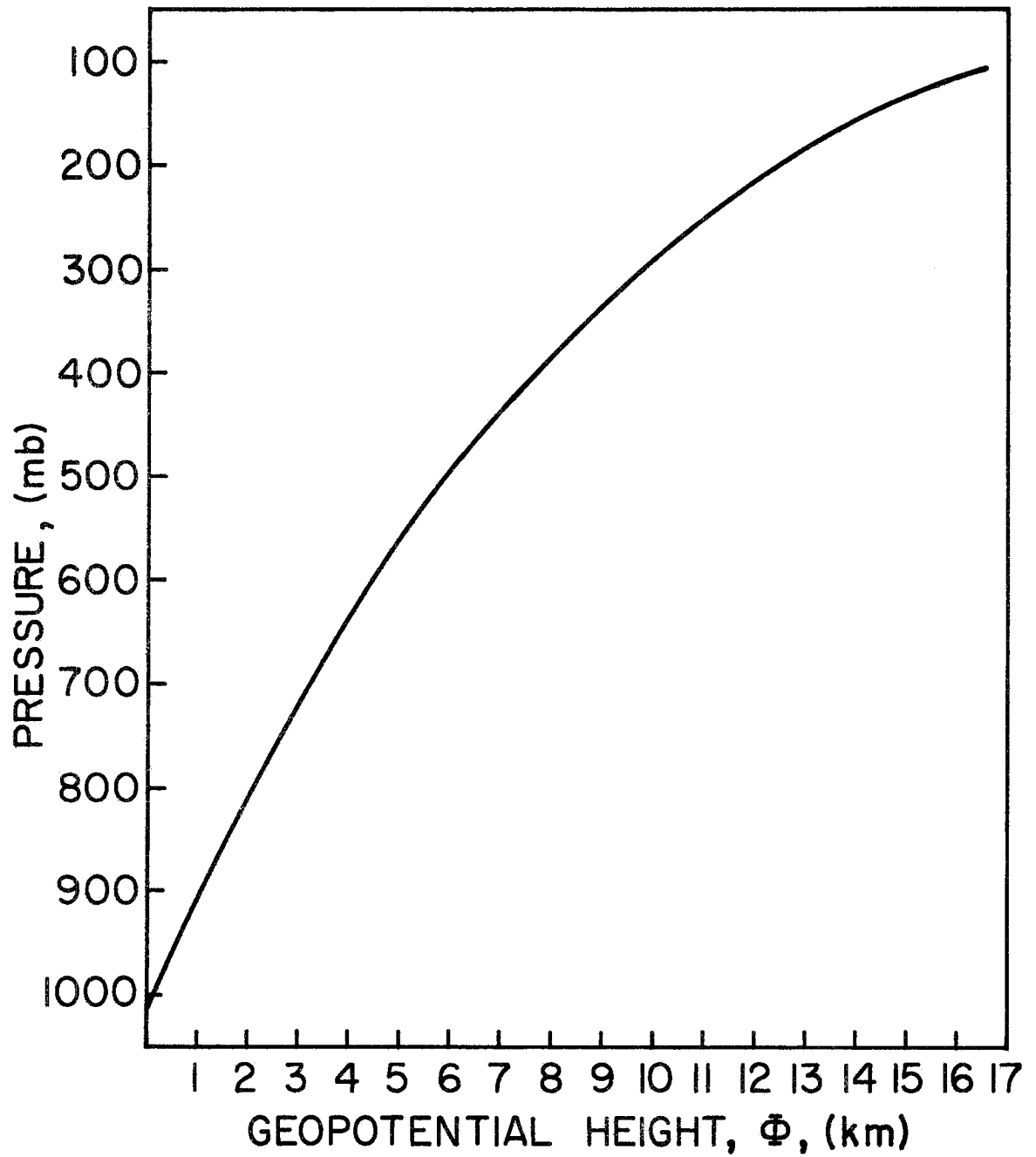
Figure 13. Relationship of geopotential height and pressure
for the mean atmosphere used in model study.

	CLOUD LOCATION RELATIVE TO LAYER		
LAYER	ABOVE	WITHIN	BELOW
1	——	——	$*$
2	——	——	$*$
3	——	$\overline{+}13$ mb ($\sim \pm206$ m)	±165 mb
4	±36 mb	$\overline{+}20$ mb ($\sim \pm239$ m)	±120 mb
5	±70 mb	$\overline{+}33$ mb (±339 m)	——

Table 4. Maximum allowable uncertainty of cloud top height location, δp_{CT}, to achieve an accuracy of $\delta Q_{IR} = \pm0.2°C \cdot day^{-1}$ for the standard layer in which the cloud occurs and the layers above and below. Clouds are assumed to have $\Delta p_C = 50$ mb and $\varepsilon^*=1.0$. It is also assumed that the standard layer in which the cloud occurs is known. An asterisk denotes a value of $\delta p_{CT} > \pm500$ mb in magnitude. The corresponding uncertainty in the geometric height is also noted. Assumptions are discussed in the text.

of the cloud layer with the vertical temperature and water vapor distributions. As cloud top becomes higher in the middle troposphere, the atmosphere above rapidly becomes semi-transparent to infrared radiation in the water vapor bands. As cloud base becomes higher, the incident upward radiation due to water vapor emission increases slowly. The upward and downward fluxes at cloud top and cloud base also decrease as the cloud boundaries become higher and colder according to Eqs. 4.1 and 4.2. The net effect is a high sensitivity of the radiative heating of the standard layer in which the cloud occurs to the location of the cloud boundaries. It is noted that for thin water clouds, which are not black, the allowable δP_{CT} increases. Thus, the data in Table 4 represent the maximum accuracy required.

Table 5 is similar to Table 4. The data were computed for simulated ice clouds in the 450 to 125 mb layer. The clouds were assumed to be 25 mb thick and were assigned to ε^* of 0.5 and 0.05. These values span the range of ε^* encountered in the large majority of tropical ice clouds. In general, the basic pattern is the same, however, the sensitivity to P_{CT} is greater. It is noted that the location of an optically thin (i.e. small ε^*) ice cloud is less sensitive than for an optically thick ice cloud. In Fig. 14, the limiting values of δP_{CT} are drawn for each of the above cases.

The data given in Table 4 and 5 pertain equally well to the location of cloud top and cloud base. If a cloud straddles a standard pressure layer, cloud top and cloud base must be known to the accuracy noted above for the layers in which they occur.

Computations were made to determine the sensitivity of the total atmospheric infrared heating, TQ_{IR}, to the location of these model

LAYER	CLOUD LOCATION RELATIVE TO LAYER					
	ABOVE		WITHIN		BELOW	
	$\varepsilon^* = 0.5$	0.05	0.5	0.05	0.5	0.05
1	——	——	$\mp$10 mb (±410 m)	$\mp$15 mb (±620 m)	±100 mb	±219 mb
2	±61 mb	±90 mb	$\mp$10 mb (±240 m)	$\mp$30 mb (±730 m)	——	——
3	±50 mb	±80 mb	$\mp$10 mb (±160 m)	$\mp$36 mb (±570 m)	——	——
4	±57 mb	±75 mb	——	——	——	——
5	±104 mb	±91 mb	——	——	——	——

Table 5. Same as Table 4 except Δp_c = 25 mb and ε^* = 0.05 and 0.50.
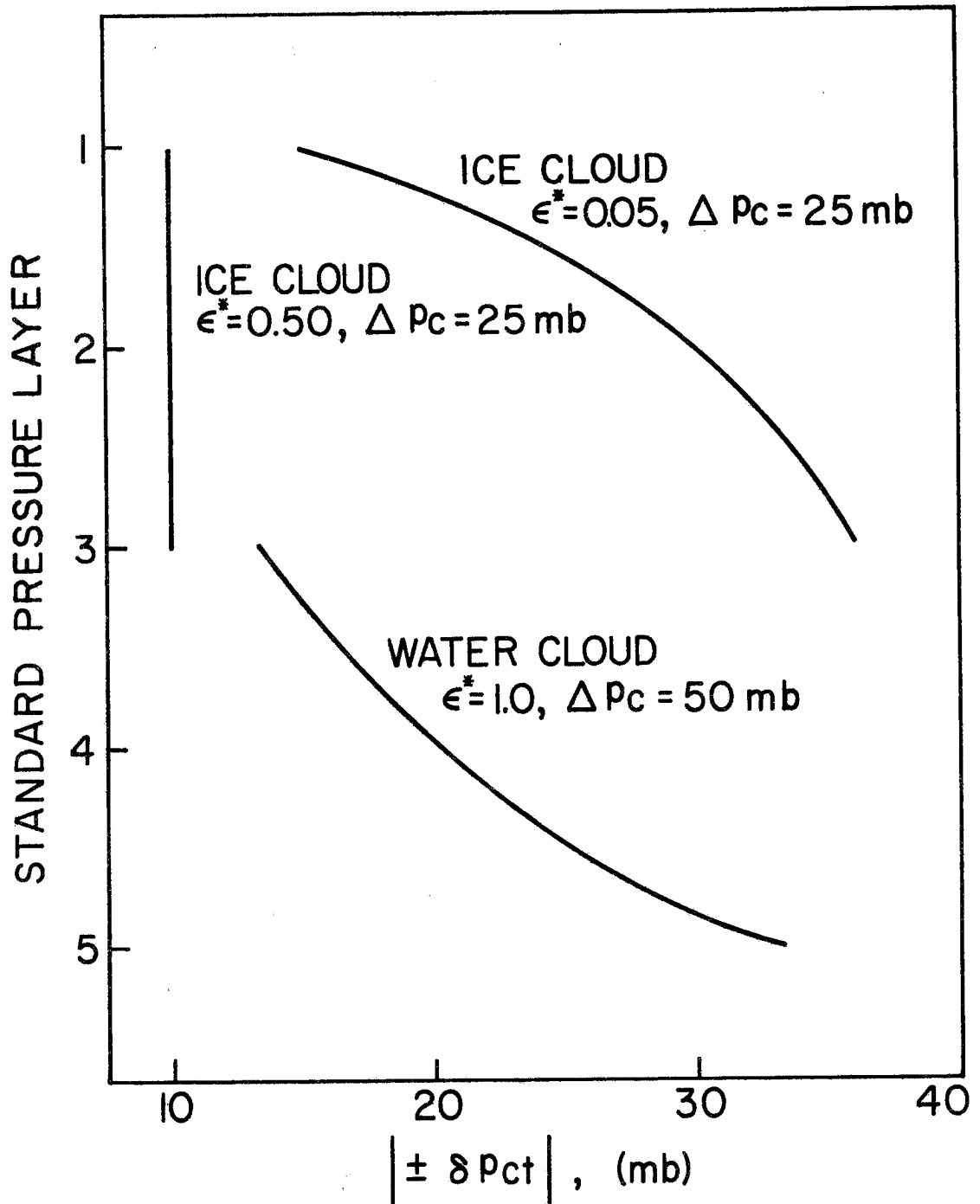
Figure 14. Magnitude of the maximum allowable uncertainty in the location of cloud top height within a standard layer, such that an accuracy of $\delta Q_{IR} = \pm 0.2°C \cdot day^{-1}$ may be achieved for all standard layers for various cloud thicknesses and effective infrared broadband emissivities. (e.g. if $\delta p_{CT} = \pm x$ mb, then $|\pm \delta p_{CT}| = x$ mb)

clouds. The allowable uncertainty in cloud top location, δp_{CT}, was determined such that TQ_{IR} may be deduced to within $\pm 0.2°C \cdot day^{-1}$. In the case of the water cloud and thin and thick ice clouds, the cloud top location must be known to within ∓ 290 mb, $\mp > 500$ mb, and ∓ 127 mb, respectively.

For the case of clouds of large vertical extent, i.e. cumulus congestus and cumulonimbus, only the layer in which the cloud top occurs and the layers above that layer are sensitive. The emissivity of such clouds is taken as unity. To deduce the TQ_{IR} to within $\pm 0.2°C$ per day we need to know the cloud top to within ∓ 76 mb. To fulfill the proposed accuracy requirement for all layers, cloud top must be known to the accuracy noted in Fig. 15. Thus, for a cloud top within the layer defined by the vertical extent of the solid lines, the tolerable uncertainty of cloud top location is that noted on the abscissa. The lower the cloud top pressure is, the greater the accuracy required in the location of cloud top pressure.

3. Areal Cloud Cover

The tolerable uncertainty of percent areal cloud coverage, $\delta \alpha$, is defined:

$$\delta \alpha \equiv \frac{\pm 0.2°C \text{ per day}}{Q_{IR}(\text{cloud}) - Q_{IR}(\text{clear})} * 100\%. \tag{4.8}$$

Thus, $\delta \alpha$ is the maximum allowable uncertainty of percent cloud area such that an accuracy of $\delta Q_{IR} = \pm 0.2°C$ per day may be achieved for the layer to which Q_{IR} pertains. It is always assumed that the area not occupied by the cloud is clear. That is, if the cloud cover is 20% then the other 80% is clear. This is done in order to normalize the results. Fig. 16 displays the $\delta \alpha$ requirement to deduce the TQ_{IR} to within $\pm 0.2°C$
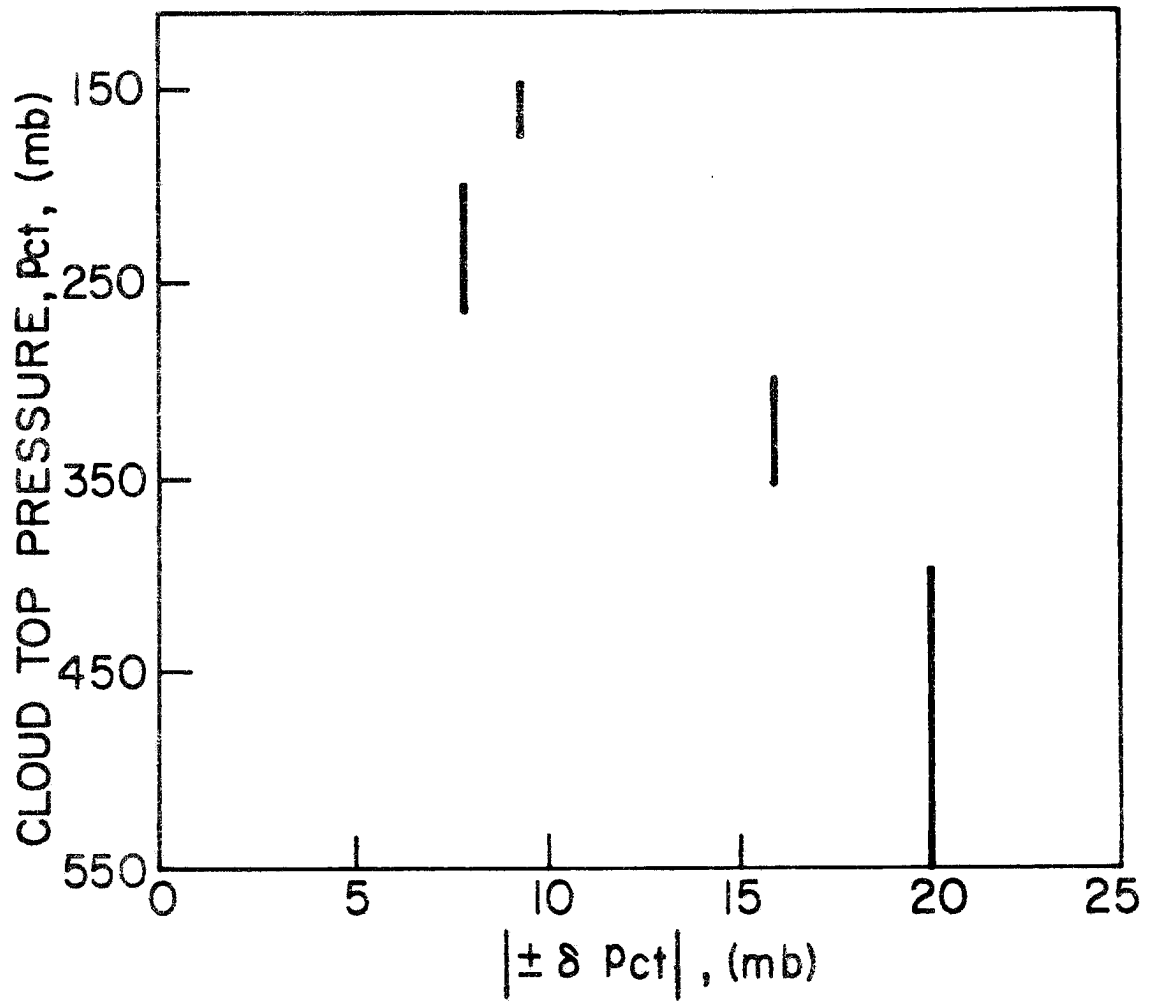
Figure 15. Magnitude of the maximum allowable uncertainty in the location of cloud top height within a standard pressure layer, such that an accuracy of $\partial Q_{TR} = \pm 0.2°C\cdot day^{-1}$ may be achieved for all standard layers for black clouds of large vertical extent.
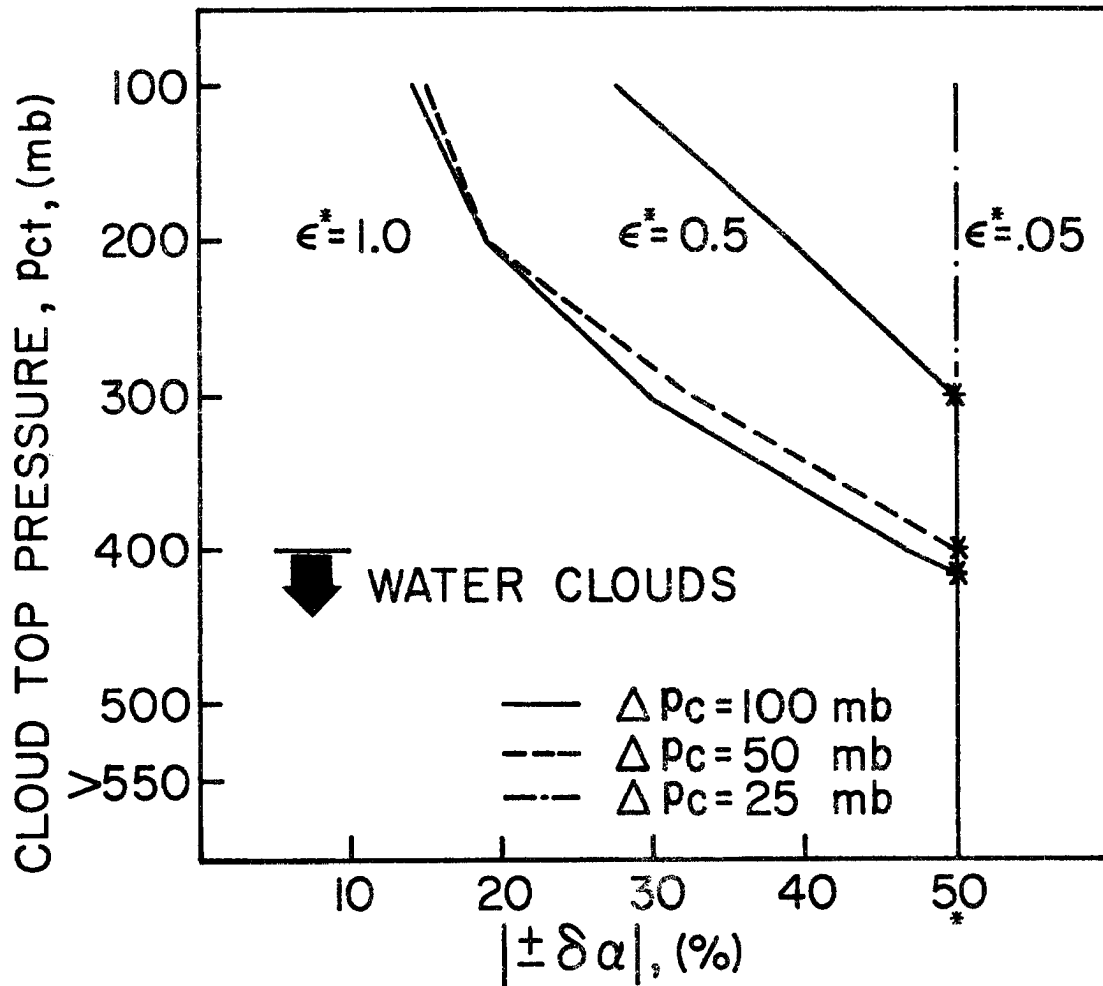
Figure 16. Magnitude of the maximum uncertainty allowed in the specification of percent area cloud cover, such that an accuracy of $\delta TQ_{IR} = +0.2°C \cdot day^{-1}$ may be achieved for the total atmospheric column, as a function of cloud top height for various cloud thicknesses and effective infrared broadband emissivities. (i.e., if $\delta\alpha = \pm$ x%, then $|\pm \delta\alpha|$ = x%)

per day for clouds of various emissivities and thicknesses as a function of P_{CT}. A value of $\delta\alpha > \pm 50\%$ implies that the TQ_{IR} is insensitive to the amount of cloud. It is seen that water clouds and very optically thin clouds do not alter the TQ_{IR} beyond the $\pm 0.2°C$ per day limit no matter what the areal coverage is. The less the ε^* of the cloud, the less we need to know about the areal coverage. The maximum accuracy of cloud area information required is for the high ice cloud, where it must be known to approximately $\pm 15\%$.

Figure 17 depicts the $\delta\alpha$ for clouds of various p_{CT}, Δp_c and ε^* such that the proposed Radiation Subprogram accuracy requirement may be ful-filled for all 200 mb thick standard pressure layers. Q_{IR} is relatively insensitive to the area cloud cover of lower tropospheric water clouds and high, very optically thin ice clouds. In general, the areal cloud cover must be known to better than approximately $\pm 10\%$ for middle and upper tropospheric clouds. The most sensitive layers are the layer the cloud occurs within and the layers below.

The percent areal cloud cover for clouds of large vertical extent must be known to within $\pm 7\%$ to $\pm 4\%$ for cloud top ranging from 550 mb to 150 mb, respectively.

4. The Multi-Layered Configuration

Information on cloud layers existing below cirrus clouds is required. Whereas, the addition of single or multiple water clouds below a cirrus layer does not substantially alter the TQ_{IR}, the vertical distribution of Q_{IR} is altered.

This may be seen in Fig. 18, which is a plot of the infrared heating rate, Q_{IR}, in each standard pressure layer for various cloud configurations.
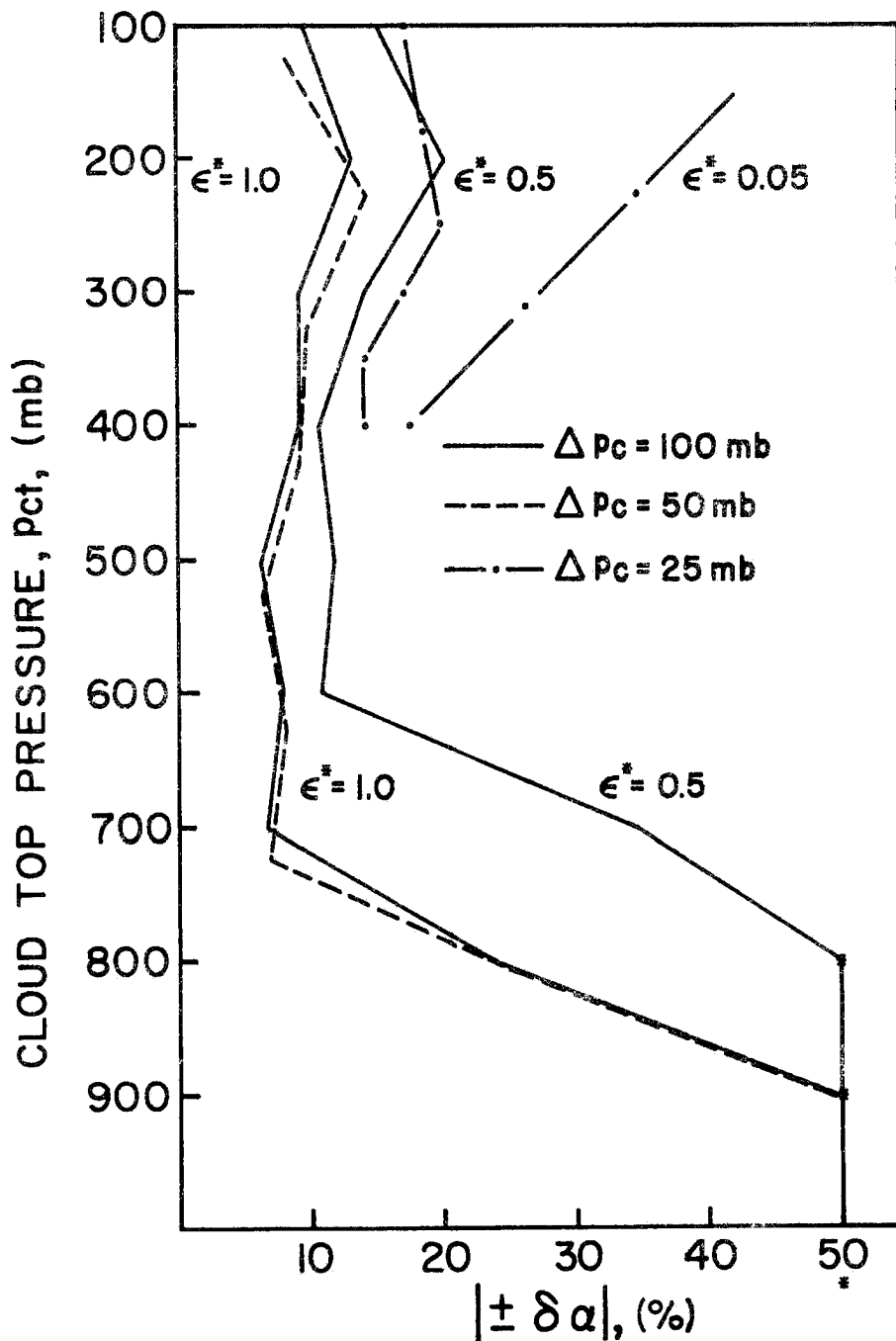
Figure 17. Magnitude of the maximum uncertainty allowed
in the specification of percent area cloud cover,
such that an accuracy of $\delta Q_{IR} = \pm 0.2°C \cdot day^{-1}$ may
be achieved for all standard pressure layers, as
a function of cloud top height for various cloud
thicknesses and effective infrared broadband
emissivities.
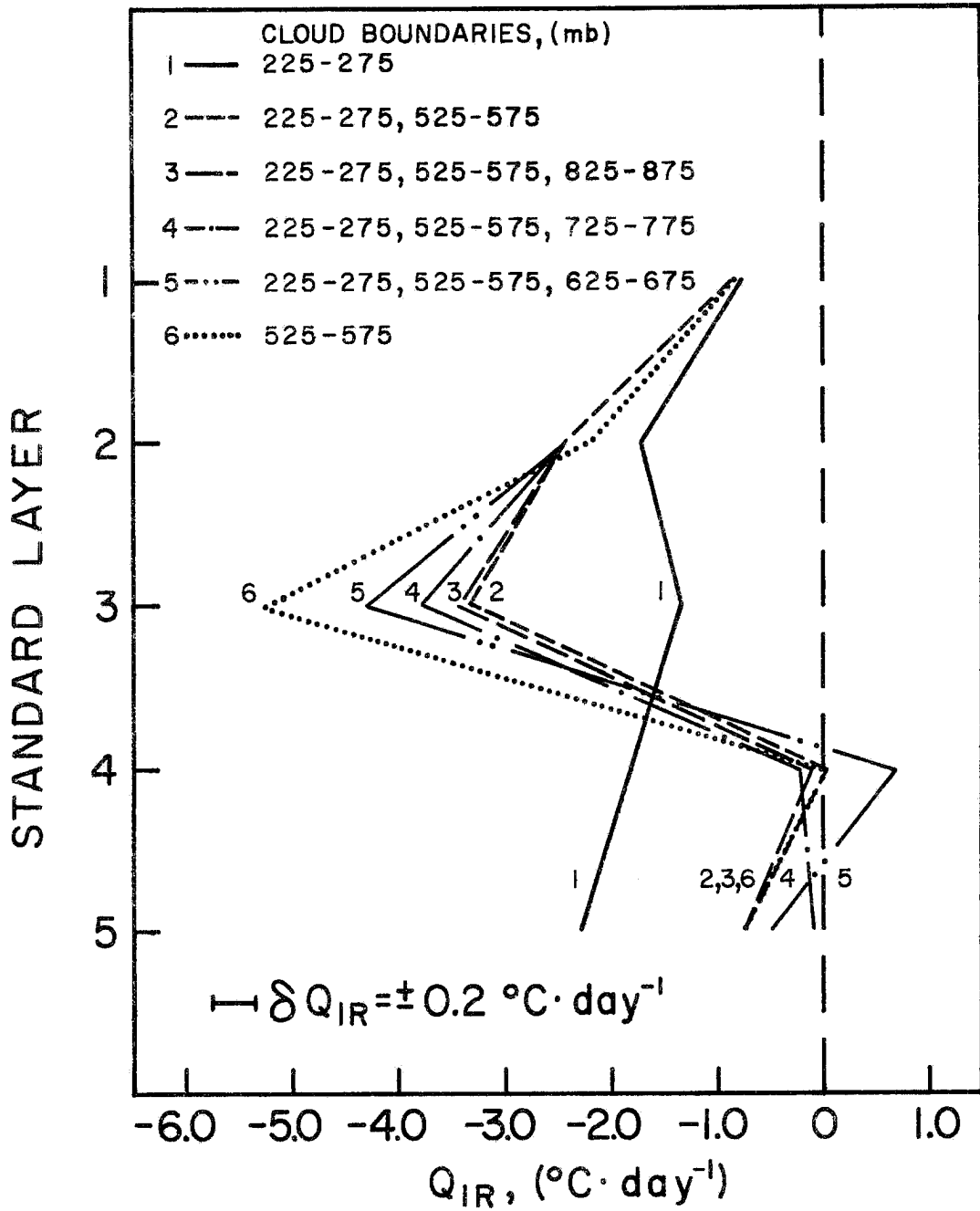
Figure 18. Infrared heating rates for various multilayered cloud configurations for the standard pressure layers. The cloud radiative properties are as noted in the text.

The emissivity of the cirroform cloud was assumed to be 0.42. The cloud top height is 225 mb and the thickness is 50 mb. Thus, it is totally within standard layer 2. The water clouds were assumed to have emissivities of unity. The cloud top heights are 525 mb, 625 mb, 725 mb, and 825 mb. The cloud thickness is taken as 50 mb for all clouds. Thus, the lower level clouds are totally contained within standard layers 3, 4, 4, and 5. respectively. It is seen that the layer above the cirroform cloud, layer 1, is relatively insensitive to additional cloud layers deep within the troposphere. It is noted that the sensitivity of upper tropospheric layers to the description of upper tropospheric ice clouds remains nearly the same as in the case of cirroform clouds only. Since the limiting values of $\delta\epsilon^*$, δp_c and $\delta\alpha$, noted previously, for upper level clouds were derived for the most sensitive layer, which, in general, was an upper tropospheric layer, the allowable uncertainty in the description of cirrus clouds remains substantially the same whether it overlies water clouds or not.

An example of the situation of a single water cloud below a cirroform layer is plotted as curve 2. The effect of the overlying cirrus cloud is to reduce the cooling in the standard layer in which the water cloud occurs. In this example, the cooling in layer 3 is reduced by approximately 60%, compared to the water cloud only case, curve 6. However, due to the blackness of water clouds, the cirrus cloud has no effect on the cooling below the water cloud. Referring to Table 3, in most cases, it is the layers below which are most sensitive to the specification of the ϵ^* of a water cloud. Thus, the limiting $\delta\epsilon^*$ is nearly the same for the single water cloud underlying a cirroform cloud as when there is no cirrus. The δp_{CT} for the underlying cloud layer is slightly greater than in the case of no cirrus.

This is due to the decreased vertical gradient of Q_{IR} above the water cloud when cirrus clouds are present. It is still critical to know in which standard layer the water cloud occurs. The improvement in δp_{CT} for the example noted here is only approximately ± 2 mb. The uncertainty allowed in the percent areal cloud cover of this water cloud alone is given as $\pm 6\%$ in Fig. 14. This was derived for the most sensitive layer, which is the standard pressure layer in which the cloud occurs. In the case of overlying cirrus, the most sensitive layer is the standard layer below that in which the water cloud occurs. The uncertainty allowed in this case is $\delta \alpha = \pm 8\%$. Thus, Q_{IR} is slightly less sensitive to the areal cloud cover prescribed for a water cloud underlying a cirroform cloud compared to when there is no overlying cirrus cloud.

In the situation of multiple water clouds, the description of the uppermost water cloud must be accurate to within the limits given above for a single water cloud layer or a single water cloud layer underlying an ice cloud. If two black water clouds occur within the same standard pressure layer, they may be regarded as one cloud with cloud top and cloud base corresponding to the top and base of the upper and lower cloud, respectively. The limits of allowable uncertainty of the cloud description pertain to these boundaries. Curves 3, 4 and 5 in Fig. 18 correspond to the case of multiple water cloud layers not occurring in the same standard pressure layer. In these cases, the $\delta \epsilon^*$ for the lower water cloud is approximately twice that given in Fig. 12. The δp_{CT} is nearly ± 50 mb, the $\delta \alpha > \pm 40\%$ for the lower water cloud when compared to the case of the upper water cloud only, curve 2. Thus, in the situation of multiple water cloud layers, the required accuracy in the description of the lower water cloud layers is much less than for the uppermost layer.

C. Sensitivity of the Solar Component

1. Cloud Radiative Properties

The significant cloud radiative properties affecting the short wave or solar component of the radiative transfer are the cloud reflectivity, ρ_c, the cloud absorptivity, a_c, and the nature of the cloud transmission, i.e. direct beam or diffuse. As noted in section IV.B, the large natural variability of the microphysical properties of clouds implies a variability of cloud optical properties.

The magnitude of potential errors in Q_{SW} due to uncertainty as to whether a cloud is a diffuse or direct beam transmitter is shown in Fig. 19. This curve was computed for a cloud base of 500 mb. The difference in the instantaneous short wave heating rates, Q_{SW} (diffuse) - Q_{SW} (direct), is given as a function of solar zenith angle for the 500 mb to 700 mb layer. The cloud reflectivity was specified as 0.30 and the cloud absorptivity as 0.05. Since this effect is maximized just below the cloud, this curve may be regarded as the maximum effect within any standard layer. It was found to be representative for a cloud with these broadband radiative properties at any level of the atmosphere. Over the entire day, the difference averages to approximately 0.1°C per day. The difference in total solar warming rate, TQ_{SW}, for the total atmospheric column, i.e.

$$TQ_{SW} = \int_{p_T = 0.1 \text{ mb}}^{p_0 = 1013 \text{ mb}} Q_{SW}(p') \, dp' \cdot \left(\frac{1}{p_0 - p_T}\right) \qquad (4.9)$$

averaged over the day is approximately 0.03°C per day. It is seen that errors approaching the RSP desired accuracy occur at small zenith angles, i.e. during the mid-day hours. However, the reflectivity and absorptivity of the cloud were chosen to yield a maximum difference. At larger values

DIFFERENCE IN THE INSTANTANEOUS HEATING RATES (°C·day^{-1}) Q_{SW}(DIFFUSE) − Q_{SW}(DIRECT)

SOLAR ZENITH ANGLE, θ, (deg)

$g_c^- = 0.30$ $\alpha_c^- = 0.05$
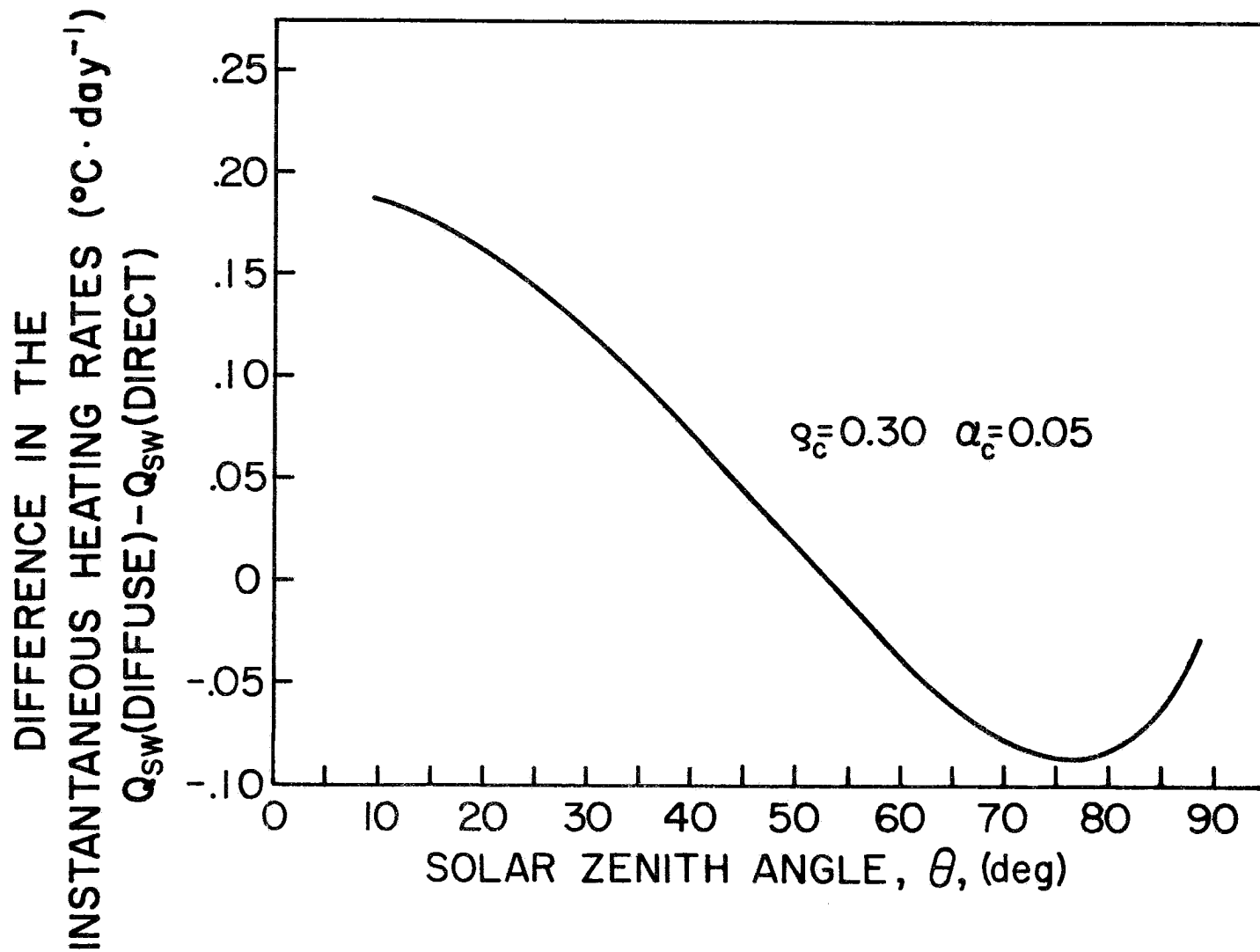
Figure 19.   Difference in the instantaneous short wave heating rate for the 500-700 mb layer as a function of solar zenith angle in the case of a cloud with base at 500 mb which transmits diffusely or directly.

of ρ_c and a_c this difference decreases markedly. It must also be noted that this curve represents the extremes of the angular distribution of solar irradiance transmitted by a cloud, i.e. purely direct or purely diffuse. It is probable that most natural clouds fall within these extremes. Furthermore, the degree of diffusivity of the transmitted irradiance is likely to be positively correlated with cloud reflectivity, i.e. clouds with large reflectivities in the short wave may be assumed to be diffuse transmitters. Some manner of relating these quantities is needed if the RSP objectives are to be met on a time resolution exceeding three hours. For the remainder of this chapter, all clouds are assumed to be diffuse transmitters, and all short wave heating rates are the total integrated heating per day. To interpret these data for average instantaneous conditions during the daylight hours, the reader should consult section IV.A.

The maximum uncertainty in cloud absorptivity, δa_c, allowed in order to achieve an accuracy of $\delta Q_{SW} = \pm 0.2°C$ per day for all standard pressure layers is approximately ± 0.01 for very high clouds and approximately ± 0.015 for very low clouds. To convert to power units, multiply by the daily incident solar irradiance at cloud top as in Eq. 4.5. The standard layers below the cloud layer are relatively insensitive when compared to the cloud layer.

In Fig. 20, the maximum allowable uncertainty in cloud reflectivity, $\delta \rho_c$, such that Q_{SW} may be determined to within $\pm 0.2°C$ per day for 200 mb thick atmospheric layers is given as a function of cloud top height. Variations of absorptivity do not affect the sensitivity. These data are the result of computations based on a standard pressure layer scheme and also on a cloud centered scheme. Thus, they represent the maximum allowable
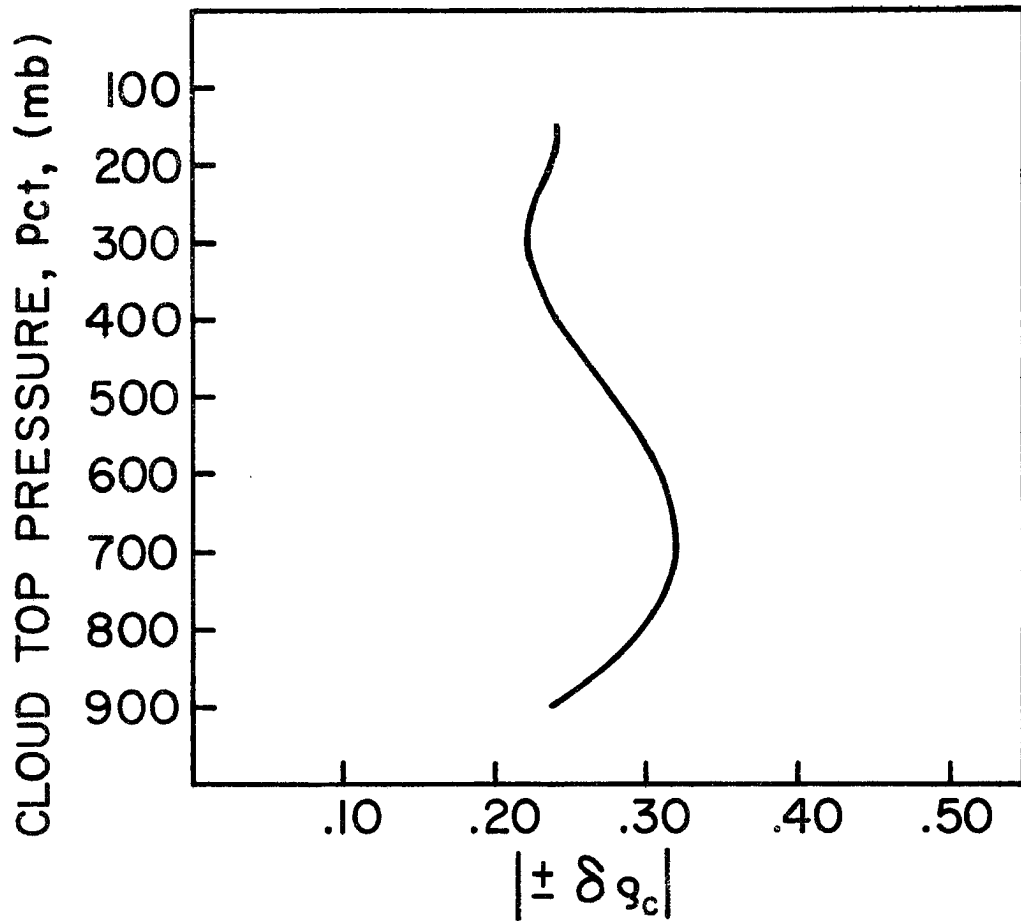
Figure 20. Magnitude of the maximum allowable uncertainty in the short wave reflectivity of a cloud, such that an accuracy in short wave radiative heating rate, δQ_{SW}, of $\pm 0.2°C \cdot day^{-1}$ may be achieved for all standard layers as a function of cloud top height. (i.e. if $\delta \rho_c = \pm x$, then $|\pm \delta \rho_c| = x$)

uncertainty even in the case of close proximity of cloud boundaries and standard pressure layer boundaries. Maximum sensitivity occurs in the cases of very high clouds and very low clouds. For the very high clouds, the layer most sensitive is standard layer 3. This may be seen in Fig. 21, where the curve represents the maximum allowable uncertainty such that the RSP desired accuracy may be fulfilled for each standard pressure layer in the case of a cloud top of 150 mb. Layer 2 is less sensitive because of its significantly smaller water vapor mass compared to layer 3. The sensitivity of lower layers is somewhat less. This is due to the spectral nature of the gaseous absorption. For mid-tropospheric clouds, the layer of maximum sensitivity is the sub-cloud layer where large values of ρ_c greatly suppress the short wave heating. As a cloud is imbedded deeper and deeper into the lower tropospheric water vapor mass, the above-cloud layer sensitivity increases until it is of equal magnitude and opposite sign compared to the sub-cloud layer sensitivity for cloud top below about 700 mb. Since the sensitivity is of opposite sign in the regions above the cloud and of equal magnitude, if a lower level cloud occurs in the center of a standard pressure layer, then the sensitivity of this layer to uncertainty in cloud reflectivity is greatly decreased. The maximum sensitivity is then found in the next standard layer below. This maximum sensitivity is $\delta\rho_c \approx \pm 0.32$ or greater in all cases. Thus, for clouds whose boundaries are in close proximity to standard pressure levels, the proper specification of cloud reflectivity is more critical.

Korb and Möller (1962) have performed theoretical computations of the broadband absorptivity and reflectivity of model clouds. They have reported solar absorption of from 0.07 to 0.21 and reflectivity of from 0.33 to 0.82 for their model clouds. These values correspond well with
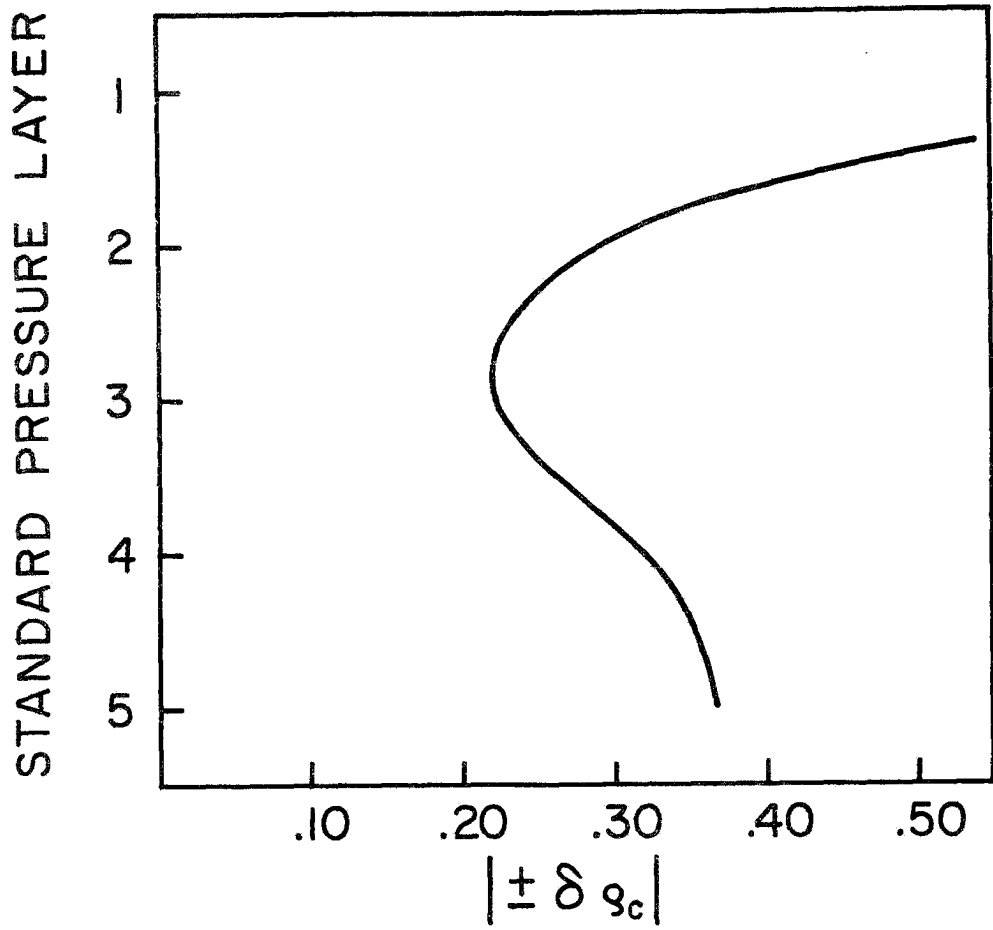
Figure 21. Magnitude of the maximum allowable uncertainty in the short wave reflectivity of a cloud with top at 150 mb, such that an accuracy of $\delta Q_{SW} = \pm 0.2°C \cdot day^{-1}$ may be achieved for each standard layer.

those summarized by Kondratyev (1969) from observational and theoretical work. Kondratyev (1969) and Fleming and Cox (1973) have noted the dependence of a_c and ρ_c on solar zenith angle. Thus, there exists a relatively wide range of values of a_c and ρ_c for natural clouds when compared to the accuracy with which they must be known for our purposes. Therefore, it is evident that some method of specifying these quantities from the field data is needed.

2. Cloud Height

To determine the sensitivity of the short wave radiative warming of the atmosphere to uncertainties in the vertical location of a cloud, tests were made using a cloud with a reflectivity of 0.5 and an absorptivity of 0.05 and 0.10.

In Fig. 22, the TQ_{SW} as a function of cloud top pressure, P_{CT}, is shown. The range of heating rates for a cloud top of from 925 mb to 150 mb and $\delta a_c = \pm 0.025$ does not exceed $\pm 0.2°C$ per day. The shape of these curves is representative for any a_c. The maximum slope occurs at about 350 mb and implies a $\delta p_{CT} = \pm 295$ mb to fulfill this accuracy requirement.

As in the long wave case, it is imperative that the standard layer in which the cloud occurs is known. If a cloud straddles a standard pressure level, the distance from that level to cloud top must be known such that a proper partitioning of the in-cloud absorption between the two layers may be accomplished. If a cloud top is more than 1000 m above a standard level, then the absorption is primarily in the upper layer. This may be inferred from the data presented by Korb and Möller (1962). Once the standard layer in which the cloud occurs is determined, the allowable uncertainty in the location of that cloud within that layer such that
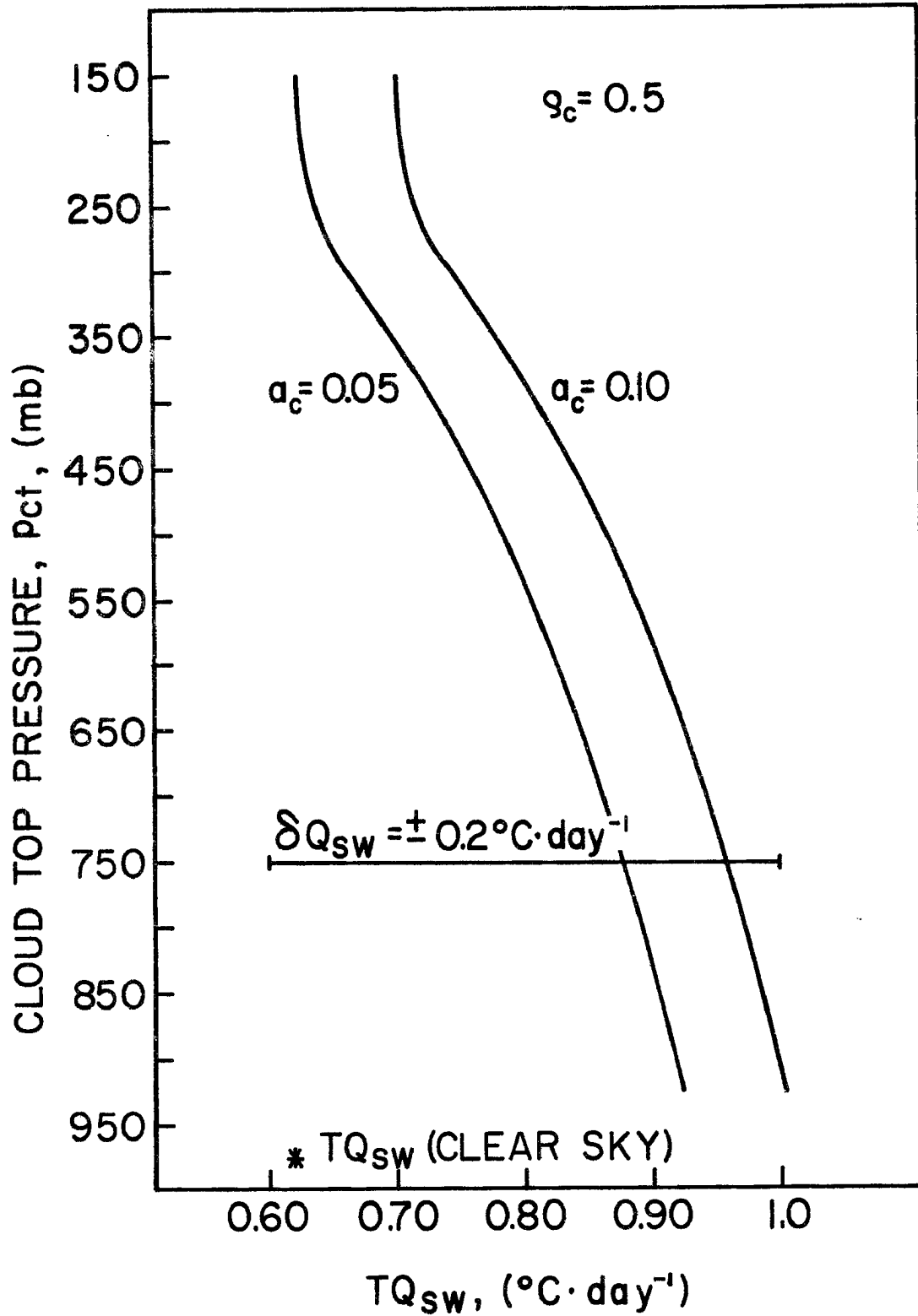
Figure 22. Daily short wave heating rate for the total atmospheric
column as a function of cloud top height for clouds with
short wave broadband absorptivities of 0.05 and 1.10.
The clear sky short wave heating is noted.

Q_{SW} may be determined to within $\pm 0.2°C$ per day for all standard layers may be seen in Fig. 23. A relative minima of $\delta p_{CT} = \pm 55$ mb occurs for clouds in the 400 mb to 600 mb layer. It is evident that simply locating in which layer the cloud occurs is nearly sufficient except in the case of boundary proximity to a standard level. The only effect of increasing the cloud absorptivity is to increase the sensitivity when the cloud boundary is in close proximity to a standard pressure level. The sensitivity tends to decrease slightly with increasing cloud reflectivity. This is particularly true of upper and middle tropospheric clouds.

3. Areal Cloud Cover

The tolerable uncertainty of areal cloud cover, as is used here, is identical with that given by Eq. 4.8 except that Q_{SW} was subtituted for Q_{IR}. Thus, the results are normalized to the clear sky case, as before. The cloud reflectivity was assumed to be 0.5. Effects due to variations of this quantity are discussed below.

For clouds with absorptivities ranging from 0.025 to 0.20, the areal cloud cover need not be known to better than $\delta\alpha = \pm 50\%$ to deduce the TQ_{IR} to within $\pm 0.2°C$ per day for clouds at any level of the tropical atmosphere. Figure 24 displays the $\delta\alpha$ required to achieve an accuracy of $\delta Q_{SW} = \pm 0.2°C$ per day for all standard pressure layers for $a_c = 0.025$, 0.05 and 0.1. The plotted points correspond to the accuracy needed for the standard layer in which the cloud occurs. The standard layers above and below the cloud layer are relatively insensitive. It is noted that as cloud top approaches the lower boundary of a layer, the sensitivity is maximized. This is because both the heating due to cloud absorption and increased heating above the cloud due to the reflected irradiance are
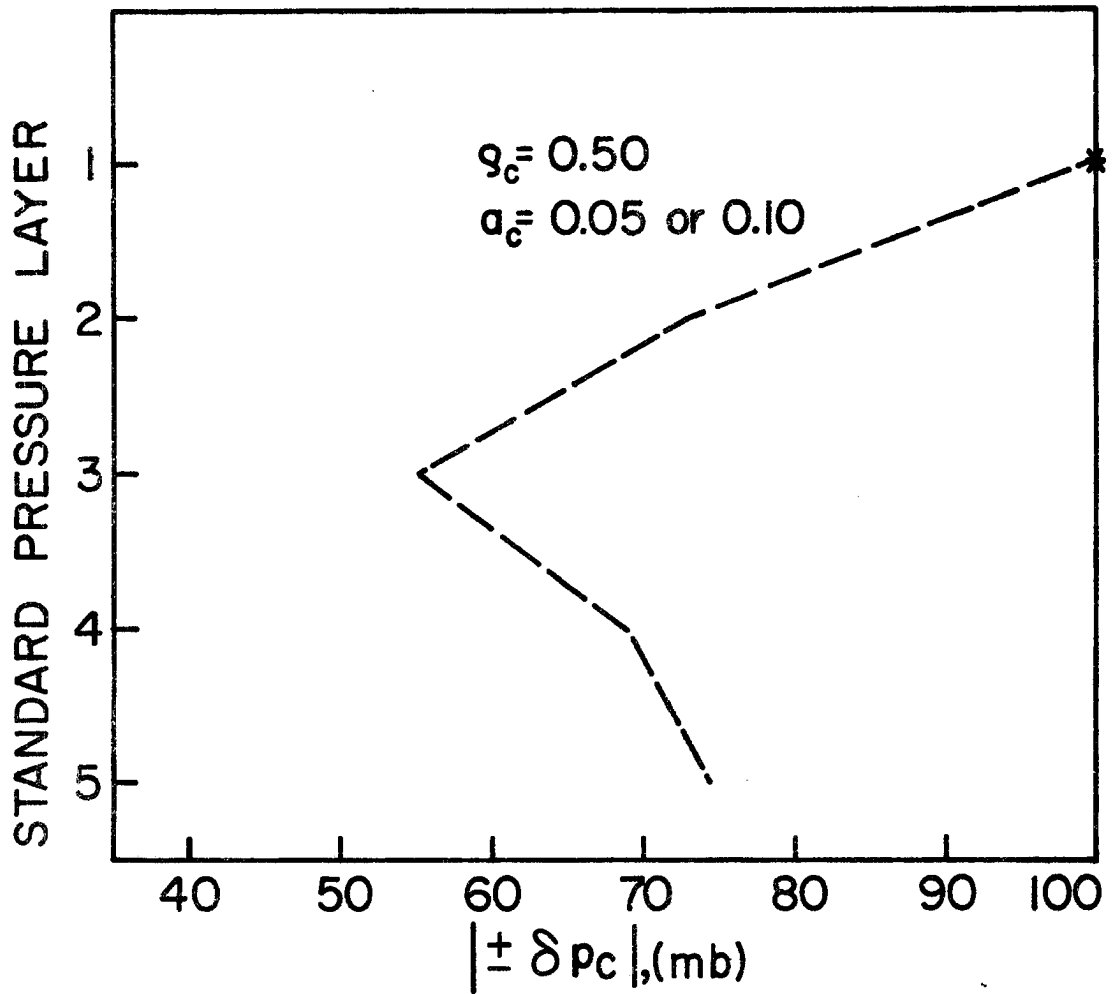
Figure 23. Magnitude of the maximum allowable uncertainty in the location of cloud top height within a standard layer, such that an accuracy of $\delta Q_{SW} = \pm 0.2°C \cdot day^{-1}$ may be achieved for all standard layers.
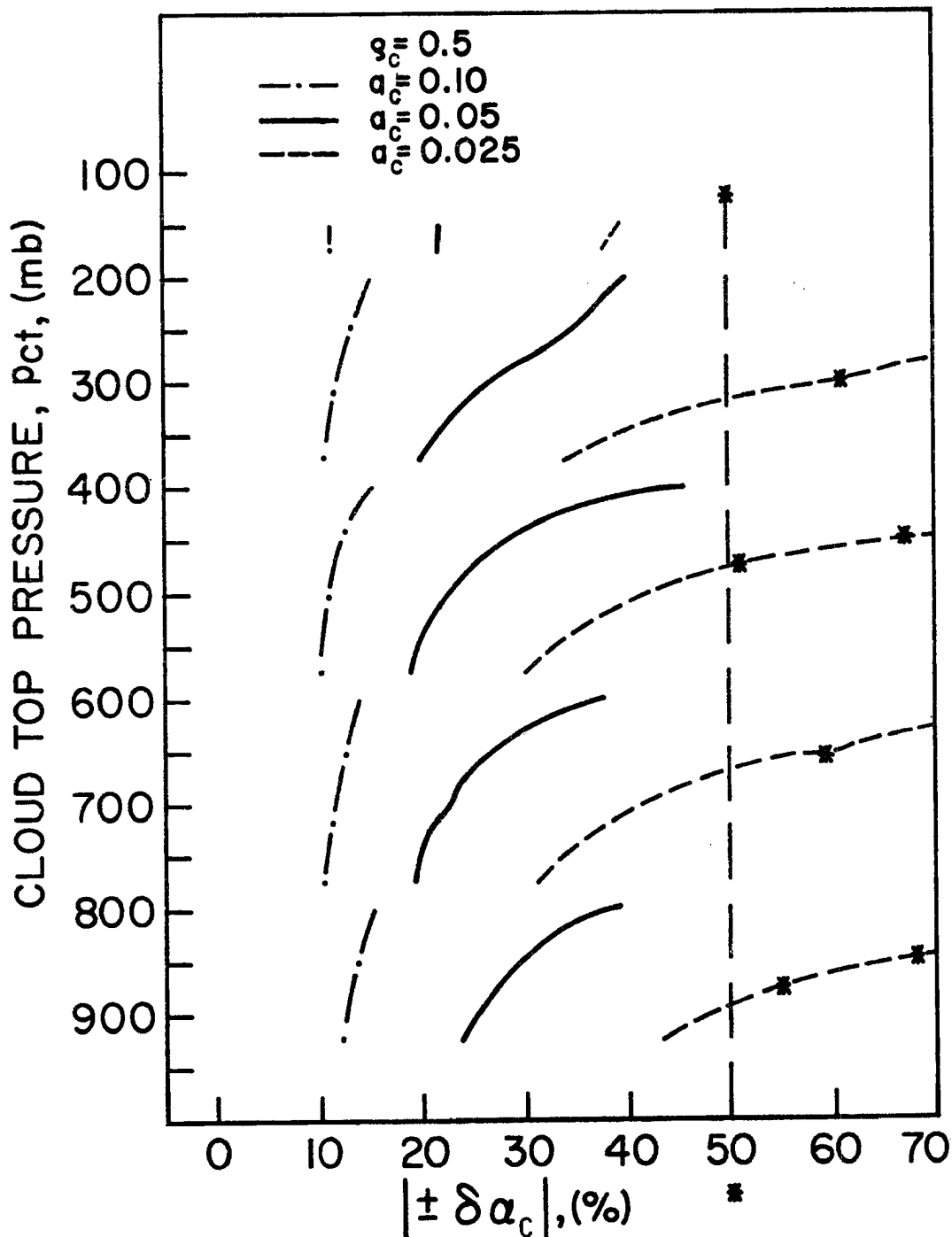
Figure 24. Magnitude of the maximum allowable uncertainty in the specification of areal cloud cover, such that an accuracy of $\delta Q_{SW} = \pm 0.2°C \cdot day^{-1}$ may be achieved, as a function of cloud top height for various values of cloud short wave absorptivity and a cloud short wave reflectivity of 0.50.

concentrated within that layer. Thus, the maximum accuracy required is $\delta\alpha \simeq \pm 30\%$, $\pm 20\%$, and $\pm 10\%$ for cloud absorptivities of a_c = 0.025, 0.05, and 0.10, respectively.

A higher value of cloud reflectivity increases the sensitivity in the standard layer above that in which the cloud occurs; very high values of ρ_c increase substantially the sensitivity of the standard layers below the cloud layer. However, in the case of high cloud reflectivity, the cloud absorptivity is large, as in the case of a cloud of large vertical extent. Thus, the cloud layer still predominates in this regard. Therefore, even for the case of high cloud reflectivity, the above limiting values are representative. For lower values of cloud reflectivity, consider that a cloud which reflects only a small portion of the incident solar irradiance also absorbs only a small portion; therefore, the cloud layer sensitivity decreases.

4. The Multi-Layered Configuration

In the situation of multiple cloud layers, the uncertainty allowed in the description of the upper-most cloud layer, i.e. δa_c, $\delta\rho_c$, $\delta\alpha$, δp_{CT}, remains the same as in the case of a single cloud layer. Since an overlying cloud layer decreases the solar irradiance available to interact with lower level cloud layers, the sensitivity of Q_{SW} to the description of the lower cloud layer is also decreased. This relation may be approximated by

$$\delta x_u' = \{ \frac{1}{(1 - a_0 - \rho_0)} \} \, \delta x_u \qquad (4.10)$$

where x is one of the factors needed for the cloud description, i.e. a_c, ρ_c, p_{CT}, α; and u and o refer to the underlying and overlying cloud layers, respectively. Thus, for example, in the case of a cirrus cloud with

p_c = 0.3 and a_c = 0.05, the uncertainty allowed in the specification of the absorptivity of an underlying water cloud at 900 mb may be approximated as $\delta a_c'$ = ± 0.023. This compares to a value of δa_c = ± 0.015, when there is no overlying cloud layer.

For clouds of similar microphysical properties, which may be anticipated to have similar spectral interaction with the irradiance fields, the radiative properties prescribed for the lower layer in a multilayered configuration should be less in magnitude than in the case of a single cloud layer.

V. IMPLICATIONS FOR AN OBJECTIVE CLOUD FIELD DETERMINATION

A. Cloud Radiative Properties

Based on the foregoing analyses, it is evident that if the RSP objectives are to be met, then it is imperative that information as to the infrared emissivity, short wave absorptivity and reflectivity, and diffusivity of transmitted short wave irradiance associated with the cloud fields be generated. Further efforts should be made to explicitly quantify relationships among the radiative properties for particular cloud types by theoretical or observational means. Various authors (e.g. Korb and Möller (1962), Davis (1970), Hansen (1971), Hunt (1973), Shenk and Curran (1973), and Platt (1974, 1975)) have presented data from which such relationships could be derived. However, their data are limited to the particular model or natural clouds considered and in some cases to small spectral intervals. It is unlikely that they are representative for all the major cloud forms occurring in the GATE area. It may be concluded from their results that the general relationship of a positive correlation of ϵ^*, a_c, and ρ_c for a given cloud type exists,

i.e. $\dfrac{\partial \epsilon^*}{\partial a_c}$, $\dfrac{\partial \epsilon^*}{\partial \rho_c}$, $\dfrac{\partial \rho_c}{\partial a_c}$, $\dfrac{\partial \rho_c}{\partial \epsilon^*}$, $\dfrac{\partial a_c}{\partial \rho_c}$ and $\dfrac{\partial a_c}{\partial \epsilon^*} \geq 0$. (5.1)

It may also be seen that,

$$\frac{\partial \epsilon^*}{\partial (\Delta p_c)}, \quad \frac{\partial a_c}{\partial (\Delta p_c)} \quad \text{and} \quad \frac{\partial \rho_c}{\partial (\Delta p_c)} \geq 0. \qquad (5.2)$$

Thus, for example, a thick water cloud tends to have a large ϵ^* approaching unity. The short wave absorptivity and reflectivity are also maximized, and the transmitted solar irradiance is predominantly diffuse. Knowledge of the exact magnitude of the terms in Eq. 5.2 along with appropriate boundary conditions for various cloud types would enable the radiative properties to be specified as a function of basic parameters, such as p_{CT} and Δp_c.

For the nighttime situation, only the ε^* must be specified. The ε^* prescribed must meet the tolerances given in IV.B.1.

For the daytime situation, ε^*, a_c, and ρ_c must be specified. It is likely that equations utilizing the coefficients given in Eq. 5.1 and 5.2 will be used to deduce the radiative properties of clouds from observations of one or more of the quantities a_c, ρ_c, ε^*, p_{CT}, and Δp_c. If it is hypothesized that the correct magnitudes of the coefficients and the appropriate boundary conditions are known for the various cloud forms, then a decrease in the sensitivity of Q_R to the specification of the cloud radiative properties results. That is, if an overestimate is made of the ε^* of a cloud then the estimates of a_c and ρ_c are also too large. However, a positive error in each of these quantities results in corresponding errors in Q_R which tend to cancel in some of the different layers.

For example, the maximum allowable uncertainty in ε^*, a_c and ρ_c such that Q_R may be determined to within $\pm 0.2°C$ per day for a cloud with $p_{CT} = 500$ mb and $\Delta p_c = 100$ mb for the 200 mb thick layers above and below the cloud and for the cloud layer itself, is shown in Fig. 25. An asterisk implies no significant dependency. These maximum allowable uncertainties were derived independently as in previous sections. It is noted that the magnitudes of $\delta\varepsilon^*$, δa_c and $\delta\rho_c$ are not directly comparable. An absolute error in ε^* is not numerically equivalent to the absolute error in a_c or ρ_c but is dependent upon the hypothesized formulation. Thus, an error in ε^* of +0.20 may correspond to errors in a_c and ρ_c of +0.05 and +0.10, respectively. Considering the above cloud layer, a positive error in ε^* and ρ_c results in a positive error in Q_R for this layer. The errors due to the overestimation of each radiative property are of the same sign and cumulative. However, this is the least sensitive layer.
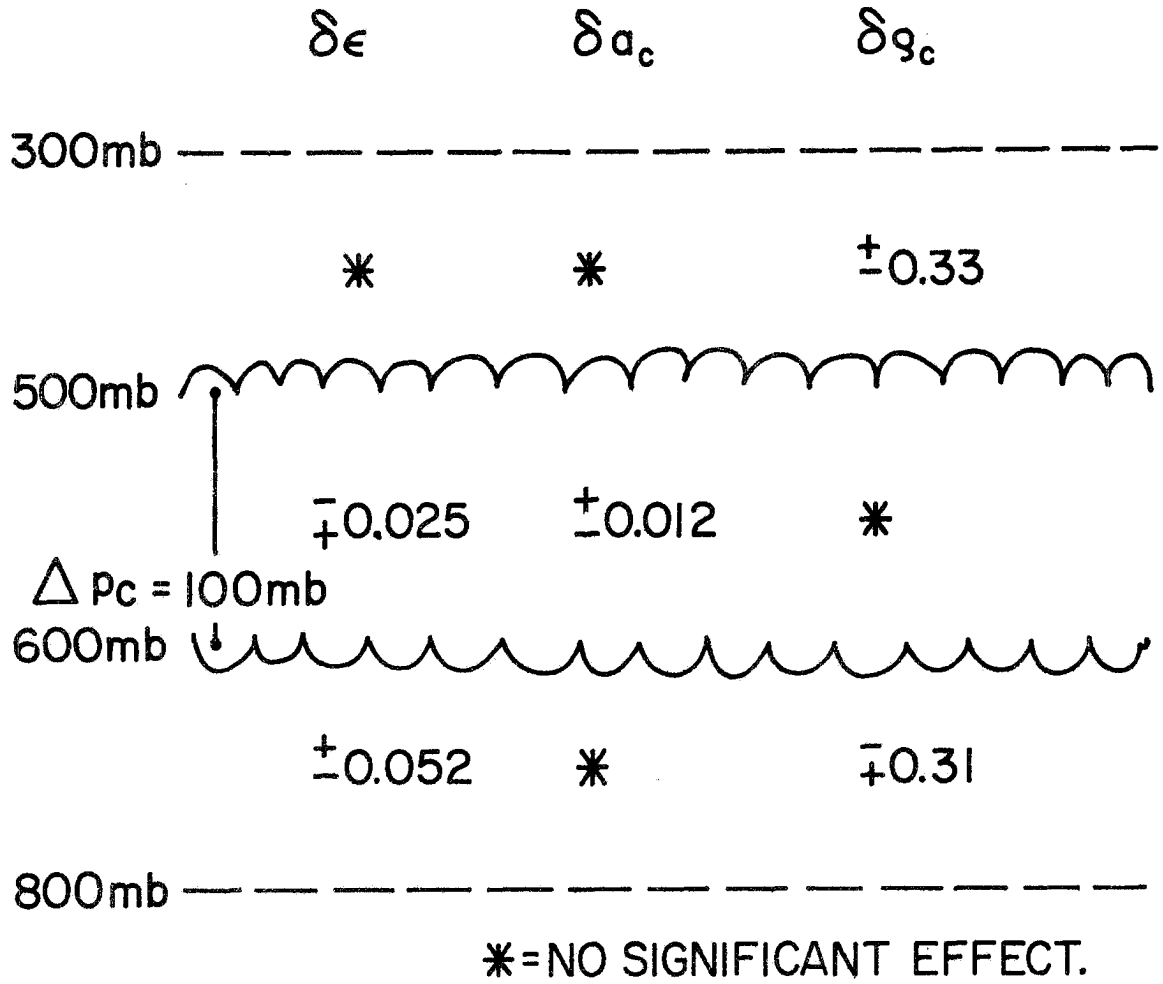
Figure 25. Maximum allowable uncertainty in the infrared and short wave radiative properties of a 100 mb thick cloud with cloud top of 500 mb, such that an accuracy of $\delta Q_{IR} = \delta Q_{SW} = \pm 0.2°C \cdot day$ may be achieved for the cloud layer and the 200 mb thick layers immediately above and below the cloud. An asterisk denotes no significant requirement.

For the cloud layer, the induced errors in Q_R due to the positive errors in ϵ^* and a_c are of opposite sign. A cancellation takes place. Thus, Q_R in this layer is less sensitive to consistent errors in ϵ^* and a_c than to independent errors. The below cloud layer is sensitive to the ϵ^*, a_c, and r_c specified. However, as in the cloud layer, the errors induced in the short wave at least partially cancel the error induced in the long wave region. Thus, the two layers exhibiting the largest sensitivity to the cloud radiative properties prescribed are less sensitive in the daytime if the radiative properties are specified in a consistent fashion. Therefore, the maximum allowable uncertainty of the radiative properties is larger in the daytime than at night.

In lieu of the development of adequate methods of specifying the radiative properties of clouds, any data pertaining to these quantities should be retained in an objective cloud field determination.

B. Cloud Height

With respect to the nighttime situation, the results given in section IV.B.2 are definitive. For the daytime, the long wave and short wave analyses must be combined. In Fig. 26, the allowable uncertainty of cloud top pressure such that an accuracy of $\delta Q_R = \pm 0.2°C$ per day may be achieved for all standard pressure layers as a function of the layer in which the cloud occurs is shown by the solid curves. It was assumed that the standard layer in which the cloud occurs is known. For comparison, the results shown in Figs. 14 and 23, which were derived for $\delta Q_{IR} = \delta Q_{SW} = \pm 0.2°C$ per day for all standard layers, are shown as dotted and dashed curves, respectively. The set of curves represents the cases of a thin ice cloud, a thick ice cloud, and a typical water cloud.
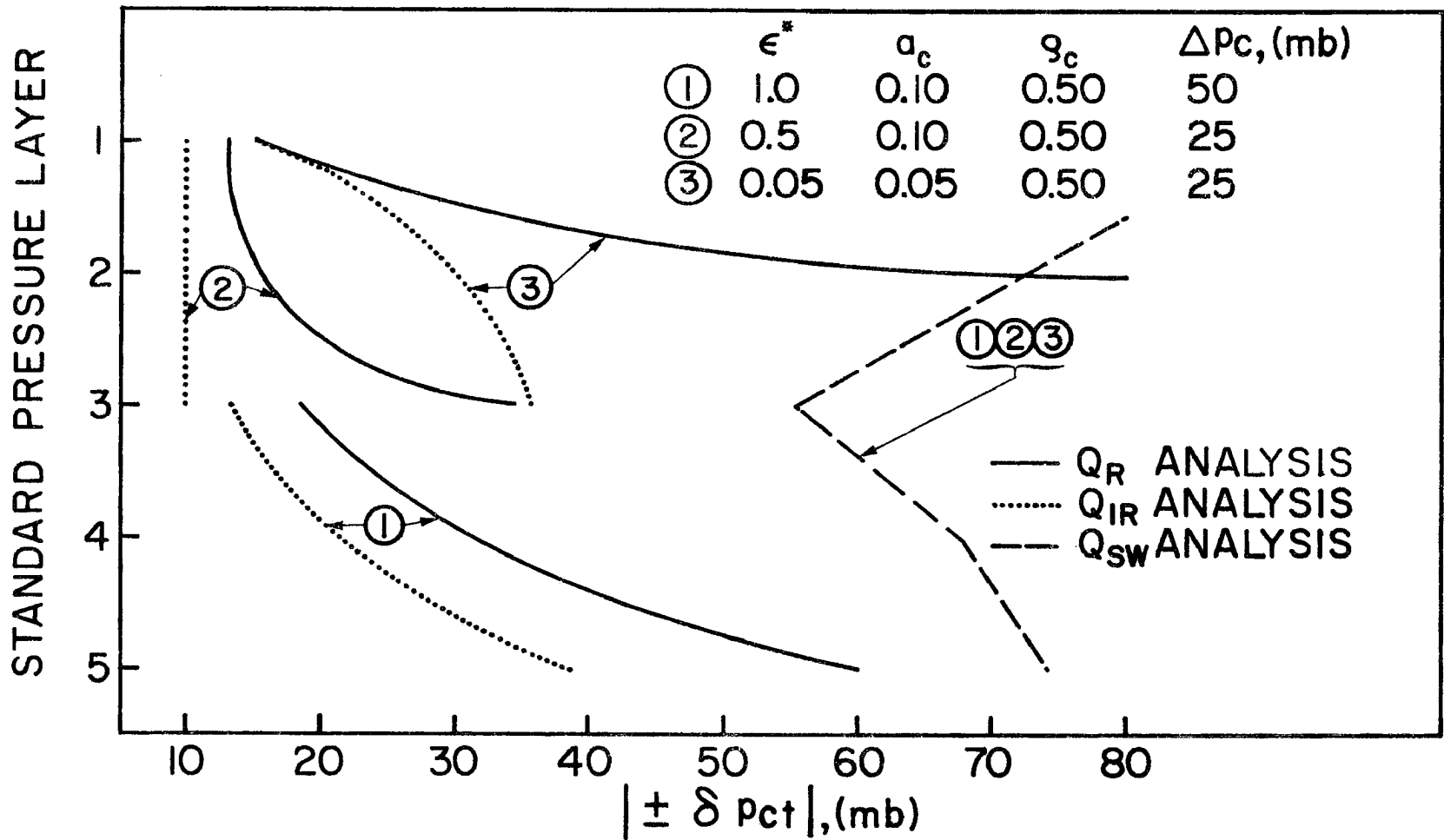
Figure 26. Magnitude of the maximum allowable uncertainty in the location of cloud top height, within a standard layer, such that an accuracy in the radiative heating rate, δQ_R, of $\pm 0.2°C \cdot day^{-1}$ may be achieved for all standard layers for clouds which possess infrared and short wave radiation properties and cloud thicknesses as noted. Curves corresponding to the short wave and infrared components for the same clouds are also drawn.

It is evident that in the daytime case, the location of cloud top need not be as precise as in the nighttime case. As noted previously, the standard pressure layer in which the cloud occurs must be known to avoid large errors in the vertical distribution of Q_R. The allowable uncertainty of the cloud location when the cloud is within 500 m to 1000 m of a standard pressure level is on the order of $\pm$100 m. This is true for both the nighttime and daytime cases.

C. Area Cloud Cover

The results given in section IV.B.3 describe the sensitivity in the nighttime situation. For the daytime case, the allowable uncertainty in areal cloud cover in percent as a function of cloud top pressure is shown in Fig. 27 for the case of water clouds and thick and thin ice clouds. Compared to the nighttime case, Fig. 17, more information is required for the lower tropospheric water clouds and very high ice clouds. Less information is required as to the area cloud cover of ice clouds in the 200 mb to 400 mb layer. For the situation of middle tropospheric water clouds, there is no real difference. The slope of the curves tends to change in the vicinity of the standard pressure levels. This is particularly true at upper and middle levels. This is a reflection of the change in the standard pressure layer in which the cloud occurs and, thus, the change in the relative position of the cloud within the layer in which it occurs. Errors in the areal cloud cover exceeding approximately $\pm$10% to $\pm$ one octal can be expected to seriously compromise a radiative divergence calculation.
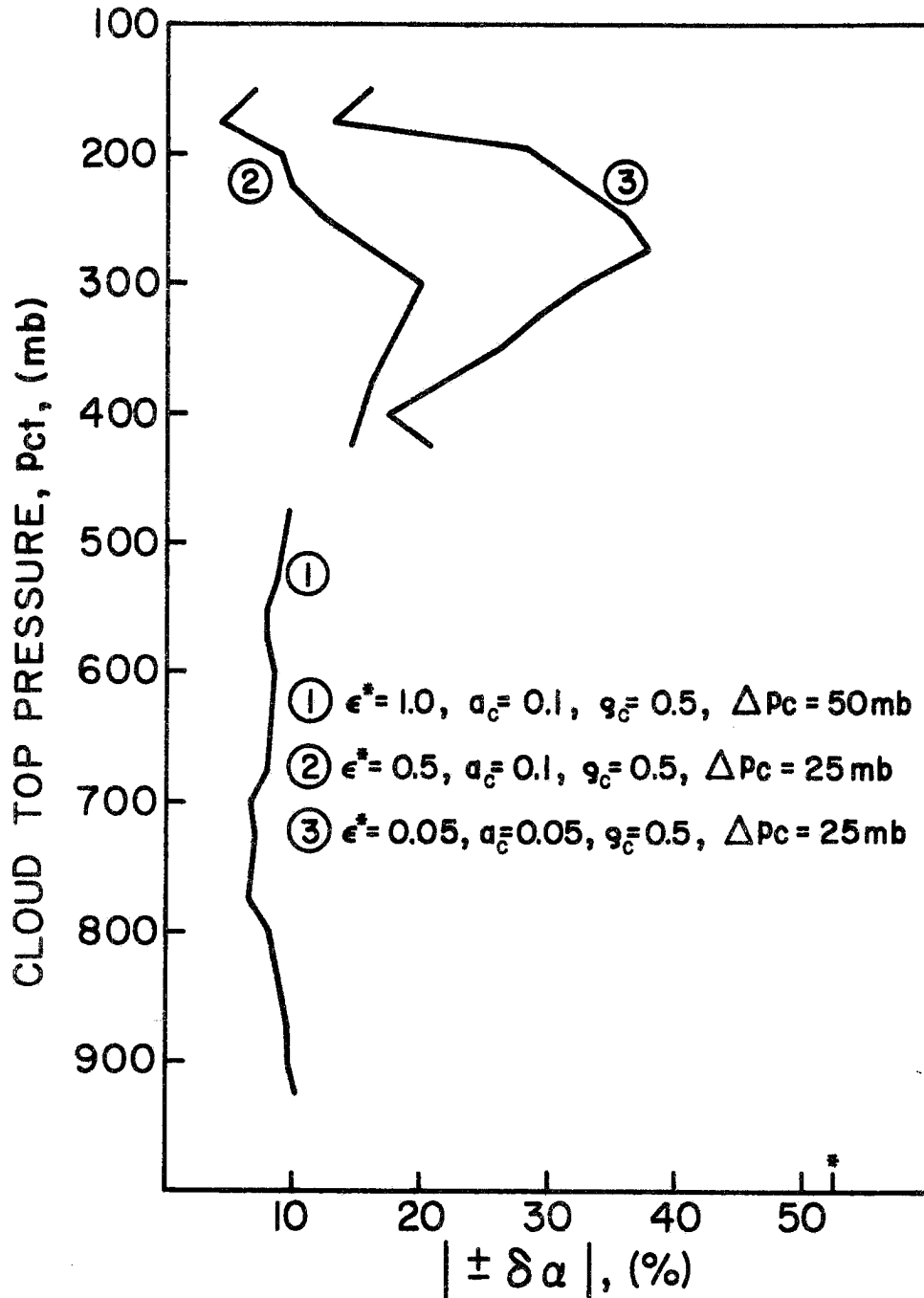
Figure 27. Magnitude of the maximum allowable uncertainty in
the specification of areal cloud cover, such that
an accuracy of $\delta Q_R = \pm 0.2°C \cdot day^{-1}$ may be achieved
for all standard layers, as a function of cloud top
height for clouds which possess the infrared and
short wave radiative properties and cloud thicknesses
as noted.

D. Simultaneous Uncertainty of Various Cloud Parameters

The previous analyses were performed by determining the sensitivity of Q_R, Q_{SW}, and Q_{IR} to uncertainties in the cloud radiative properties, cloud height, and areal cloud cover in an independent fashion where some or all factors relating to the cloud field description other than that being tested were held constant. An objective analysis scheme, which generates a description of the cloud fields from field data, is likely to exhibit some uncertainty in all factors simultaneously. However, in the process of generating the cloud field description, some factors may be determined in a dependent manner. Thus, the case of multiple uncertainty and particularly the case of dependent uncertainties must be evaluated in light of the RSP accuracy requirements. To this purpose, three example cases are presented. In Table 6, the values of $\delta\varepsilon^*$, δp_{CT}, and $\delta\alpha$ are given for each standard layer for the situation of cloud top at 200 mb, 500 mb, and 800 mb, respectively. All clouds were assumed to be 100 mb thick. The data entries are the maximum uncertainty allowed in ε^*, p_{CT}, and α of the given cloud such that an accuracy of $\delta Q_{IR} = \pm 0.2°C\cdot day^{-1}$ may be achieved for the layer. They result from the analyses reported in section IV.B. The layer in which the cloud occurs was assumed to be known. Thus, the values of $\delta\varepsilon^*$, δp_{CT}, and $\delta\alpha$ quantify the degree of sensitivity of Q_{IR} to each factor. Large values should be viewed in this light. These examples portray the nighttime situation.

Considering the case of cloud top of 200 mb, the sign of each allowable uncertainty given in Table 6 is the same in all standard layers except in layers 1 and 2, where the sign of δp_{CT} is opposite to that of $\delta\varepsilon^*$ and $\delta\alpha$. This implies that an error in Q_{IR} due to an overestimate/ underestimate of any one factor is at least partially compensated in

Table 6. Maximum allowable uncertainty in the specification of the effective infrared broadband emissivity, $\delta\epsilon^*$, the cloud top location, δp_{CT}, and the areal cloud cover, $\delta\alpha$, of a cloud to achieve an accuracy of $\delta Q_R = \delta Q_{IR} = \pm 0.2°C \cdot day^{-1}$ for each standard layer and the total atmospheric column for clouds contained within standard layers 2, 3, and 5, i.e. approximate cloud top heights of 200 mb, 500 mb, and 800 mb, respectively. Table 6 is continued on the next page.

$p_{CT} = 200$ mb, $\Delta p_C = 100$ mb				
LAYER	$\delta\varepsilon^*$	δp_{CT}, (mb) $\varepsilon^* = 0.5$	$\delta\alpha$, (%) $\varepsilon^* = 1.0$	$\delta\alpha$, (%) $\varepsilon^* = 0.5$
1	∓0.15	+100	∓66	∓35
2	±0.08	∓10	+30	±15
3	±0.13	+50	+25	+13
4	±0.15	+57	+23	+13
5	±0.19	+104	+20	+13
TQ_{IR}	±0.20	∓127	±36	+19

$p_{CT} = 500$ mb, $\Delta p_C = 100$ mb				
LAYER	$\delta\varepsilon^*$	δp_{CT}, (mb) $\varepsilon^* = 1.0$	$\delta\alpha$, (%) $\varepsilon^* = 0.5$	$\delta\alpha$, (%) $\varepsilon^* = 1.0$
1	∓2.81	+604	∓98	∓84
2	∓1.74	+738	∓282	∓153
3	∓0.04	∓13	∓34	∓6
4	±0.04	+36	±23	+7
5	±0.16	+70	±11	+9
TQ_{IR}	±0.76	∓290	±110	±71

$p_{CT} = 800$ mb, $\Delta p_C = 100$ mb				
LAYER	$\delta\varepsilon^*$	δp_{CT}, (mb) $\varepsilon^* = 1.0$	$\delta\alpha$, (%) $\varepsilon^* = 0.5$	$\delta\alpha$, (%) $\varepsilon^* = 1.0$
1	∓5.16	+604	∓172	∓147
2	∓16.0	+738	∓556	∓500
3	∓2.91	+165	∓350	∓286
4	∓0.15	+120	+180	∓56
5	±0.16	∓33	+98	+24
TQ_{IR}	+8.0	∓290	±298	+364

layers 3, 4, and 5 if there is a corresponding underestimate/overestimate
of either of the other two factors. However, the standard layer most
sensitive to an error in either of these quantities differs according
to the factor considered. Layer 2 is most sensitive to errors in ε^* or
p_{CT}. Lower tropospheric layers are most sensitive to errors in α. Note
that a positive error in p_{CT} implies the cloud height estimate is lower
in the troposphere than it actually is. One of the primary data sources
for an objective cloud field determination scheme, particularly at upper
levels, is the infrared satellite observations. In the interpretation
of such data, the ε^*, p_{CT} and α of clouds are solved for in a dependent
fashion (Smith, et al., 1974). The infrared radiative flux, H_o, which
the satellite sensor samples, may be approximated in a gross way as:

$$H_o = (1-\alpha) \cdot H_s + \alpha\{(1- \varepsilon^*) H_s + \varepsilon^*\sigma T_{CT}^4\} \qquad (5.3)$$

where H_s is the upward infrared flux from the earth's surface and the
lower troposphere, σ is the Stefan-Boltzman constant, and T_{CT} is the
cloud top temperature. It is noted that $H_s \geq H_o$ and $H_s \geq T_{CT}^4$. Thus,
a positive/negative error in the estimate of the ε^* of a cloud results
in a negative/positive error in the estimate of α and/or a positive/
negative error in the estimate of p_{CT}. If, for example, the estimate of
ε^* for a moderately thick upper tropospheric cloud is 0.08 too high,
then the induced error in Q_{IR}, in $°C \cdot day^{-1}$, is -0.11, +.20, +0.12, +0.11,
and +0.09 for layers 1 through 5, respectively. However, if the over-
estimate of ε^* generates an overestimate of p_{CT} of 10 mb, then the
induced error in Q_{IR} through the cumulative effect of the errors in both
ε^* and p_{CT} is -0.15, 0.0, +0.16, +0.14, and +0.11 $°C \cdot day^{-1}$ for layers 1-5,
respectively. Thus, in the case of a dependent relation between errors

in ε^* and p_{CT}, there is a degradation in layers 1, 3, 4 and 5. Schemes solving for ε^* and p_{CT} in a dependent manner tend to minimize the effect of any errors in the layer in which the cloud occurs. However, the error in all other layers is increased. In the same way, if an error in the estimate of ε^* of +0.08 generates an error in α of -20%, then the resultant cumulative error in Q_{IR} is +0.05, +0.07, -0.04, -0.06, and -0.11°C·day^{-1} for layers 1-5, respectively. Thus, in the case of a dependent relation between errors in ε^* and α, there is improvement in the accuracy of Q_{IR} in all layers except for layer 5, where there is a slight decrease in the accuracy. For no layer does the cumulative error exceed the RSP accuracy requirements. This implies that schemes solving for ε^* and α in a dependent fashion tend to reduce the error in Q_{IR} at most levels and, consequently, satisfy the RSP requirements. The same general conclusions result in the case of a cloud in layer 1. The cumulative error in layers 2-5 is large if ε^* and p_{CT} are deduced in a dependent fashion. The error in Q_{IR} is reduced in all layers in the case of a dependent solution for ε^* and α. Layer 2 exhibits the largest error in this case. Therefore, any objective cloud field determination scheme relying on satellite data to generate upper level cloud field statistics should attempt to specify the cloud height and also thickness from independent data sources such as rawinsonde and aircraft observations. If this is done, then the infrared satellite data may be used to generate values of ε^* and α in a dependent manner. This would assure the highest degree of accuracy in the determination of Q_{IR}.

Consider the case of a thick mid-tropospheric cloud. For a cloud top of 500 mb, layers 1 and 2 are virtually completely insensitive to errors in the estimate of ε^*, p_{CT}, and α. The sign of each allowable

uncertainty in layers 3, 4, and 5 are the same. Therefore, in all layers where there is a significant effect, an underestimate/overestimate of any one parameter is at least partially compensated if there is a corresponding overestimate/underestimate of either of the other two factors. If, for example, an overestimate of ε^* of 0.04 is made, then the resultant error in Q_{IR} is -0.20, +0.12, +0.02°C·day^{-1} for layers 3, 4, and 5, respectively. An error in ε^* of +0.04 and a consequent error in p_{CT} of +13 mb induces a cumulative error in Q_{IR} of -0.4, +0.2, and +0.05°C·day^{-1} in layers 3, 4, and 5, respectively. An error in ε^* of +0.04 and a consequent error in α of -6% induce a cumulative error in Q_{IR} of 0.0, -0.05, and -0.12°C·day^{-1} for layers 3, 4, and 5, respectively. Thus, if ε^* and p_{CT} are generated in a dependent fashion, then there is substantial degradation in the accuracy of Q_{IR} in all layers where there is a significant sensitivity. This is particularly true for the layer in which the cloud occurs. If ε^* and α are generated in a dependent fashion, then there is substantial improvement in the accuracy of Q_{IR} in layers 3 and 4. However, the high sensitivity of layer 5 to errors in α, coupled with the decreased sensitivity to ε^* in this layer, results in an increase in the cumulative error in Q_{IR} in this layer. Therefore, an objective cloud field determination scheme which generates ε^* and α in a dependent fashion, as from satellite infrared data, for middle tropospheric clouds may yield a much higher degree of accuracy in the resultant Q_{IR} values compared to a scheme which generates these parameters in an independent fashion. This implies that such a scheme should attempt to use such data sources whenever possible, when attempting to deduce statistics relating to middle tropospheric clouds. As in the case of high cloudiness, independent information as to the proper p_{CT} is more desirable than for α.

It may also be noted here that if the assumption of an $\varepsilon^* = 1.0$ for a tropical water cloud is employed, which may tend to be slightly too high, and the cloud top height is determined from radar data, which tends to give a positive error in p_{CT} (Mason, 1971; and Battan, 1973), then the cumulative errors in Q_{IR} due to each of these factors are in the same direction. Thus, much care is required in the interpretation of radar data with the above assumption to avoid large errors in Q_{IR}. If radar data is used to estimate α, which tends to underestimate α, and ε^* is assumed to be unity, then the cumulative errors in Q_{IR} due to each of these factors are in the opposite direction. Thus, there is a favorable aspect in utilizing radar data to estimate α if there is a tendency to overestimate ε^*.

In the case of the lower tropospheric cloud with cloud top of 800 mb, layers 1, 2, and 3 are very insensitive to the specification of either ε^*, p_{CT}, or α. Moreover, layer 4 is relatively insensitive to the p_{CT} or α prescribed. In layers 4 and 5 the sign of the allowable uncertainty of ε^* and α given in Table 6 is the same, the sign of δp_{CT} is the opposite. As before, this implies that if ε^*, p_{CT}, and α are solved for in a dependent fashion from the satellite data, then the induced error in Q_{IR} is less than the case of independent errors. However, it is unlikely that satellite data could be used to generate cloud statistics for such low clouds. The presence of overlying clouds or haze, which are relatively active in the "atmospheric window", greatly limits the usefulness of satellite observations. Therefore, it may not be possible to determine ε^*, p_{CT}, and α in a dependent fashion at lower levels. If the values of ε^*, p_{CT}, and α are generated from independent information at this or any level of the troposphere, the allowable uncertainty of ε^* is $b\delta\varepsilon^*$, of p_{CT}

is $c\delta p_{CT}$, and of α is $d\delta\alpha$, where $b + c + d = 1.0$ and the δ values are those limiting values given previously. Thus, it is desirable to know as many parameters as accurately as possible so that the tolerable uncertainty in any one parameter, which may be very difficult to evaluate from the field data, is as large as possible. In this way, the Radiation Subprogram desired accuracy is most likely to be met.

For the daytime situation, the effect described in section V.A. must be combined with the results given in sections IV.D.2 and IV.D.3. It is unrealistic to attempt to quantitatively evaluate the cumulative effect of multi-uncertainty in the estimate of cloud field parameters at this time due to the lack of adequate knowledge of the relationship of ϵ^*, a_c, and ρ_c postulated in section V.A. However, a qualitative understanding of the cumulative effects of multi-uncertainty may be gained by comparing the values listed in Table 7 to those given in Table 6. The data entries in Table 7 are the maximum allowable uncertainty of ϵ^*, p_{CT}, and α such that an accuracy of $\pm0.2°C \cdot day^{-1}$ may be achieved in a determination of Q_R. The same example cases are considered. The cloud top heights and thicknesses are the same. Additionally, in Table 7, in the determination of δp_{CT} and $\delta\alpha$ for the cloud at 200 mb, the cloud was assumed to have a long wave emissivity of 0.5 and a short wave reflectivity of 0.5 and a short wave absorptivity of 0.1. For cloud top at 500 mb and 800 mb, δp_{CT} and $\delta\alpha$ were determined for a cloud with $\epsilon^* = 1.0$, $\rho_c = 0.5$, and $a_c = 0.1$. The values of $\delta\epsilon^*$ are the same as given in Table 6.

In the case of the cloud at 200 mb, if the uncertainty in ϵ^* is coupled to the uncertainty in a_c and ρ_c as in section V.A., then the net effect of a consistent simultaneous error in ϵ^*, a_c, and ρ_c may be represented by increasing the value of $\delta\epsilon^*$ in layers 2, 3, 4, and 5. The

Table 7. Same as Table 6, except for an accuracy of $\delta(Q_{IR} + Q_{SW}) = \delta Q_R = \pm 0.2°C \cdot day^{-1}$. Note the values of δp_{CT} and $\delta \alpha$ were derived for clouds with $a = 0.10$ and $\rho = 0.50$. Table 7 is continued on the next page.

p_{CT} = 200 mb, Δp_C = 100 mb			
LAYER	$\delta\epsilon^*$	δp_{CT}, (mb) ϵ^* = 0.5	$\delta\alpha$, (%) ϵ^* = 0.5
1	$\mp$0.15	$\mp$128	$\mp$232
2	+0.08	$\mp$ 25	+ 9
3	+0.13	$\pm$ 58	+ 79
4	+0.15	$\pm$ 56	+ 53
5	+0.19	+ 72	+ 29
TQ$_R$	+0.20	$\mp$105	+ 27

p_{CT} = 500 mb, Δp_C = 100 mb			
LAYER	$\delta\epsilon^*$	δp_{CT}, (mb) ϵ^* = 1.0	$\delta\alpha$, (%) ϵ^* = 1.0
1	+2.81	+625	$\mp$126
2	$\mp$1.74	>+1000	$\mp$541
3	$\mp$0.04	$\mp$190	$\mp$ 17
4	+0.04	$\pm$ 45	+ 9
5	+0.16	+555	+ 9
TQ$_R$	+0.76	$\mp$195	+ 34

p_{CT} = 800 mb, Δp_C = 100 mb			
LAYER	$\delta\epsilon^*$	δp_{CT}, (mb) ϵ^* = 1.0	$\delta\alpha$, (%) ϵ^* = 1.0
1	$\mp$5.16	+1000	$\mp$303
2	$\mp$16.0	>+1000	>$\mp$500
3	$\mp$2.91	>+1000	>+500
4	$\mp$0.15	+ 47	$\mp$286
5	+0.16	$\mp$ 30	+ 8
TQ$_R$	+8.0	>$\mp$1000	+ 45

sign remains the same for all layers and for layers 2 and 3 the increase may be as much as a factor of 2. The value of $\delta\varepsilon^*$ in layer 1 decreases slightly. This implies that the sensitivity of all layers is nearly the same. The values of δp_{CT} and $\delta\alpha$ for the daytime case are all of the same sign as in the nighttime case. Thus, the same general conclusions as in the nighttime case are also valid in the daytime. The magnitude of δp_{CT} is greater in the upper troposphere, nearly the same in the middle troposphere and less in the lower troposphere. The magnitude of $\delta\alpha$ is greater in all layers except layer 2, in which the cloud occurs. The net effect is that due to the nearly equal values of $\delta\varepsilon^*$ at all levels and the greatly variable values of δp_{CT} and $\delta\alpha$, the cumulative error in Q_R generated by solving for the cloud parameters in a dependent fashion is larger in most layers than in the nighttime case.

For the case of a middle tropospheric cloud with top at 500 mb, consistent errors in ε^*, a_c, and ρ_c may be represented by slightly decreasing the values of $\delta\varepsilon^*$ in layers 1 and 2, increasing by as much as a factor of 2 the values in layers 3 and 4, and slightly increasing the value of $\delta\varepsilon^*$ in layer 5. The signs of δp_{CT} and $\delta\alpha$ are the same as in the nighttime case and the magnitudes are somewhat larger. Noting the relative magnitudes for the various layers, the cumulative error in Q_R may best be minimized if ε^* and α are generated in a dependent manner. Conversely, if ε^* and p_{CT} are generated in a dependent manner, the cumulative error in Q_R in the lowest layers is even larger than in the nighttime case.

For the case of a lower tropospheric cloud with cloud top of 800 mb, the values of $\delta\varepsilon^*$, in the same sense as above, are of the same sign and smaller above the cloud top level, when compared to the nighttime case.

The value of $\delta\varepsilon^*$ in layer 4 may be less than that listed in Table 7 by a factor of 0.5. The value of $\delta\varepsilon^*$ in layer 5 is somewhat larger. The values of δp_{CT} are of the same sign and larger compared to the nighttime situation. The sensitivity of Q_R to α in layer 5 is greatly increased. Due to the large inconsistent variance of the relative magnitudes of $\delta\varepsilon^*$, δp_{CT}, and $\delta\alpha$ in the lowest layers, the utilization of an objective scheme for specifying ε^*, p_{CT}, and α in a dependent fashion would yield no improvement and possibly generate greater inaccuracies in Q_R when compared to an independent method of specifying ε^*, p_{CT}, and α.

If these results are incorporated into satellite data analysis techniques, improvement in the interpretation of satellite radiometric data in the case of broken clouds at sub-satellite resolution may result. In particular, bi-spectral methods, which generate cloud field data at a resolution exceeding sensor resolution, such as in Reynolds and Vonder Haar (1976), should be modified to reflect these conclusions. It must be noted that improvement results only in the application to a radiative heating rate determination. In the absolute sense, the accuracy in the estimate of ε^*, p_{CT} and α may not be increased.

E. Resolution, Accuracy, and Scale

As was stated at the beginning of Chapter 4, it is unrealistic to attempt to formulate an objective cloud field determination scheme, which would resolve all cloud features in detail for the GATE A/B and B-scales. The limit on the spacial resolution of satellite observations, the significant distance between surface observations, the restricted time coverage of aircraft observations, and the response characteristics of radar observations necessitate this conclusion. To specify in detail

the radiative properties of the clouds, on an individual basis, poses an even greater problem due to the limited observations and large variability. Even if these data could be generated, a statistical stratification into more general classifications would be required to make it feasible to apply any of the proposed methods of computing the radiative divergence on the proposed scale. A more acceptable method of specifying the cloud fields is to attempt to determine the mean statistics directly. One may, from the limited observations, be able to typify the cloud structure within limited volumes. In the same way, the mean radiative properties associated with the various cloud structures could be more readily deduced from the observations. In regions where the radiative properties of specific clouds were not observed, values observed as typical of such cloud forms could be assigned. For small volumes, the data generated in this manner may be substantially in error. However, the larger the volume and, consequently, the more observations available, the greater the probability that the mean statistics are representative of the cloud structure within that volume. Thus, more confidence may be placed in the resultant values of Q_R for the resolution proposed in Fig. 4, than in the values of Q_R generated for the various structures and sub-volumes within these grid volumes. In a similar manner, the mean radiative divergence for a 1° x 1° grid volume is likely to be more accurate than the values specified for the 0.5° x 0.5° volumes. The point is that the cumulative effect of truly random errors is to approach the mean as the sampling volume is increased.

The accuracies to which cloud parameters must be specified to achieve an accuracy of $\delta Q_R = \pm 0.2°C \cdot day^{-1}$, as have been reported in this work,

are applicable to the mean statistics of these parameters as well as for the individual cloud. The true value of such an approach is particularly evident in the case of cloud boundary proximity to a standard pressure level, where the values of Q_R for both layers are extremely sensitive to the exact boundary location. A knowledge of the mean cloud height and an estimation of its variance allows for a suitable partitioning of Q_R for the two layers.

Systematic or bias errors may be corrected by a comparison of deduced and observed values of Q_R for specific times when a dense observing network (multiple aircraft missions) was deployed.

Studies of C-scale phenomena require a greater spacial and temporal resolution to adequately describe the phenomena. To achieve a resolution campatible with the requirements of C-scale studies, requires a different approach. The surface observing network was more dense than on the larger scale. Additionally, for limited times, aircraft observations of state parameters, clouds and the radiative fluxes were made at as many as five different flight levels, concurrently. Thus, the resolution of input parameters to a computational method is quite good. The accuracy of these data should also be enhanced due to the density of observations. It may, therefore, be possible to generate the fields of radiative heating at this resolution by more detailed computations. Such determinations could be readily verified using the direct observations of the radiative fields.

VI. THE SENSITIVITY OF THE RADIATIVE SURFACE FLUXES

In addition to the determination of the radiative divergence of atmospheric layers, the determination of the radiative fluxes at the surface is also essential to the fulfillment of the RSP objectives. Knowledge of the upward and downward long wave and short wave surface fluxes is required for the purposes of the Oceanographic and Boundary Layer Subprograms of the GATE.

Kraus, et al (1973) have suggested that a determination of the hourly mean surface fluxes is necessary. The observing network, which was deployed in the GATE area (Fig. 1), provides a fairly extensive and continuous record of the upward and downward radiative fluxes at the ocean surface, (Cox and Kraus, 1975). These direct observations comprise a basic data set, which is superior in resolution and continuity when compared to those available for the radiative divergence determination. However, area averaged values of the surface fluxes are needed. The horizontal resolution required of a surface flux determination is comparable to that required for the radiative divergence determination (Fig. 4). Thus, the direct observation may be insufficient to accurately specify the hourly mean area averaged surface fluxes on this resolution. This is analogous to the radiative divergence determination in that the representativeness of the hourly mean fluxes observed at a point for the surrounding grid area must be verified. Therefore, analysis techniques, which utilize the direct observations and other pertinent meteorological data, may be necessary in order to generate the required fields. Kraus, et al (1973) have stated that the determination of the individual hourly mean fluxes should be accurate to within 7 $W \cdot m^{-2}$ + 5% of the true value.

That is:

$$\delta H_s \leq \pm \{ 7 \ W \cdot m^{-2} + 0.05 \ H_s \} \tag{6.1}$$

where H_s is the upward or downward long wave or short wave radiative flux at the surface.

In this section, the sensitivity of the computed radiative surface fluxes to the vertical distribution of temperature, moisture and clouds is investigated.

A. Infrared Upward Irradiance

The upward long wave radiative flux at the surface, $H_{IR}(\uparrow)_s$, is primarily a function of the sea surface temperature, T_s, according to the Stefan-Boltzman Law. That is:

$$H_{IR}(\uparrow)_s = \epsilon_s \ \sigma \ T_s^4 \tag{6.2}$$

where ϵ_s is the sea surface broadband long wave emissivity and σ is the Stefan-Boltzman constant. The long wave emissivity of the sea surface is very nearly unity (Kondratyev, 1972). Thus, effectively, the sea surface temperature is the only variable quantity on the right hand side of Eq. 6.2. Radiometric and thermometric observations of sea surface temperature were routinely made from the GATE ships (see GATE Report No. 19). A mean map of the sea surface temperature for the tropical East Atlantic Ocean for Phase I has been compiled by Nicholson (1975). These data were composited from daily maps generated from the ship observations. A mean value of $\sim +27°C$ occurred in the GATE B-scale area. Variations of from $+22°C$ to $+28°C$ were encountered in the GATE A/B-scale area. Employing Eqs. 6.1 and 6.2 for a surface temperature of $+25°C$, a limiting accuracy constraint of $\sim \pm29°W \cdot m^{-2}$ for the upward long wave flux determination is found. This implies that the sea surface temperature

must be known to within $\sim$ $\pm4.5°C$. Thus, even the simple assumption of a mean sea surface temperature of $+25°C$ will meet the RSP proposed accuracy standard. Therefore, the utilization of observed sea surface temperatures and observed upward long wave fluxes should yield results which substantially exceed the RSP proposed accuracy for the upward long wave surface flux determination.

B. Infrared Downward Irradiance

Simplified formulas exist for the determination of the downward longwave radiative flux at the surface. Rodgers (1972) and Kondratyev (1969) have discussed the accuracy and applicability of such techniques. In general, they are based upon the water vapor content and temperature of the lowest atmospheric layers. However, the results of numerous computations using the radiative transfer model described in section III.A. imply that for tropical maritime conditions, the downward long wave radiative flux at the surface is relatively invariant. The downward flux for the mean model atmosphere (see section IV.A.) was 450 $W \cdot m^{-2}$. This implies a limiting accuracy constraint of $\sim$ ±29 $W \cdot m^{-2}$. Computations made for black ($\varepsilon^*=1.0$) clouds existing in the mean model atmosphere at heights of from 100 mb to 900 mb yielded long wave downward surface fluxes of from 450 $W \cdot m^{-2}$ to 452 $W \cdot m^{-2}$, respectively. Thus, even in the case of the low lying black cloud, a change of only $+$ 2 $W \cdot m^{-2}$ in the downward long wave surface flux results when compared to cloud free conditions. Computations for grey ($\varepsilon^*=0.5$) clouds gave an even smaller deviation from the mean case. It may thus be concluded that a knowledge of the cloud fields is not required to meet the RSP proposed accuracy standard for the downward long wave radiative flux at the surface. Even

in the case of an atmosphere, which is saturated at all levels, the computed downward surface flux was only 471 $W \cdot m^{-2}$ or 21 $W \cdot m^{-2}$ greater than in the mean model case. For an atmosphere which is 20% drier at all levels compared to that given in Fig. 9, a downward surface flux of 443 $W \cdot m^{-2}$ was computed. This is only 7 $W \cdot m^{-2}$ less than in the mean case. Computations made for atmospheres, which are 2°C warmer or cooler at all levels compared to the mean atmosphere given in Fig. 9, yielded surface fluxes of 470 $W \cdot m^{-2}$ and 448 $W \cdot m^{-2}$, respectively. It is noted that in none of the above cases does the downward surface flux in the infrared vary by more than ±29 $W \cdot m^{-2}$ from that computed for the mean model atmosphere. This relative invariance of the downward long wave radiative flux at the surface may be attributed to the high vapor pressures and the resulting continuum absorption in the boundary layer. The semi-permanent presence of such a layer over the tropical oceans is a well-known feature of tropical meteorology (v. Ficker, 1936). It is thus evident that if the data on the temperature, humidity and cloud fields are generated to the accuracy required for the radiative divergence determination (section IV and V), then the accuracy of downward surface flux determinations in the long wave may be expected to substantially exceed the proposed accuracy requirement.

C. Solar Incident Irradiance

One may deduce the sensitivity of the incident short wave irradiance at the surface for a grid area by considering a simple, one layer approximation to the atmospheric radiative transfer processes. That is:

$$K(\downarrow)_s = K(\downarrow)_0 \cdot \left\{ \int_0^{p_s} t_a(p') \cdot dp' \cdot (1 - \alpha) + \left\{ \int_0^{p_{CT}} t_a(p') \cdot dp' \cdot \right.\right.$$

$$\left. \int_{p_{CT}}^{p_{CB}} t_c(p')\cdot dp' \cdot \int_{p_{CB}}^{p_s} t_a(p')\cdot dp' \right\} \cdot \alpha \right| \tag{6.3}$$

where $K(\downarrow)$ is the downward solar irradiance, $t_a(p)$ is the broadband short wave transmissivity of the free atmosphere, $t_c(p)$ is the broadband short wave transmissivity of the clouds, α is the percent area cloud cover over the grid area, and p is the pressure. The subscripts s, o, CT, and CB refer to the ocean surface, the top of the atmosphere ($p \sim 0$ mb), cloud top and cloud base, respectively. It is noted that:

$$t_a \equiv \int_0^{p_s} t_a(p')\cdot dp'$$

and

$$t_c \equiv \int_{p_{CT}}^{p_{CB}} t_c(p')\cdot dp' = 1 - a_c - \rho_c.$$

One may also approximate the transmissivity of the free atmosphere in the cloudy column as:

$$t_a = \int_0^{p_{CT}} t_a(p')\cdot dp' \cdot \int_{p_{CB}}^{p_s} t_a(p')\cdot dp'.$$

Thus,
$$K(\downarrow)_s = K(\downarrow)_0 \cdot \{t_a\cdot(1 - \alpha) + t_a\cdot t_c\cdot\alpha\}. \tag{6.4}$$

This equation ignores the spectral dependence of the transmissivities. Thus, it may tend to underestimate the transmissivity in the cloudy column. This implies that the sensitivity of $K(\downarrow)_s$ to the specification of t_a, t_c and α is slightly too large in Eq. 6.4. Differentiating Eq. 6.4, substituting from Eqs. 6.1 and 6.4 and rearranging terms, yields:

$$\pm \delta K(\downarrow)_0 = \frac{7 \ W\cdot m^{-2}}{t_a\cdot(1-\alpha) + t_a\cdot t_c\cdot\alpha} + 0.05 \cdot K(\downarrow)_0 \tag{6.5}$$

$$\pm \delta t_a = \frac{7 \ W \cdot m^{-2}}{K(\downarrow)_0 \cdot \{(1-\alpha) + t_c \cdot \alpha\}} + 0.05 \cdot t_a \qquad (6.6)$$

$$\pm \delta t_c = \frac{7 \ W \cdot m^{-2}}{K(\downarrow)_0 \cdot t_a \cdot \alpha} + 0.05 \cdot \{\frac{1-\alpha}{\alpha} + t_c\} \qquad (6.7)$$

$$\pm \delta \alpha = \frac{7 \ W \cdot m^{-2} + 0.05 \cdot K(\downarrow)_0 \cdot \{t_a \cdot (1-\alpha) + t_a \cdot t_c \cdot \alpha\}}{K(\downarrow)_0 \cdot \{t_a \cdot t_c - t_a\}} \qquad (6.8)$$

where the quantities $\delta K(\downarrow)_0$, δt_a, δt_c, and $\delta \alpha$ are the maximum uncertainty allowed in the specification of $K(\downarrow)_0$, t_a, t_c, and α in order that $K(\downarrow)_s$ may be determined to within 7 $W \cdot m^{-2}$ + 5% of its true value. Thus, the δ values may be determined for various combinations of the four variables t_a, t_c, $K(\downarrow)_0$ and α.

Consider first the sensitivity of the incident solar irradiance at the surface to the specification of the incident solar irradiance at the top of the atmosphere (Eq. 6.5). By simple examination of Eq. 6.5, one may see that the less the attenuation (i.e. large t_c, and t_a, and small α), the more sensitive $K(\downarrow)_s$ is to $K(\downarrow)_0$. In Table 8, values of $\delta K(\downarrow)_0$ are given for various combinations of t_c, t_a, α. The value of $K(\downarrow)_0$ was assumed to be $\sim$ 500 $W \ m^{-2}$. The magnitudes of $\delta K(\downarrow)_0$ should be increased by 25 $W \cdot m^{-2}$ for $K(\downarrow)_0 \cong$ 1000 $W \cdot m^{-2}$ or decreased by 20 $W \cdot m^{-2}$ for $K(\downarrow)_0 \cong$ 100 $W \cdot m^{-2}$.

The maximum accuracy required in the specification of $K(\downarrow)_0$ may be determined by evaluating Eq. 6.5 for $\alpha = 0$, and $t_a = 0.85$. In this case, for $K(\downarrow)_0 \sim$ 500 $W \cdot m^{-2}$, $\delta K(\downarrow)_0 = \pm 33.2 \ W \cdot m^{-2}$ or for $K(\downarrow)_0 \sim$ 1000 $W \cdot m^{-2}$, $\delta K(\downarrow)_0 = \pm 58.2 \ W \cdot m^{-2}$.

Examining Eq. 6.6, it is seen that the maximum sensitivity (i.e. minimum δt_a) of the incident solar irradiance at the surface occurs in

| | t_c | $\delta K(\downarrow)_o$, $(W \cdot m^{-2})$ | | |
		$\alpha = 20\%$	$\alpha = 50\%$	$\alpha = 80\%$
$t_a = 0.60$	0.1	± 39.2	± 46.2	± 66.7
	0.3	± 38.5	± 43.0	± 51.5
	0.5	± 38.0	± 40.6	± 44.5
	0.7	± 37.4	± 38.7	± 40.4
	0.9	± 37.0	± 37.3	± 37.7
$t_a = 0.85$	0.1	± 35.0	± 40.0	± 54.4
	0.3	± 34.6	± 37.7	± 43.7
	0.5	± 34.2	± 36.0	± 38.7
	0.7	± 33.8	± 34.7	± 35.8
	0.9	± 33.4	± 33.7	± 34.0

Table 8. Maximum allowable uncertainty in the specification of the incident solar irradiance at $p \sim 0$ in order that the incident solar irradiance at the surface may be determined to within 7 $W \cdot m^{-2}$ + 5% of its true value for various values of t_a, t_c and α and for $K(\downarrow)_o \sim 500$ $W \cdot m^{-2}$. To interpret for different values of $K(\downarrow)_o$, refer to the text.

the case of small values of α, t_c, and t_a and large values of $K(\downarrow)_0$. Thus, the less cloudiness there is, and the less optically thick the clouds are, the greater the sensitivity is. Also, the greater the incident solar irradiance at the top of the atmosphere, the greater is the sensitivity. In a similar manner, the less transparent the atmosphere is, the greater the sensitivity. If one employs the mean instantaneous value of $K(\downarrow)_0$ for the conditions noted in section IV.A (i.e. $K(\downarrow)_0 \sim 800$ $W \cdot m^{-2}$) and assumes $\alpha = 0$ (i.e. no clouds), then a value of $\delta t_a \cong \pm 0.04$, ± 0.05 results for $t_a \cong 0.60$, 0.85, respectively. That the values of $t_a \cong 0.60$ and 0.85 correspond to the extreme values of clear sky atmospheric transmissivity for the GATE A/B-scale area may be inferred from the observational results of Kondratyev, et al (1976). Thus, these are the lower limiting values of the uncertainty which can be tolerated in the specification of the transmissivity of the free atmosphere. The presence of clouds may increase this lower limit by up to ± 0.04 (i.e. $\delta t_a \cong \pm 0.08$ for $t_c = 0.1$ and $\alpha = 80\%$) in the mean instantaneous situation.

In the situation of a small solar zenith angle and thus a small value of $K(\downarrow)_0$ corresponding to the time periods near sunrise and sunset, the sensitivity is substantially decreased. If one assumes a cloud free atmosphere, a value of $K(\downarrow)_0 = 100\ W \cdot m^{-2}$, and $t_a \sim 0.60$, then $\delta t_a \cong \pm 0.10$.

Table 9 is a compilation of the values of δt_c resulting from the evaluation of Eq. 6.7 for various values of $K(\downarrow)_0$, t_a, t_c and α. It is seen that the less the solar attenuation in the clear region, the more sensitive $K(\downarrow)_s$ is to the specification of t_c. It may also be noted that as areal cloud cover increases or as the optical thickness

		δt_c		
		$K(\downarrow)_o = 100 \ W\cdot m^{-2}$		
	t_c	$\alpha = 20\%$	$\alpha = 50\%$	$\alpha = 80\%$
$t_a = 0.60$	0.1	±0.79	±0.29	±0.16
	0.9	±0.83	±0.33	±0.20
$t_a = 0.85$	0.1	±0.62	±0.22	±0.12
	0.9	±0.66	±0.26	±0.16
		$K(\downarrow)_o = 500 \ W\cdot m^{-2}$		
	t_c	$\alpha = 20\%$	$\alpha = 50\%$	$\alpha = 80\%$
$t_a = 0.60$	0.1	±0.32	±0.10	±0.04
	0.9	±0.36	±0.14	±0.08
$t_a = 0.85$	0.1	±0.29	±0.09	±0.04
	0.9	±0.33	±0.13	±0.08
		$K(\downarrow)_o = 1000 \ W\cdot m^{-2}$		
	t_c	$\alpha = 20\%$	$\alpha = 50\%$	$\alpha = 80\%$
$t_a = 0.60$	0.1	±0.27	±0.08	±0.03
	0.9	±0.31	±0.12	±0.07
$t_a = 0.85$	0.1	±0.25	±0.07	±0.03
	0.9	±0.29	±0.11	±0.07

Table 9. Maximum uncertainty allowed in the specification of the cloud transmissivity in order that the incident solar irradiance at the surface may be determined to within 7 $W\cdot m^{-2}$ + 5% of its true value for various values of t_a, t_c, α and $K(\downarrow)_o$.

of the clouds increase (i.e. decreasing t_c), the sensitivity increases (i.e. decreasing δt_c). Evaluating Eq. 6.7 for $K(\downarrow)_0 = 800$ W·m^{-2}, $t_a = 0.85$ and $\alpha = 100\%$ yields values of $\delta t_c = \pm 0.015$, ± 0.035 and ± 0.055 for $t_c \simeq 0.1$, 0.5, and 0.9, respectively. These values of δt_c are the lower limit of the allowable uncertainty in t_c for the mean instantaneous case. Referring to section IV.C.1, the comparable requirement for the radiative divergence determination is $\delta t_c \stackrel{\simeq}{=} \pm 0.105$ to 0.155. Thus, the surface flux determination is much more sensitive to the specification of the cloud radiative properties in the short wave portion of the spectrum. This arises because the radiative heating is not nearly as sensitive to the cloud reflectivity.

In Table 10, the values of $\delta\alpha$ are given for various combinations of $K(\downarrow)_0$, t_a, t_c. and α. It is seen that the sensitivity of $K(\downarrow)_s$ to the specification of α increases with (1) increasing cloudiness, (2) increasing $K(\downarrow)_0$, (3) decreasing cloud transmissivity, and (4) increasing transmission in the cloud free atmosphere. Thus, in general, the greater the difference in transmissivity of the clear and cloudy regions, the greater the sensitivity (i.e. small magnitudes of $\delta\alpha$). The limiting value of $\delta\alpha$, which resulted from the radiative divergence determination for the mean instantaneous condition (see sections IV.C.3 and V.C.), was approximately $\pm 5\%$. The comparable number for the surface flux determination is $\sim \pm 10\%$. This results in the case of $K(\downarrow)_0 \stackrel{\simeq}{=} 800$ W·m^{-2}, $t_c \sim 0.5$, and $t_a = 0.85$. Thus, the accuracy of the surface flux determination should exceed the RSP proposed accuracy by up to a factor of 2 if the data on the percent areal cloud cover meets the accuracy constraint imposed for a radiative divergence determination. However,

	$\delta\alpha$, (%)		
	$K(\downarrow)_0 = 100 \ W \cdot m^{-2}$		
t_c	$\alpha = 20\%$	$\alpha = 50\%$	$\alpha = 80\%$
$t_a = 0.60$			
0.1	∓ 17.5	∓ 16.0	∓ 14.5
0.5	∓ 32.3	∓ 30.8	∓ 29.3
0.9	∓ 166.0	∓ 164.2	∓ 162.7
$t_a = 0.85$			
0.1	∓ 13.7	∓ 12.2	∓ 10.7
0.5	∓ 25.5	∓ 24.0	∓ 22.5
0.9	∓ 131.4	∓ 129.9	∓ 128.4
	$K(\downarrow)_0 = 500 \ W \cdot m^{-2}$		
t_c	$\alpha = 20\%$	$\alpha = 50\%$	$\alpha = 80\%$
$t_a = 0.60$			
0.1	∓ 7.2	∓ 5.7	∓ 4.2
0.5	∓ 13.7	∓ 12.2	∓ 10.7
0.9	∓ 72.3	∓ 70.8	∓ 69.3
$t_a = 0.85$			
0.1	∓ 6.4	∓ 4.9	∓ 3.4
0.5	∓ 12.3	∓ 10.8	∓ 9.9
0.9	∓ 65.5	∓ 64.0	∓ 62.5
	$K(\downarrow)_0 = 1000 \ W \cdot m^{-2}$		
t_c	$\alpha = 20\%$	$\alpha = 50\%$	$\alpha = 80\%$
$t_a = 0.60$			
0.1	∓ 5.9	∓ 4.4	∓ 2.9
0.5	∓ 11.4	∓ 9.9	∓ 8.4
0.9	∓ 60.6	∓ 59.1	∓ 57.6
$t_a = 0.85$			
0.1	∓ 5.5	∓ 4.0	∓ 2.5
0.5	∓ 10.7	∓ 9.2	∓ 7.7
0.9	∓ 57.3	∓ 55.8	∓ 54.3

Table 10. The maximum allowable uncertainty in the specification of the percent areal cloud cover in order that the incident solar irradiance at the surface may be determined to within 7 $W \cdot m^{-2}$ + 5% of its true value for various values of $K(\downarrow)_0$, t_a, t_c, and α.

it must be noted that the greater sensitivity of $K(\downarrow)_s$ to the specification of t_c, when compared to Q_R or Q_{SW}, will tend to partially cancel this beneficial relation.

D. Solar Reflected Irradiance

The upward short wave flux at the surface, $K(\uparrow)_s$ is determined by the broadband short wave surface reflectivity and the incident, downward short wave flux according to:

$$K(\uparrow)_s = \rho_s \cdot K(\downarrow)_s \tag{6.9}$$

Differentiating Eq. 6.9, substituting from Eqs. 6.1 and 6.9, and rearranging terms yields:

$$\delta\rho_s = 0.05 \, \rho_s + \frac{7 \; W \cdot m^{-2}}{K(\downarrow)_s} \tag{6.10}$$

where $\delta\rho_s$ is the maximum uncertainty allowed in the specification of ρ_s in order that $K(\uparrow)_s$ may be determined to within $7 \; W \cdot m^{-2}$ + 5% of its true value.

Except for the case of large solar zenith angle, Kondratyev, et al (1976) have observed that the surface reflectivity in the short wave for the GATE region varies from 0.04 to 0.16 depending on the diffuseness of the downward irradiance. The maximum values of ρ_s were observed in very dusty conditions where the incident solar irradiance at the surface was very diffuse. Evaluating Eq. 6.10 for $\rho \sim 0.04$ and $K(\downarrow)_s$ = 100, 500, and 1000 $W \cdot m^{-2}$ yields values of $\delta\rho_c$ = ±0.072, ±0.016, ±0.009, respectively. In a similar manner, in the case of $\rho \sim 0.16$, $\delta\rho_s$ equals ±0.078, ±0.022, ±0.015. Thus, in the situation of a large incident irradiance, the surface reflectivity must be known to within $\sim$ ±0.01 to ±0.02. Also, the smaller the surface reflectivity is, the better it must be known.

Thus, it is evident that some manner of deducing the diffusivity of the incident irradiance is needed. In addition to the presence of aerosols, the presence of clouds also affects the diffusivity. The problem of aerosols may be adequately handled utilizing the results of Kondratyev, et al, (1976). However, to deduce the effect of clouds, analysis of the ship observations will be required.

Due to the small magnitude of ρ_s, if $K(\downarrow)_s$ is determined to within the RSP proposed accuracy then $K(\uparrow)_s$ is only slightly sensitive to the uncertainty in $K(\downarrow)_s$.

E. Net Radiative Flux at the Surface

Based on the foregoing analyses, it may be concluded that the determination of the net long wave flux at the surface should be accurate to within 7 $W \cdot m^{-2}$ + 5% of its true value. However, the determination of the net short wave flux will be more difficult. This is due to the large variability of the solar incident irradiance. It is noted that the effect of an uncertainty in $K(\downarrow)_s$ on the net solar flux will be slightly compensated in the determination of $K(\uparrow)_s$.

VII. CONCLUSIONS

The research reported in this paper defines the constraints, which data analysis techniques must meet if the GATE Radiation Subprogram accuracy objectives are to be met, in terms of the conventional independent variables used in radiative transfer computations. The need for an objective cloud field determination scheme and the proposed methods of deducing the radiative divergence fields from cloud field data and other pertinent meteorological data have been reviewed in light of the GATE RSP objectives. The desired resolution of the radiative divergence product is specified as 0.5° latitude by 0.5° longitude in the horizontal and 200 mb in the vertical every one to three hours. Area averaged values of the radiative divergence are desired at this resolution. Statistical information on the three dimensional cloud fields and other meteorological parameters within the grid volumes is needed. This conclusion results from a consideration of the computational feasibility of the proposed methods and the desired resolution and accuracy. Thus, data at a limited number of geographic locations are insufficient; in addition, the bulk radiative properties of the cloud fields must be known.

The required accuracy in the cloud field description, which an objective cloud field determination scheme must meet such that the RSP accuracy requirement of $\pm 0.2°C \cdot day^{-1}$ in the radiative heating rates may be achieved, has been evaluated. The radiative transfer was simulated by means of a simplified isothermal, broadband flux emissivity transfer model in the long wave spectral region and a simplified broadband flux transmissivity transfer model in the short wave regime. In the long wave region, clouds were modelled in terms of a broadband effective

emissivity (i.e. grey body approximation) and in the short wave in terms of a broadband absorptivity and reflectivity. The maximum allowable uncertainty in the specification of each of the bulk radiative properties, the height, the thickness and the percent areal coverage of clouds, such that the RSP accuracy requirement may be met, has been determined for the short wave and long wave radiative components, and for the total radiation. The sensitivities are directly applicable to the mean daily situation. A constant multiplier must be used to reinterpret the short wave component in terms of the average instantaneous situation.

- The accuracy required in the description of the temperature and moisture fields has also been evaluated. In addition, the influence of aerosols upon the radiative heating rates has been investigated. Similar limiting constraints for the radiative surface flux determination have been developed. The RSP proposed accuracy limit for the individual hourly surface fluxes is 7 $W \cdot m^{-2}$ + 5% of the true value.

The primary results of this study are stated below:

1. State Parameters

Random or systematic errors in the specification of the water vapor mixing ratio must not exceed ± 0.2 $g \cdot kg^{-1}$ in a 200 mb thick atmospheric layer. Similarly, errors in the mean layer temperature should not exceed $\pm 2.5°C$. Observational verification of the accuracy of the proposed methods in their treatment of the radiative transfer for tropical cloud free conditions is needed before any method is applied.

2. Aerosols

The contribution of atmospheric aerosols to the radiative heating rates is significant. Dust "clouds" of Saharan origin are the primary

radiatively active aerosol in the GATE region. Kondratyev, et al (1976) have measured radiative heating rates due to aerosol absorption of short wave radiation in the GATE region of $4°C \cdot day^{-1}$ to $5°C \cdot day^{-1}$. Thus, as many as ten stratifications of dustiness might be required in the data analysis. However, based on their measurements, this constraint may be able to be relaxed in light of the uniformity of the effect when dust "clouds" are present. Further research into the variability of the dust influence and ways of detecting the dust "clouds" is needed.

3. Areal Cloud Cover

Errors in the specification of percent areal cloud cover must not exceed $\pm 10\%$ at any level. Exceptions to this are: lower tropospheric water clouds at night, clouds which are not very radiatively active (i.e. very thin stratus and cirrus whose bulk radiative properties are very small in magnitude), and water clouds occurring beneath other water clouds. In these cases, the sensitivity of the radiative heating to the percent areal cloud cover is significantly less.

4. Cloud Structure

It is critical to know in which standard 200 mb thick pressure layer(s) a cloud occurs. The accuracy with which the cloud boundaries must be located within the layer(s) in which they occur, at night, ranges from $\sim \pm 10$ mb to $\sim \pm 35$ mb for radiatively active high and low clouds, respectively. In the daytime case, the radiative divergence is less sensitive to the boundary location within a layer by as much as a factor of 2-3 at many levels. Less information is needed for water clouds occurring below water clouds and clouds which are relatively radiatively inactive.

5. Bulk Radiative Properties of Clouds

In general, the accuracy to which the bulk radiative properties must be specified is substantially greater than the range of naturally occurring values. This is particularly true for upper and middle level clouds and their associated long wave effective emissivity and short wave absorptivity. Thus, methods must be developed to deduce the cloud radiative properties from the data obtained during the GATE Field Phase. In this regard, detailed modelling and observations of the interaction of finite size cloud elements and broken cloud fields with the radiative fields is needed such that adequate methods of specifying the associated radiative properties may be developed.

6. Interrelation of Cloud Bulk Radiative Properties

Further effort is needed in the formulation of quantitative dependent relations among the effective long wave emissivity (both upward and downward), short wave absorptivity and reflectivity, the diffusivity of transmitted short wave irradiance and cloud height or type and cloud thickness. Both observational and theoretical studies should be undertaken. Without such information, the RSP objectives are unlikely to be met due to the lack of direct observations on the required time and space scales. In lieu of the development of adequate methods for specifying the radiative properties of cloud fields, all information relating to these quantities should be retained in any objective cloud field determination scheme.

7. Data Analysis and Dependent Solutions

The case of simultaneous uncertainty in the specification of various cloud parameters has been treated. In the case of independent

errors the allowable uncertainties in the cloud field parameters is substantially reduced. Realistically, however, in many instances, these quantities will be deduced in a dependent fashion from a particular data source (e.g. satellite radiometric data). The effect of compensating errors due to a dependent solution for the various cloud parameters has been evaluated for three example cases. The parameters for which a dependent solution would yield the greatest accuracy in the radiative divergence are given. In a similar manner, those quantities for which independent information is most desirable are also given.

8. Surface Fluxes

The upward and downward infrared fluxes at the surface are relatively invariant over the tropical oceans. The sea surface temperature must be known to within $\pm 4.5°C$. It has been found that if the accuracy of the description of the temperature and water vapor distributions meets the limits noted above for the radiative divergence determination, then the individual and net surface flux determinations in the long wave region may be expected to easily meet the RSP proposed accuracy. Due to the large vapor pressures and continuum absorption in the tropical oceanic boundary layer, the effect of clouds on the infrared surface fluxes is nearly negligible.

The downward solar flux at the surface is, in general, less sensitive than the radiative divergence to uncertainties in the cloud field description and the transmission of the free atmosphere. However, it is significantly more sensitive to the broadband short wave reflectivity of clouds. To deduce the upward short wave surface flux, the sea surface reflectivity must be determined to within $\pm 1\%$ to $\pm 2\%$ in most cases.

Since the surface reflectivity depends on the angular distribution of the incident irradiance, some manner of prescribing the diffusivity of solar irradiance transmitted by clouds and aerosols must be developed.

LITERATURE CITED

Albrecht, B.A., S.K. Cox and M. Poellot, 1974: Pyrgeometer Measurements
From Aircraft. Rev. Sci. Instrum., 45, pp. 33-38.

Albrecht, B.A. and S.K. Cox, 1975: The Large Scale Response of the
Tropical Atmosphere to Cloud Modulated Infrared Heating. J. Atmos.
Sci., 32, pp. 16-24.

Battan, L.J., 1973: Radar Observation of the Atmosphere. University
of Chicago Press, 324 pp.

Betts, A.K., 1975: Personal communication.

Bignell, K.J., 1970: The Water Vapor Infrared Continuum. Quart. J. Roy.
Meteor. Soc., 96, pp. 390-403.

Cox, S.K., 1968: A Radiation Model in which the Effects of Clouds are
Simulated from Moisture and Temperature Parameters. Annual Report
on WBG 88, Dept. of Meteorology, Univ. of Wisconsin, pp. 2-50.

Cox, S. K.,1969: Observational Evidence of Anomalous Infrared Cooling
in a Clear Tropical Atmosphere. J. Atmos. Sci., 26, No. 6, pp. 1347-
1349.

Cox, S.K., 1971a: Cirrus Clouds and the Climate. J. Atmos. Sci., 28,
No. 8, pp. 1513-1515.

Cox, S.K., 1971b: Infrared Radiation Models for the Tropics. Proceedings
of the Miami Workshop on Remote Sensing, A.M.S., pp. 161-178.

Cox, S.K., 1972: Radiative Energy Components for the BOMEX Core Experiment.
Conference on Atmospheric Radiation, Fort Collins, CO, A.M.S.,
pp. 188-190.

Cox, S.K., T.H. Vonder Haar, K. Hanson, and V. Suomi, 1972: Measurements
of Absorbed Short Wave Energy in a Tropical Atmosphere. J. Solar
Energy, 14, No. 2.

Cox, S.K., 1973: Infrared Heating Calculations with a Water Vapor
Pressure Broadened Continuum. Quart. J. Roy. Meteor. Soc., 99,
pp. 669-679.

Cox, S.K., and H. Kraus, 1975: Field Phase Report, GATE Radiation
Subprogram, GARP.

Cox, S.K., 1975: Personal communication.

Cox, S.K., 1976: Observations of Cloud Infrared Emissivity. To be
published in J. Appl. Meteor.

Davis, P.A., 1970: Airborne Ruby-Lidar and Radiometric Measurements of
Cirrus and Haze During BOMEX, Final Report Contract No. E-263-68,
SRI Proj. 2334, Menlo park, California.

LITERATURE CITED - Continued

Davis, P.A., 1971: Applications of an Airborne Ruby-Lidar During a BOMEX Program of Cirrus Observations. J. Appl. Meteor., 10, pp. 1314-1323.

Fleming, J.R. and S.K. Cox, 1974: Radiative Effects of Cirrus Clouds. J. Atmos. Sci., 31, No. 8, pp. 2182-2188.

Gille, J.C., and T.N. Krishnamurti, 1972: On Radiative Interactions in a Tropical Disturbance. Conference on Atmospheric Radiation, Fort Collins, Colorado, AMS, pp. 266-268.

Goody, R.M., 1964: Atmospheric Radiation, I. Theoretical Basis, Oxford University Press, 436 pp.

Grassl, H., 1974: Influence of Different Absorbers in the Window Region on Radiative Cooling. Beitr. z. Phys. Atm., 47, pp. 1-13.

Gray, W.M., 1972: The Magnitude and Character of the Radiation Induced Vertical Circulation of the Troposphere. Conference on Atmospheric Radiation, Fort Collins, Colorado, A.M.S., pp. 255-259.

Hansen, J.E., 1971: Multiple Scattering of Polarized Light in Planetary Atmospheres. Part I. The Doubling Method. J. Atmos. Sci., 28, pp. 120-125.

Herman, B.M., and S.R. Browning, 1975: The Effects of Aerosols on the Earth-Atmosphere Albedo. J. Atmos. Sci., 32, No. 7, pp. 1430-1445.

Hunt, G.E., 1973: Radiative Properties of Terrestrial Clouds at Visible and Infrared Thermal Window Wavelengths. Quart. J. Roy. Meteor. Soc., 99, pp. 346-369.

International Scientific & Management Group (ISMG), 1975: Report on the Field Phase of the GATE. GATE Report No. 19, ICSU, WMO, 219 pp.

Jacobowitz, H., 1970: Emission, Scattering and Absorption of Radiation in Cirrus Cloud Layers. Ph.D. Thesis, Massachusetts Institute of Technology, 181 pp.

Johnson, D.R. and P.M. Kuhn, 1966: Improved Radiometersonde Observations of Atmospheric Infrared Irradiance. J. Geophys. Res., 71, pp. 367-373.

Jordan, C.L., 1958: Mean Soundings for the West Indies Area. J. Meteor. 15, pp. 91-97.

Kattawar, G.W., G.N. Plass and J.A. Guinn, 1973: Monte Carlo Calculations of the Polarization of Radiation in the Earth's Atmosphere-Ocean System. J. Phys. Oceanogr., 3, pp. 353-372.

LITERATURE CITED - Continued

Kondratyev, K.Ya., and G. Nikolsky, 1968: Direct Solar Radiation and Aerosol Structure of the Atmosphere from Balloon Measurements in the Period of IQSY. Sveriges. Met. Arch. Hydrol. Inst. Meddel., Ser. B., No. 28.

Kondratyev, K.Ya., 1969: Radiation in the Atmosphere. Academic Press, New York, 912 pp.

Kondratyev, K.Ya., 1971: Preliminary Results of the First Expedition Under the Program of the Complex Atmospheric Energetics Exp. WMO Bull., 20, pp. 160.

Kondratyev, K.Ya., 1972: Radiation Processes in the Atmosphere. WMO - M 309.

Kondratyev, K.Ya., et al, 1976: Aerosol in the GATE Area and Its Radiative Properties. Colorado State University Atmospheric Science Paper No. 247, Fort Collins, Colorado.

Korb, G. and F. Möller, 1962: Theoretical Investigation on Energy Gain by Absorption of Solar Radiation in Clouds. Final Tech. Report. Contract DA-91-591-EUC-1612 (1.1. 1961 - 30.9.1962 (U.S. Dept. of Army)).

Kraus, H., et al, 1973: The Radiation Subprogram for the GATE, GATE Report No. 4, ICSU, WMO, 109 pp.

Kuhn, P.M., 1963: Measured Effective Long Wave Emissivity of Clouds. Mon. Wea. Rev., 91, pp. 635-640.

Kuhn, P.M., and H.K. Weickman, 1969: High Altitude Radiometric Measurement of Cirrus. J. Appl. Meteor., 8, pp. 147-154.

Kuhn, P.M., and L.P. Stearns, 1971: Radiative Transfer Observations and Calculations During BOMEX. NOAA Tech. Report, ERL 203-APCL 19, 171 pp.

Manabe, S., and F. Möller, 1961: On the Radiative Equilibrium and Heat Balance of the Atmosphere. Mon. Wea. Rev., 89, pp. 503-532.

Manabe, S. and R.F. Strickler, 1964: Thermal Equilibrium of the Atmosphere with a Convective Adjustment. J. Atmos. Sci., 21, No. 4, pp. 361-385.

Manabe, S. and R.T. Wetherald, 1967: Thermal Equilibrium of the Atmosphere with a Given Distribution of Relative Humidity, J. Atmos. Sci., 24, No. 3, pp. 241-259.

Marks, F., 1975: Study of Diurnal Variations in Convection Using Quadra Radar, Phases I and II. GATE Report No. 14, ISMG, pp. 191-204.

LITERATURE CITED - Continued

Martin, D.W., 1975: Characteristics of West African and Atlantic Cloud Clusters. GATE Report No. 14, ISMG, pp. 182-190.

Mason, B.J., 1971: The Physics of Clouds. Clarendon Press, Oxford, 671 pp.

McKee, T.B. and S.K. Cox, 1974: Scattering of Visible Radiation by Finite Clouds. J. Atmos. Sci., 31, No. 7, pp. 1885-1892.

Meteorological Branch, Canadian Dept. of Transportation, 1964, 1965, 1966, 1967: Ozone Data for the World.

Nicholson, S.E., 1975: Sea-Surface Temperature Variation Off the West Coast of Africa During Phase I of GATE. GATE Report No. 14, ISMG, pp. 129-136.

Nitta, T. and S. Esbensen, 1974: Heat and Moisture Budget Analyses Using BOMEX Data. Mon. Wea. Rev., 102, pp. 17-28.

Nitta, T., 1975: Observational Determination of Cloud Mass Flux Distribution. J. Atmos. Sci., 32, No. 1, pp. 73-91.

Paltridge, G.W., 1973: Direct Measurement of Water Vapor Absorption of Solar Radiation in the Free Atmosphere. J. Atmos. Sci., 30, No. 1, pp. 156-160.

Paltridge, G.W., 1974: Infrared Emissivity, Short Wave Albedo, and the Microphysics of Stratiform Water Clouds. J. Geophys. Res., 79, No. 27, pp. 4053-4058.

Pelissier, J.M., 1972: A Numerical Model of the Tropical Upper Tropospheric Cold Core Cylcones Including Parameterized Infrared Cooling. Conference on Atmospheric Radiation. Ft. Collins, Colorado, A.M.S., pp. 260-265.

Platt, C.M.R., and K. Bartusek, 1974: Structure and Optical Properties of Some Middle Level Clouds. J. Atmos. Sci., 31, No. 4, pp. 1079-1088.

Platt, C.M.R., 1975: Infrared Emissivity of Cirrus: Simultaneous Satellite, Lidar, and Radiometric Observations. Quart. J. Roy. Meteor. Soc., 101, pp. 119-126.

Prospero, J.M., and T.N. Carlson, 1972: The Vertical and Areal Distribution of Saharan Dust Over the Western Equatorial North Atlantic Ocean. J. Geophys. Res., 77, No. 27, pp. 5255-5265.

Reed, R.J. and E.E. Recker, 1971: Structure and Properties of Synoptic-Scale Wave Distrubances in the Equatorial Western Pacific. J. Atmos. Sci., 28, pp. 1117-1133.

LITERATURE CITED - Continued

Reynolds, D.W., T.H. Vonder Haar and S.K. Cox, 1975: The Effect of Solar Radiation Absorption in the Tropical Troposphere. J. Appl. Meteor., 14, pp. 433-444.

Reynolds, D.W. and T.H. Vonder Haar, 1976: A Bi-Spectral Method for Cloud Parameter Determination. CSU Atmos. Sci. Paper No. 239.

Roach, W.T., 1961: The Absorption of Solar Radiation by Water Vapor and Carbon Dioxide in a Cloudless Atmosphere. Quart. J. Roy. Meteor. Soc., 87, pp. 364-373.

Rodgers, C.D. and C.D. Walshaw, 1966: The Computation of Infrared Cooling Rates in Planetary Atmospheres. Quart. J. Roy. Meteor. Soc., 92, pp. 67-92.

Rodgers, C.D., 1972: Report of the JOC Study Group Conference. Leningrad, GARP Publ. Series No. 8, pp. 6-19.

Ruprecht, E. and W.M. Gray, 1974: Analysis of Satellite-Observed Tropical Cloud Clusters. CSU Atmos. Sci. Paper No. 219.

Shenk, W.E. and R.J. Curran, 1973: A Multi-Spectral Method for Estimating Cirrus Cloud Top Heights. J. Appl. Meteor., 12, 7, pp. 1213-1216.

Smith, W.L., 1969: A Semi-Empirical Method for Calculating Carbon Dioxide and Water Vapor Transmission. ESSA Technical Report. NESC, 47, 20 pp.

Smith, W.L., H.M. Woolf, P.G. Abel, C.M. Hayden, M. Chalfant, and N. Grody, 1974: Nimbus-5 Sounder Data Processing System, Part I. NOAA Tech. Memo NESS 57, U.S. Dept. of Commerce, National Environmental Satellite Service, Washington, D. C. 99 pp.

Smith, W.L. and W.C. Shen, 1975: A Radiative Heating Model Derived from the GATE MSR Experiment. Ninth Tech. Conf. on Hurricanes and Tropical Meteorology of the AMS, Miami.

Stone, H.M. and S. Manabe, 1968: Comparison Among Various Numerical Models Designed for Computing Infrared Cooling. Mon. Wea. Rev., 96, pp. 735-741.

Tarbeev, Y.V., and S.R. Peterson, 1974: Ship Operations, GATE Report No. 10, ICSU, WMO, 140 pp.

Vonder Haar, T.H., et al, 1974: Final Report of Second Informal Planning Meeting for the GATE Radiation Subprogram. Fort Collins, Colorado, ICSU, WMO.

von Ficker, H., 1936: Die Passatinversion. Veröffentl. d. Meteorol. Inst. d. Univ. Berlin, Bd. I, Heft. 4.

LITERATURE CITED - Continued

Walshaw, C.D., 1957: Integrated Absorption by the 9.6 μm Band of Ozone
 Quart. J. Roy. Meteor. Soc., 83, pp. 315-320.

Williams, K.T. and W.M. Gray, 1973: Statistical Analysis of Satellite
 Observed Trade Wind Cloud Clusters in the Western North Pacific.
 Tellus, 25, pp. 313-336.

Yamamoto, G., M. Tanaka and S. Asano, 1970: Radiative Transfer in
 Water Clouds in the Infrared Region. J. Atmos. Sci., 27,
 pp. 282-292.

Yamamoto, G., M. Tanaka and S. Ohta, 1974: Heating of the Lower
 Troposphere Due to Absorption of the Visible Solar Radiation by
 Aerosols. J. Met. Soc. of Japan, 52, No. 1, pp. 61-68.

Yanai, M., S. Esbensen and J.H. Chu, 1973: Determination of Bulk
 Properties of Tropical Cloud Clusters from Large Scale Heat and
 Moisture Budgets. J. Atmos. Sci., 30, pp. 611-627.

Zdunkowski, W. G., and W.K. Crandall, 1971: Radiative Transfer of
 Infrared Radiation in Model Clouds. Tellus, XXIII, pp. 517-527.